For Typhoon Analysis Technology and Guidance

Typhoon precipitation and wind analyses using ground weather observation instruments

June 28, 2023

Pukyong National University, Busan, Korea
leedi@pknu.ac.kr
Prof. Lee, Dong-In

National Institute of Meteorological Sciences, Jeju, Korea
Dr. Cha, Eun-Jeong

- The typhoons affected or landed on the Korean Peninsula for the past 10 years (40 and 10) --- 4 typhoons affected the Korean peninsula annually. --- (2013-2022) (KMA, Mar. 2023)

Yr	Month	TY Name	Occurrence Extinction date	Landing	Max. wind speed
13	6	LEEPI	18-21		15.4
	8	KONG-REY	26-31		16.0
	10	DANAS	04-09		30.3
14	7	NEOGURI	04-11		54.0
		HALONG	29-11		18.0
		NAKRI	30-03		25.0
	10	VONGFONG	03-14		59.0
15	**6**	**CHAN-HOM**	**30-13**	**o**	**33.5**
	7	NANGKA	04-18		18.2
		HALOLA	13-27		24.0
	8	GONI	15-26		36.1
16	9	MALAKAS	13-20		49.0
		CHABA	**28-02**	**o**	**56.0**
17	7	NANMADOL	02-05		27.0
		NORU	21-02		37.0
	9	TALIM	09-18		47.0

Yr	Month	TY Name	Occurrence Extinction date	Landing	Max. wind speed
18	6	PRAPIROON	29-04		32.0
	8	RUMBIA	15-18		20.0
		SOULIK	**16-25**	**O**	**43.0**
	9	TRAMI	21-01		53.0
		KONGREY	29-07		
19	7	DANAS	16-20		24.0
	8	**FRANCISCO**	**02-06**	**O**	**32.0**
		LEKIMA	04-12		50.0
		KROSA	06-16		43.0
	9	LINGLING	02-08		47.0
		TAPAH	19-23		37.0
		MITAG	**28-03**	**O**	**37.0**
20	8	JANGMI	22-27		45.0
		BAVI	**28-02**	**O**	**56.0**
		MAYSAK	**28-03**	**O**	**49.0**
	9	**HAISHEN**	**01-07**	**O**	**55.0**
21	8	LUPIT	04-09		23.0
		OMAIS	**20-24**	**O**	**24.0**
	9	CHANTHU	07-18		55.0
22	7	AERE	01-05		20.0
		SONGDA	28-01		20.0
		TRASES	31-01		18.0
	8	**HINNAMNOR**	**28-06**	**O**	**55.0**
	9	NANMADOL	14-20		55.0

Contents

Chapter Ⅰ.

Meteorological instruments used for TY observation.

Marine	Surface	Upper-air
1) Buoy 2) Weather vessel 3) Wave Glider	1) AWS 2) Disdrometer	1) Sonde 2) Windprofiler 3) Radiometer

Radar	Satellite	Airplane
1) Doppler radar 2) Dual-Pol radar	1) TRMM 2) GPM	1) T-PARC

1. Precipitation Analysis in Typhoon using ground based meteorological instruments (Radar, Wind Profiler, Disdrometer)

Weather Radar

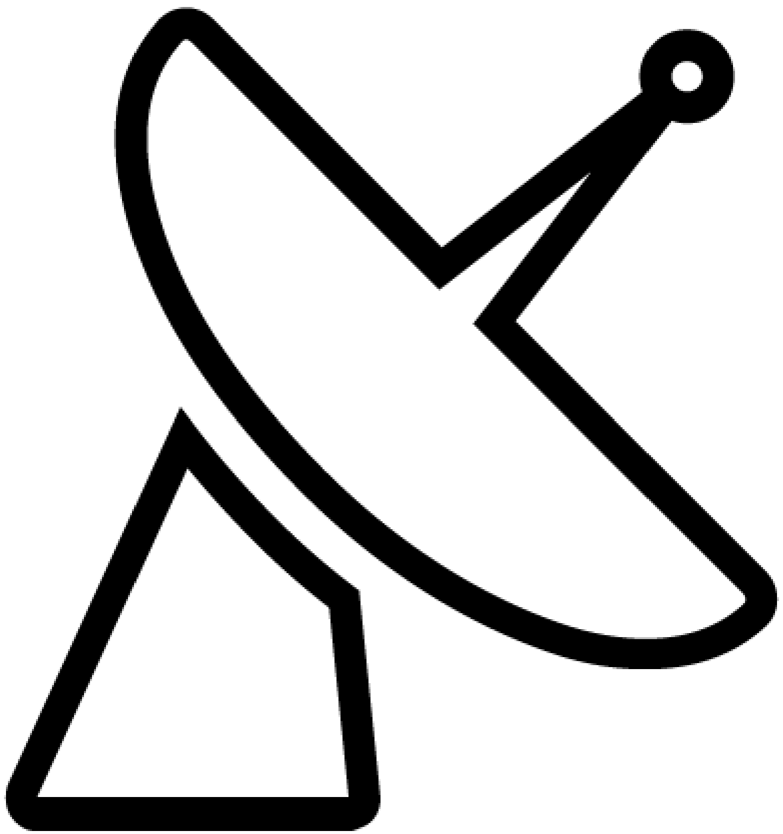

Quantitative Precipitation Estimation (QPE) and Forecasting (QPF)

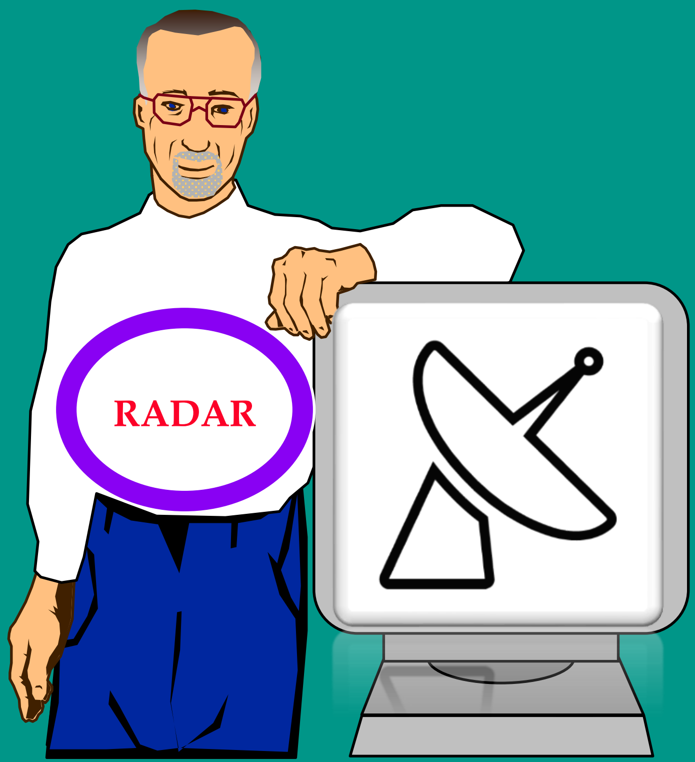

Weather Radar

The Korea Meteorological Administration (KMA) operates 15 radars across the country.

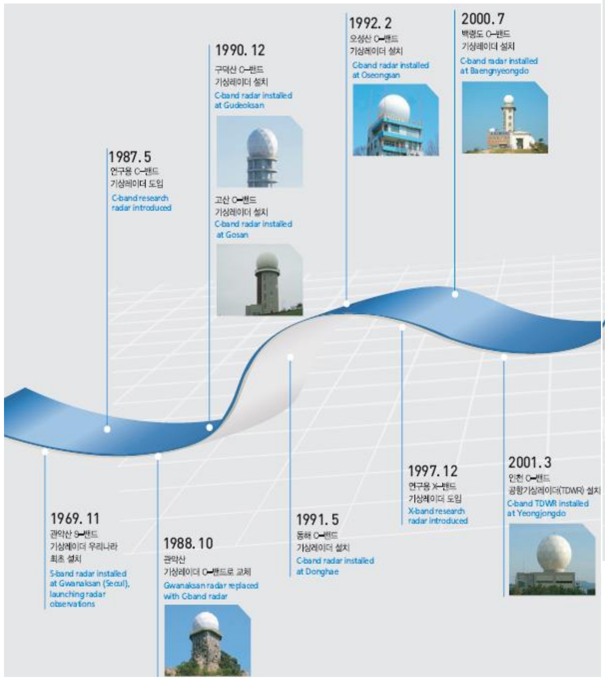

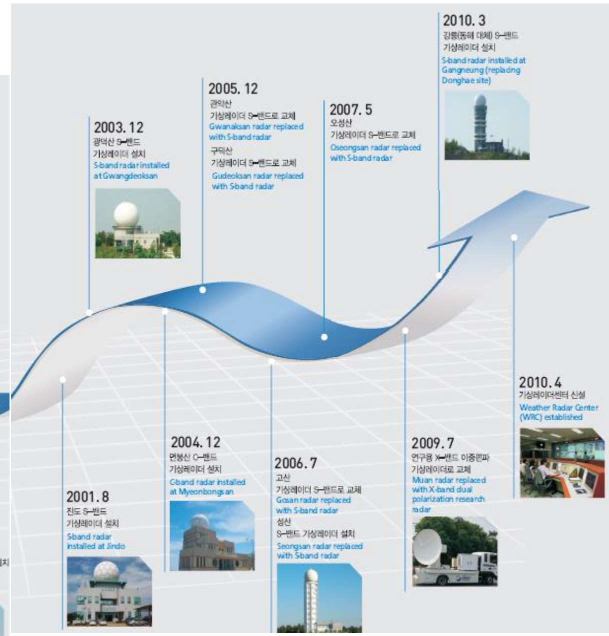

S-band (1969)
: Gwanaksan

5 C-band(1990s)
: Gwanaksan, Gudeoksan,
Gunsan, Donghae, Gosan

3 S-band, 2 C-band (2000s)
: Gwangdeoksan, Jindo, Seongsan (S)
: Myeonbongsan, Baeknyeongdo (C)

Replacing all to
Dual-Pol S-band
(2014~2019)

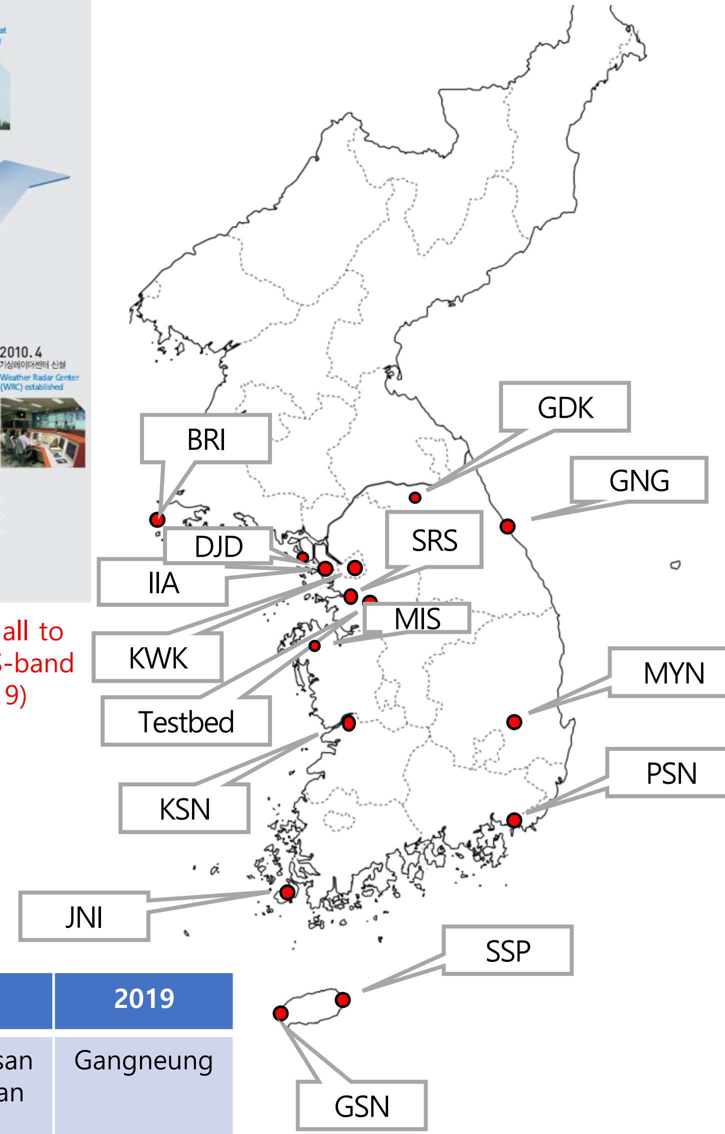

Year	2014	2015	2016	2017	2018	2019
Radar	Baeknyeongdo Testbed (Yongin)	Myeonbongsan Jindo	Gwanaksan Gudeoksan	Gwangdeoksan Gosan	Oseongsan Seongsan	Gangneung

Weather Radar

Band Designation	Frequency	Wave Length	
VHF	30 – 300 MHz	10 – 1 m	Wind Profilers (6m, 75cm, 22cm)
UHF	300 – 1000 MHz	1 – 0.3 m	
L	1 – 2 GHz	30 – 15 cm	
S	2 – 4 GHz	15 – 8 cm	Weather Radars (10, 5, 3 cm)
C	4 – 8 GHz	8 – 4 cm	
X	8 – 12 GHz	4 – 2.5 cm	
K_u	12 – 18 GHz	2.5 – 1.7 cm	Cloud radar (9mm, 3mm)
K	18 – 27 GHz	1.7 – 1.2 cm	
K_a	27 – 40 GHz	1.2 – 0.75 cm	

Weather Radar

Weather radar is ..?

a remote sensing instrument used to locate precipitation and its motion
by sending out microwaves that can be reflected back to the radar by precipitation particles.

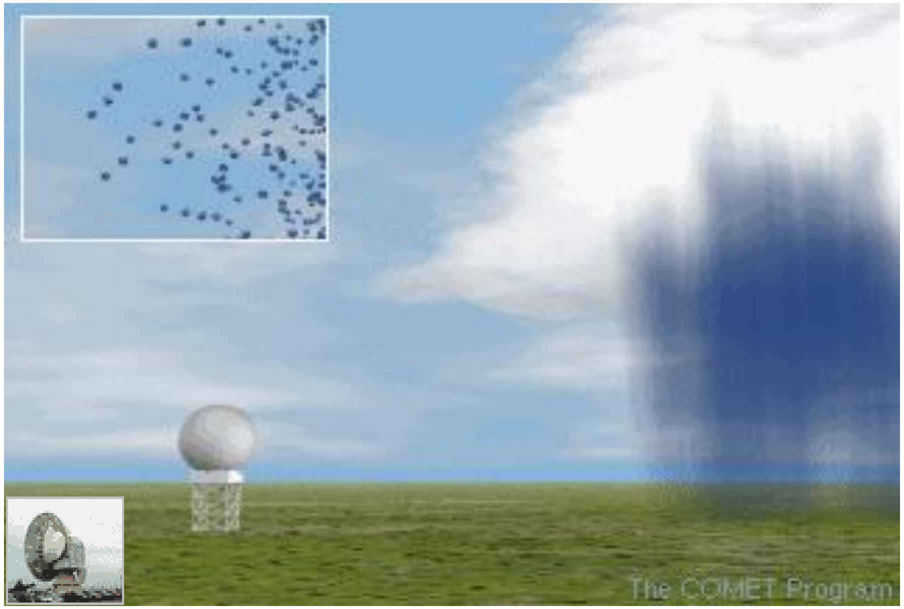

Fig. The image of radar operation.

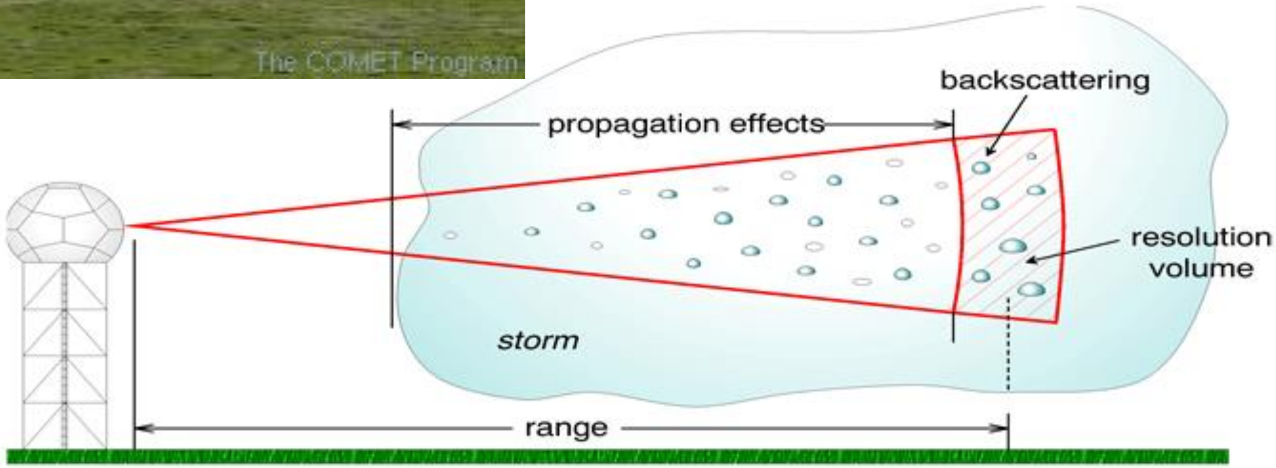

Output

- **Reflectivity (Z, dBZ) :**

  The signal strength received from the subject

  $$Z\ (dBZ) = 10\log_{10} z$$

  $$Z\ (mm^6 m^{-3}) = \int N(D) D^6 dD$$

  → **Detect the size and content in precipitation**

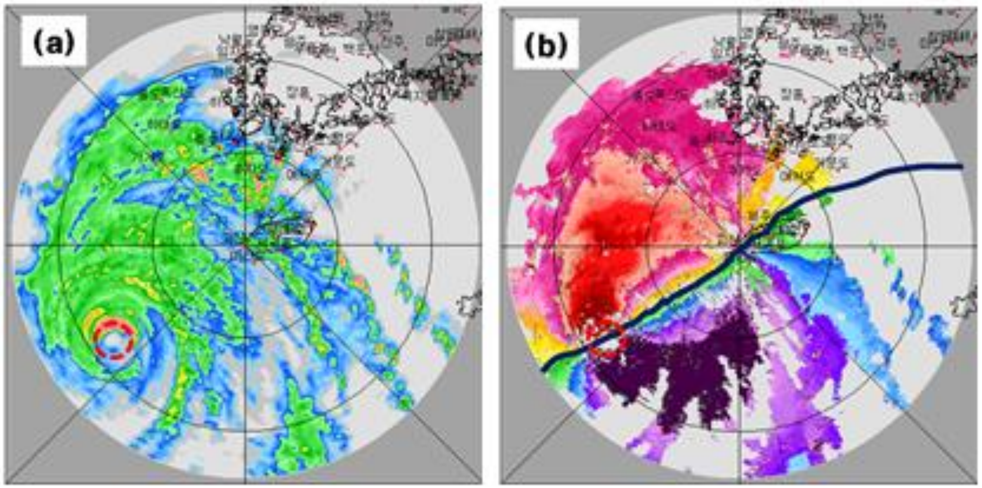

Fig. The images of Typhoon Dianmu at 18 LST in Aug. 10, 2010 from radar in Gosan (a) Reflectivity, (b) Radial velocity.

- **Radial velocity (V_r , m s^{-1}) :**

  The velocity of an object moving in the direction of the radar

  → **Estimate the wind distribution**

- **Spectrum Width (SW , m s^{-1})**

  The variation of wind distribution

  → **Determine the accuracy of wind data**

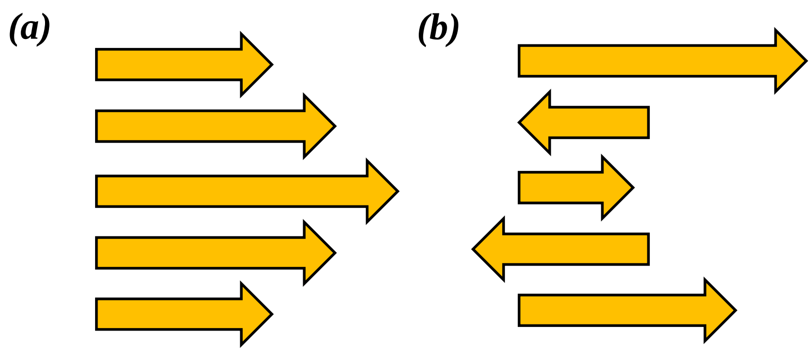

Fig. Example of the (a) narrow and (b) wide spectrum width.

QPE (Quantitative Precipitation Estimation)

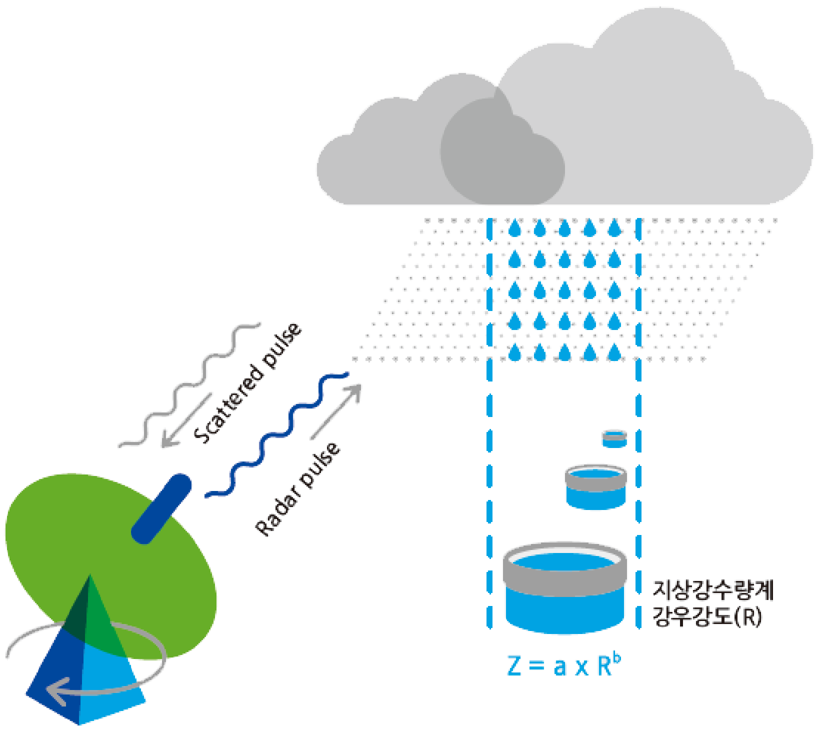

Fig. Demonstration of the QPE (by Radar center).

To make significant use of reflectivity,
Rainfall rate (R in mm hr^{-1}) can be calculated.

→ **Z-R relationship**

$$Z = AR^b$$

$$Z = 200R^{1.6}$$

Marshall and Palmer (1948)

※ Depending on the precipitation type intensity, parameter a and b changes.

The type of the precipitation system changes according to the weather conditions, so that the estimation of precipitation using the Z-R relation simply involves inherent errors.

Polarimetric weather radar

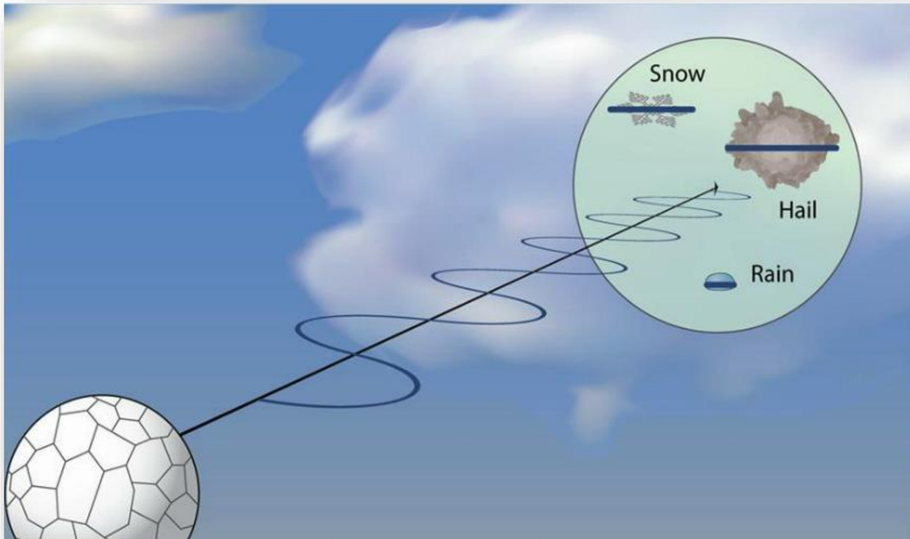

Previous Radars

- Using a horizontal wave to detect
  - ➔ Reflectivity and Radial Velocity

Dual-Pol radar

- Using Horizontal + Vertical waves
- Obtain the horizontal/vertical size of the objects
- By analyzing the differential of horizontal and vertical waves
  - ➔ **Size, Shape, Variability of the precipitation**

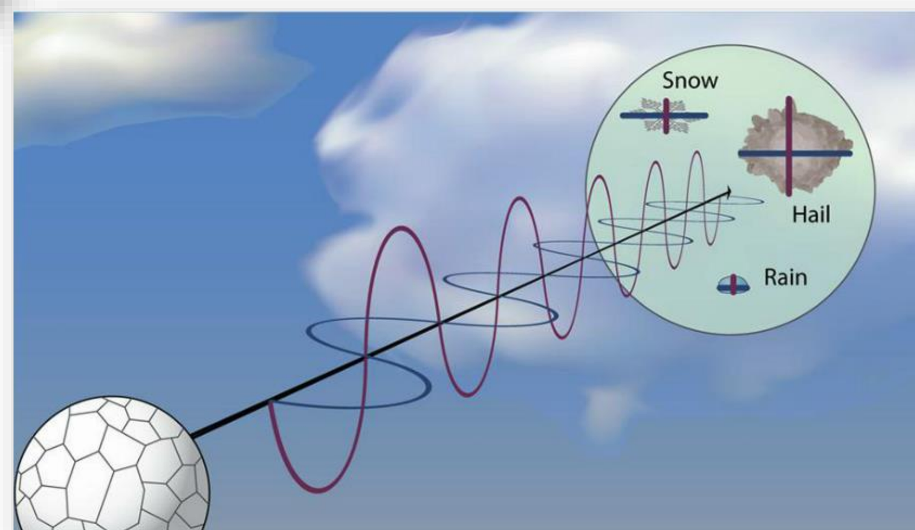

Weather Radar

Dual Polarimetric Parameters → Information of the size, shape, variability of the objects

1. **Differential reflectivity (Z_{DR})**
    - A measure of the reflectivity-factor-weighted shape of particles in the sampling volume
    - **Differentiate Rain/Hail/Snow**

3. **Differential phase (Φ_{DP})**
    - Only detects **non-spherical particles** within the sampling volume
    - Immune to radar mis-calibration and partial beam blockage
    - Immune to attenuation and differential attenuation
    - Often more useful for meteorological purposes is K_{DP}

4. **Specific differential phase (K_{DP})**
    - K_{DP} only has contributions from **non-spherical particles**.
    - Often taken as a measure of the amount of **liquid water** present in the sampling volume
    - Better for locating and quantifying heavy rainfall

5. **Cross-correlation coefficient (ρ_{hv})**
    - A measure of the **diversity of particle shapes, canting angles, physical compositions, and δ** in the radar sampling volume.
    - ρ_{hv} usually is <u>very low in non-meteorological stuff</u>

Weather Radar

Typhoon "Chanhome" (11 July, 12~24KST)

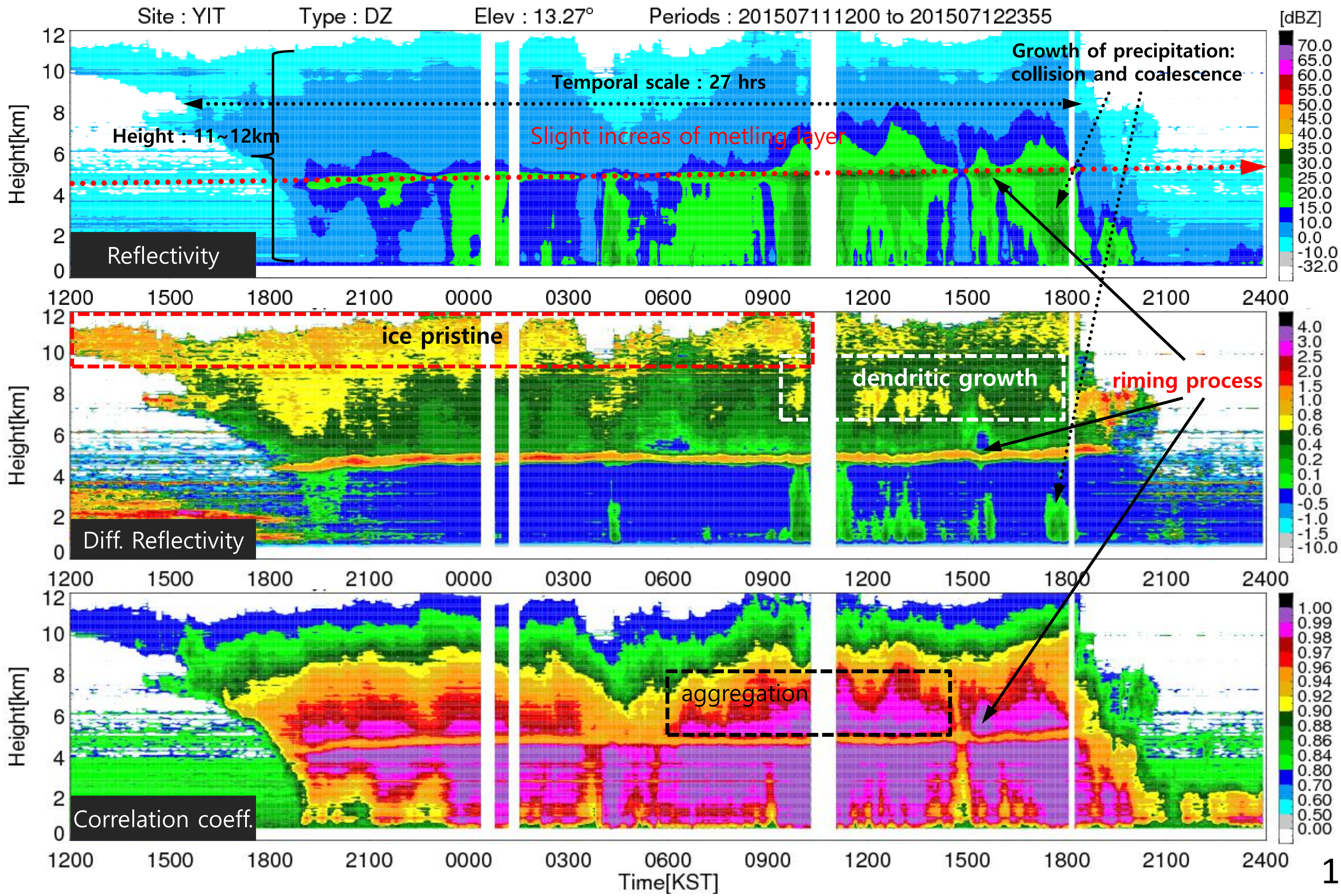

Radar Observations of Intense Orographic Precipitation Associated with Typhoon Xangsane (2000)

Yu and Cheng, 2008

Instrument :

- S-band Doppler Radar (WSR-88D) from CWB_Taiwan
- C-band Doppler Radar from Taoyuan International Airport

Target :

- Typhoon Xangsane (2000)

Objective of the study :

Orographic precipitation of Typhoon

Result :

- It is confirm that the precipitation range and strength are enhanced in the windward side of the wide and high mountain (DT)
- It shows that when the system passes, the flow velocity of the lower level is strengthened in the narrow and low mountain (NKR) area.
- The location of the maximum precipitation in each mountain area changes according to the windward side of the wind.

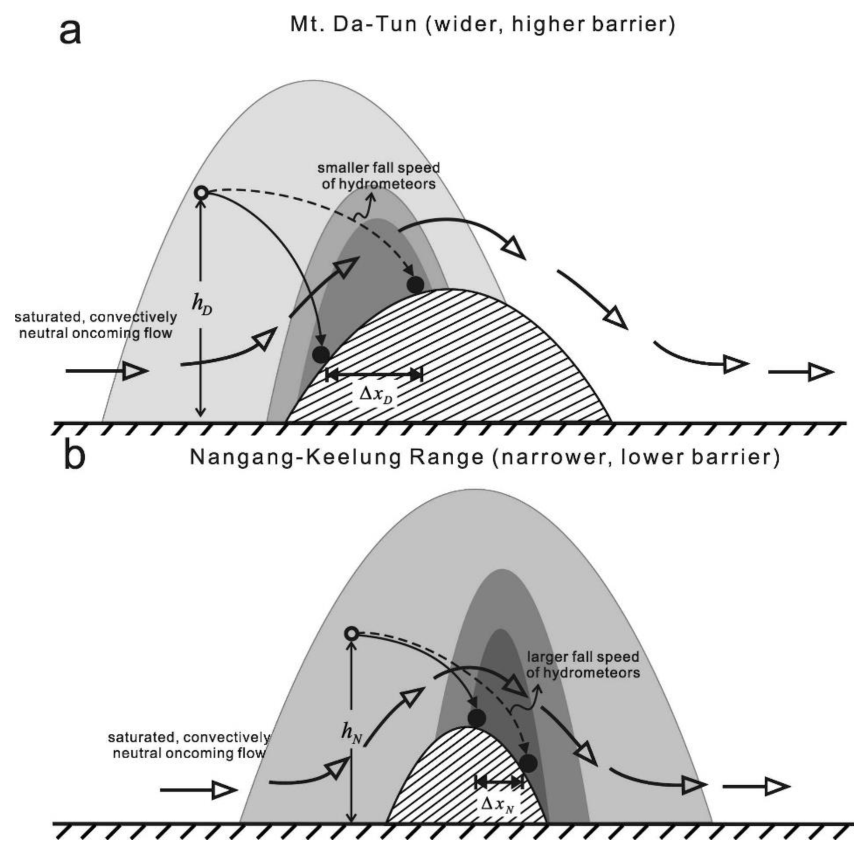

Fig. The schematic image of the result of this study. The precipitation range and strength are enhanced in the windward side of the wide and high mountain (DT), and when the system passes, the flow velocity of the lower level is strengthened in the narrow and low mountain (NKR) area.

Wind profiler (13)

Transmits UHF wave (Ultra High Frequency, 300 ~ 3000 ㎒)
to the upper atmosphere.

A upper layer observation instrument that observes
a vertical wind distribution by receiving radio signals scattered
from turbulence moving with the wind.

Observation Strategy:
Receives a Doppler-shifted radio signal according to
the atmospheric motion in each direction from the radio waves
deflected 14 to 20 °for the four orientations and the vertical
direction.

→ Three-dimensional wind field output using the five Vr.

Observation range:
Low mode: ~ 5 km
High mode: ~ 12 km

Resolution: 1-10 minutes

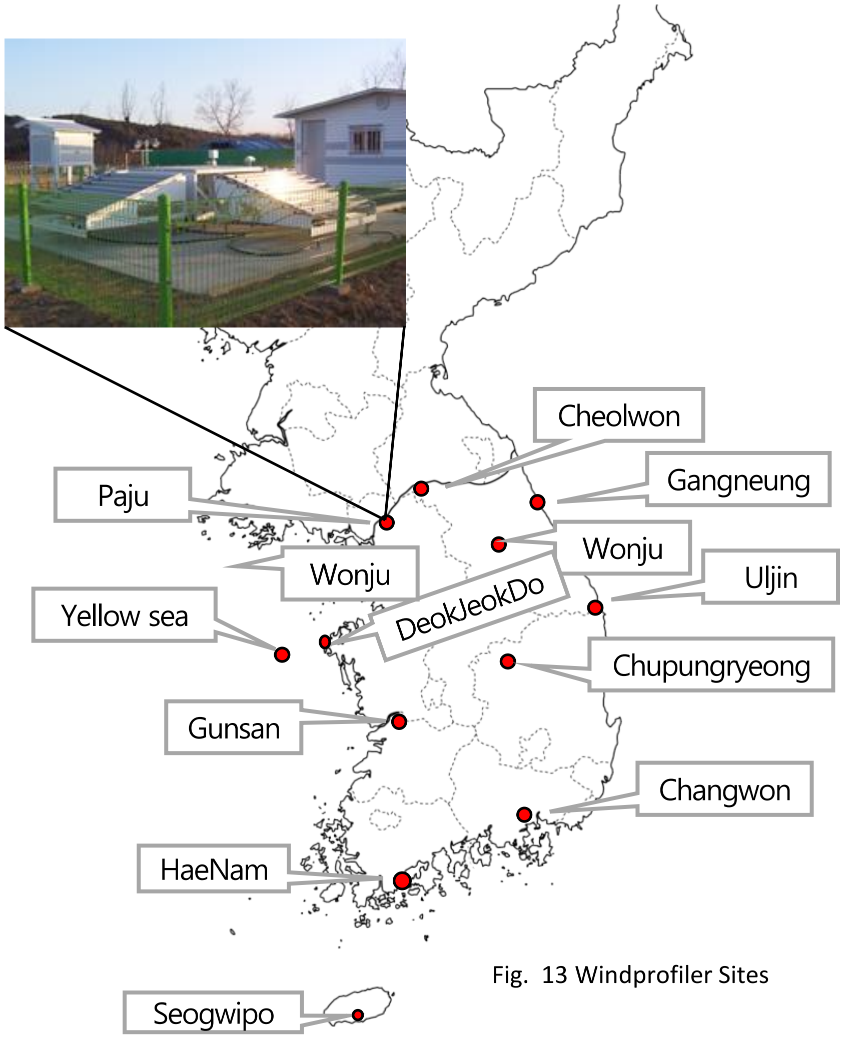

Fig. 13 Windprofiler Sites

DBS(Doppler Beam Swinging):

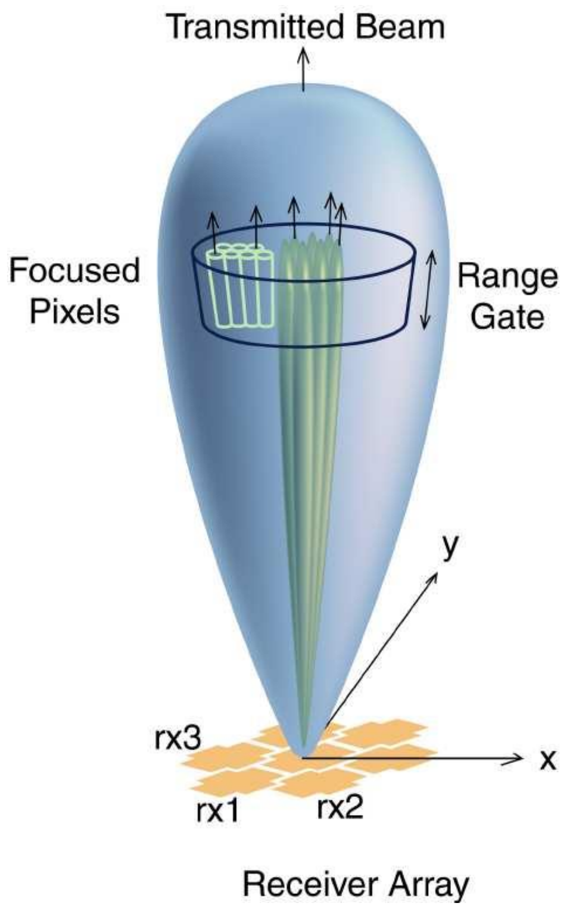

Fig. Schematic diagram of Wind Profiler (Cheong et al., 2008).

Calculation of wind components (UVW) from radial velocity (N)

$$\begin{pmatrix} sin\theta_1 cos\emptyset_1 & sin\theta_1 cos\emptyset_1 & cos\theta_1 \\ sin\theta_2 cos\emptyset_2 & sin\theta_2 cos\emptyset_2 & cos\theta_2 \\ \dots & \dots & \dots \\ sin\theta_n cos\emptyset_n & sin\theta_n cos\emptyset_n & cos\theta_n \end{pmatrix} \begin{pmatrix} u \\ v \\ w \end{pmatrix} = \begin{pmatrix} v_{r1} \\ v_{r2} \\ \dots \\ v_{rn} \end{pmatrix}$$

※ θ_i :Elevation angle, φ_i :Azimuth

- Considering 4 components of radial velocity, RMSE reduces (Cheong et al., 2008).

- Wind profiler uses five components of radial velocity

Characteristics and performance of the operational wind profiler network of the Japan Meteorological Agency

Ishihara et al., 2006

Instrument :
WINDAS(Wind profiler Network and Data Acquisition System), Japan

Research:
Typhoon Chaba, 2004

Research Purpose :
Typhoon inner core observed using WINDAS

Research result :
Track of the typhoon inner core observed using Wind profiler network(Ichiki, Kumamoto and Hamada)

The increase of environmental vertical shear around the typhoon was observed in the time-height cross sections of winds.
→ This is a typical example showing usefulness of the wind profiler network, for analyzing kinematical structure of mesoscale weather systems.

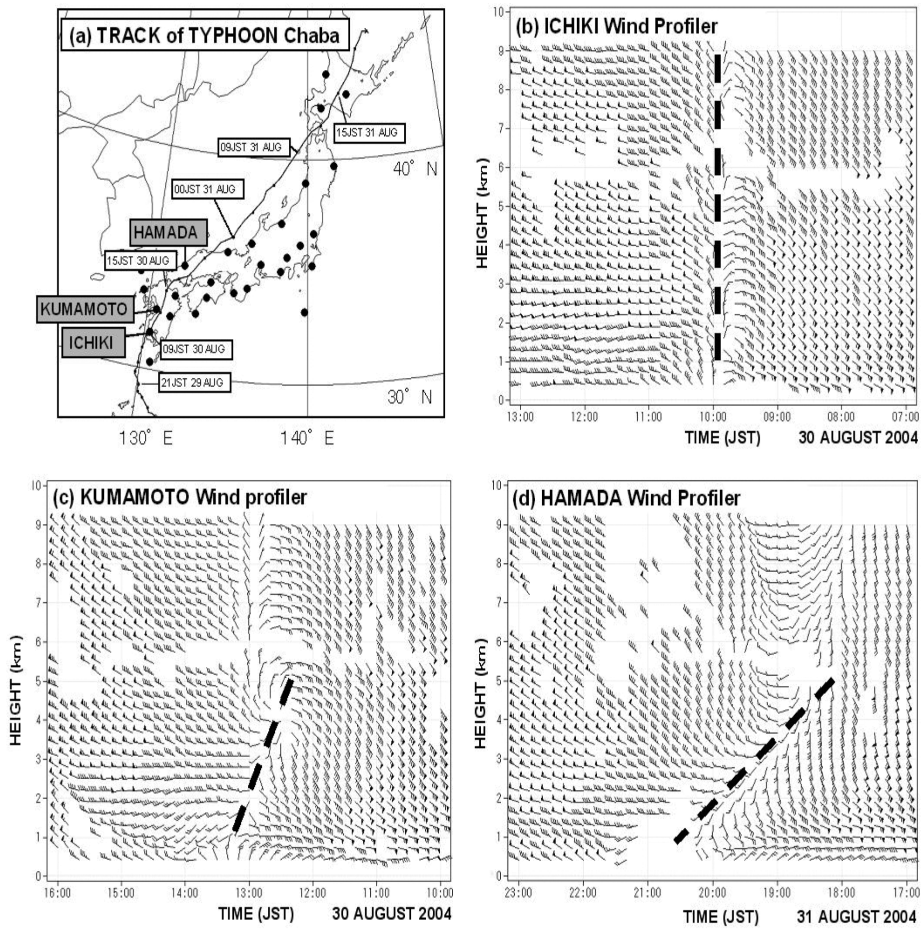

Fig. The track of the 16th Typhoon in 2004 (Chaba) (a), and time-height cross section of winds obtained from wind profilers at (b) Ichiki (31.7N, 130.3E), (c) Kumamoto (32.8 N, 130.7 E) and (d) Hamada (34.9N, 132.1N).

3) Disdrometer

Disdrometer
Advanced observation equipment that recognizes individual steel importers and observes the size and shape of steel importers.

Observation type:
Impact (e.g., JWD)
Optical (e.g., **Parsivel**, **2DVD**)
Electromagnetic (e.g., POSS)

Observation strategy :
Observation of the number concentration, size, and fall velocity passing through the observation area formed by the optical sensor.

Drop Size Distribution (DSD) can be possible to analyze the microphysical features of raindrops.

Observation range:
Observation area : 54 cm^2 (Parsivel), 100 cm^2 (2DVD)

Temporal resolution : several seconds and minutes

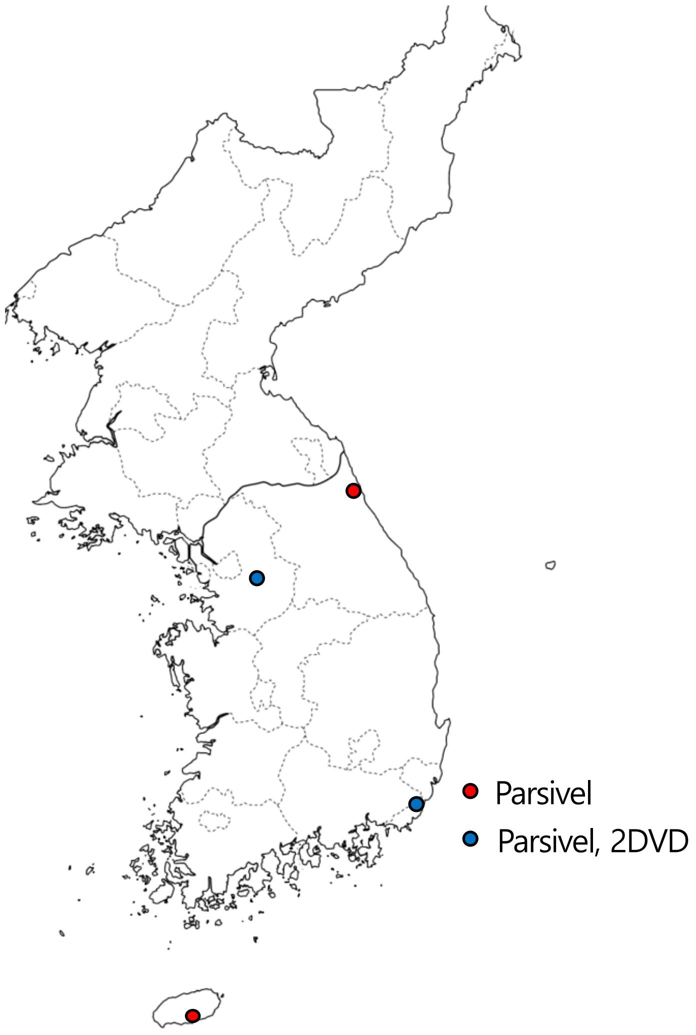

Fig. The location of Parsivel and 2DVD observation sites

3) Disdrometer - Parsivel

Parameters	Unit	Notes
$$V(D)_i = \frac{\sum_{i=1}^{32}\sum_{j=1}^{32} V_j C_{i,j}}{\sum_{i=1}^{32}\sum_{j=1}^{32} C_{i,j}}$$	m s-1	Calculated V(D) (Tokay et al., 2014)
$$V(D) = 9.65 - 10.3\exp[-0.6D]$$	m s-1	Reference line (Gunn and Kinger, 1949)
$$N(D)_i = \frac{1}{dt}\sum_{i=1}^{32}\sum_{j=1}^{32}\frac{C_{ij}}{V_j A_i dD_i}$$	mm-1 m-3	Calculated N(D)
$$A(D)_i = [180 \times (30 - 0.5D_i)] \times 10^{-6}$$	m2	Effective measuring area
$$R = 3.6 \times 10^{-3}\frac{6}{\pi}\int_0^{\infty} N(D)V(D)D^3 dD$$	mm h-1	Calculated R

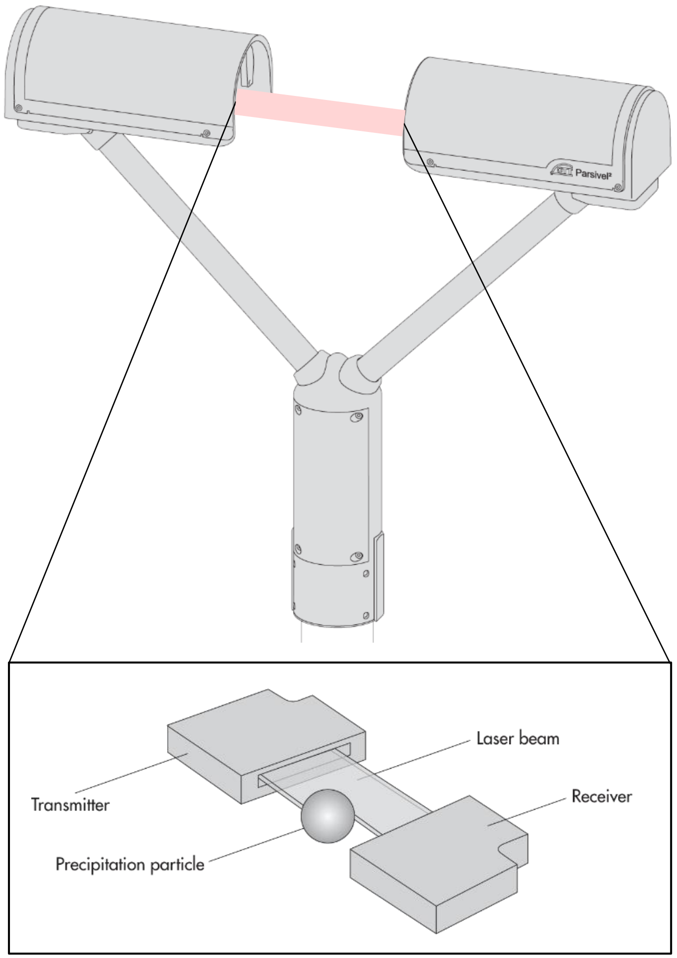

Fig. The diagram of the Parsivel

Drop-size distributions in thunderstorms measured by optical disdrometers during VORTEX2

Friedrich et al., 2013

Observation instruments :
Parsivel (Ver. 1) disdrometer
Doppler radar(CU01, CU02, DOW)

Research target :
Hurricane Ike (2008)

Purpose :
Tilting Experiment and Analysis for DSD Observation of Precise Typhoon Using Right Field.

Major results 1:
The number concentration distribution obtained by stationary observations was relatively high value more than D > 4 mm and it was also high value D < 2 mm.

This explains that the wind conditions must be considered when observing Typhoons accompanied by gusts.

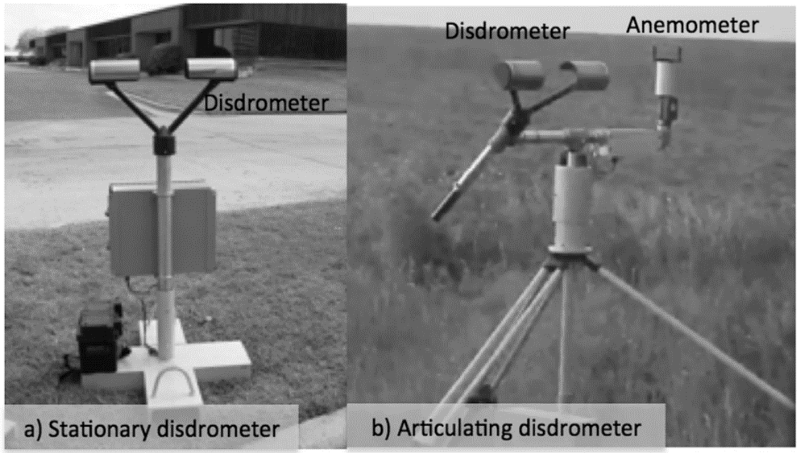

Fig.9. (a) Stationary and (b) articulating parabolic reflectometer taken during intensive observations VORTEX2 (2010).

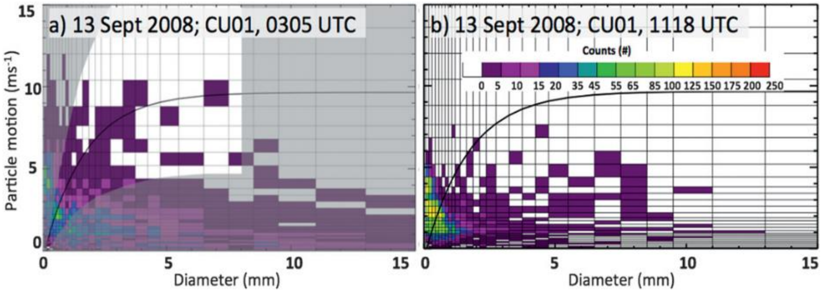

Fig. Terminal velocity distribution for hurricane Ike cases observed on September 13, 2008.

3) Disdrometer - Parsivel

Rainfall type classifications

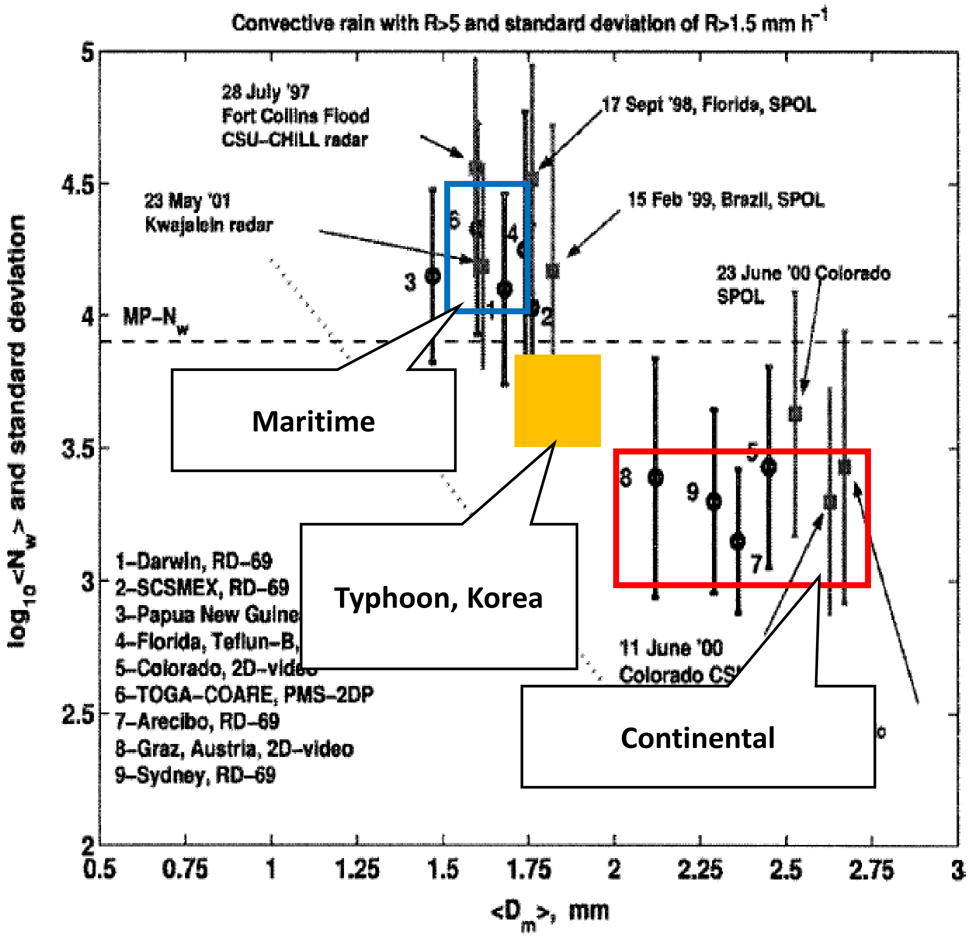

In typhoons cases, the average distributed at between the inland and ocean boundary.

$1.75<D_m<1.95$ / $3.5<LogN_w<3.8$

Representative areas of typhoon suitable for Korea ?

How about in Vietnam?

Chapter Ⅱ. IOP

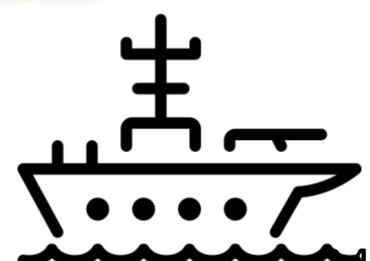

Intensive field campaigns by GEAR, PKNU, Korea

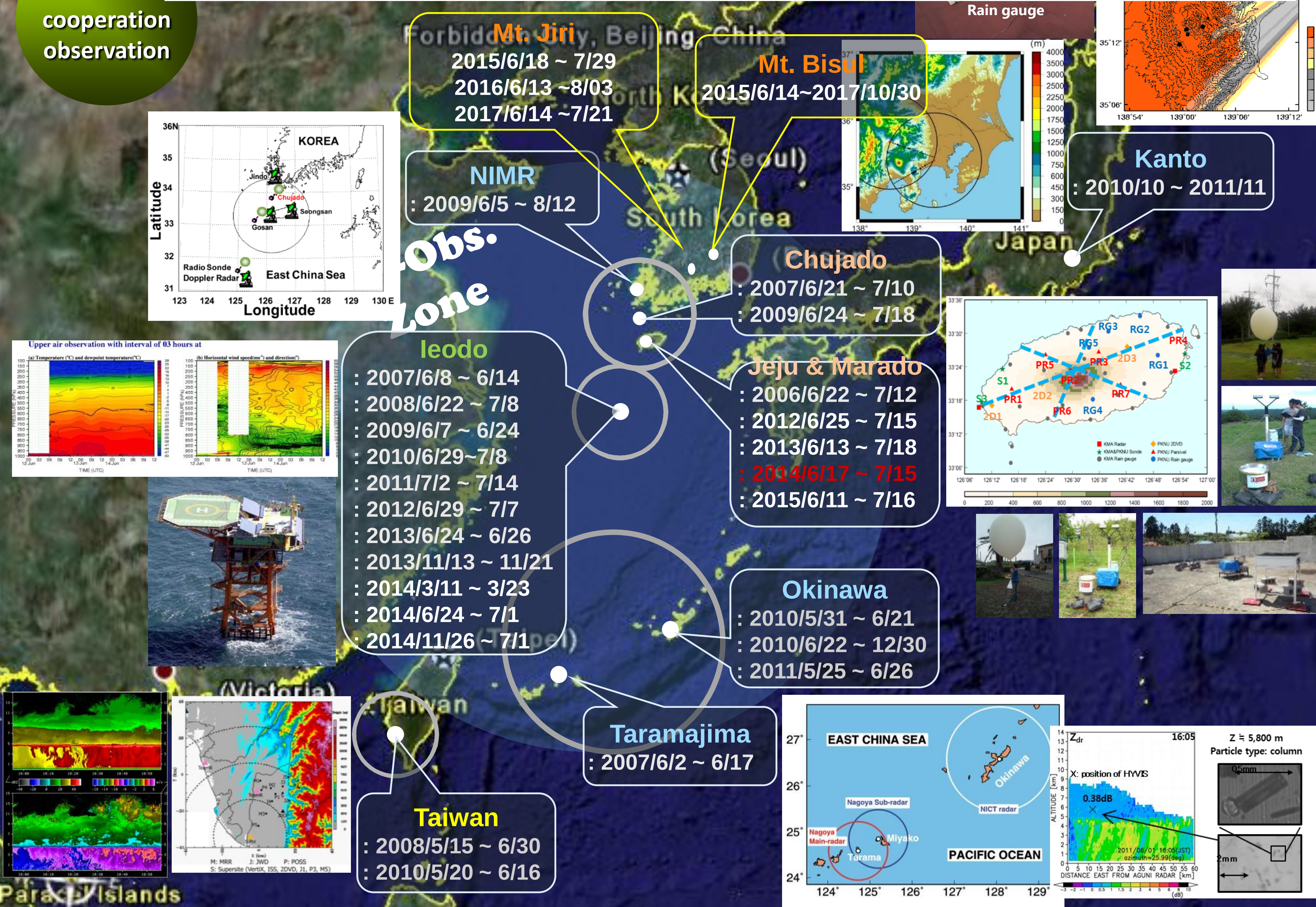

1. TY observation in Jeju
Neoguri(2014)

Observation map & instruments

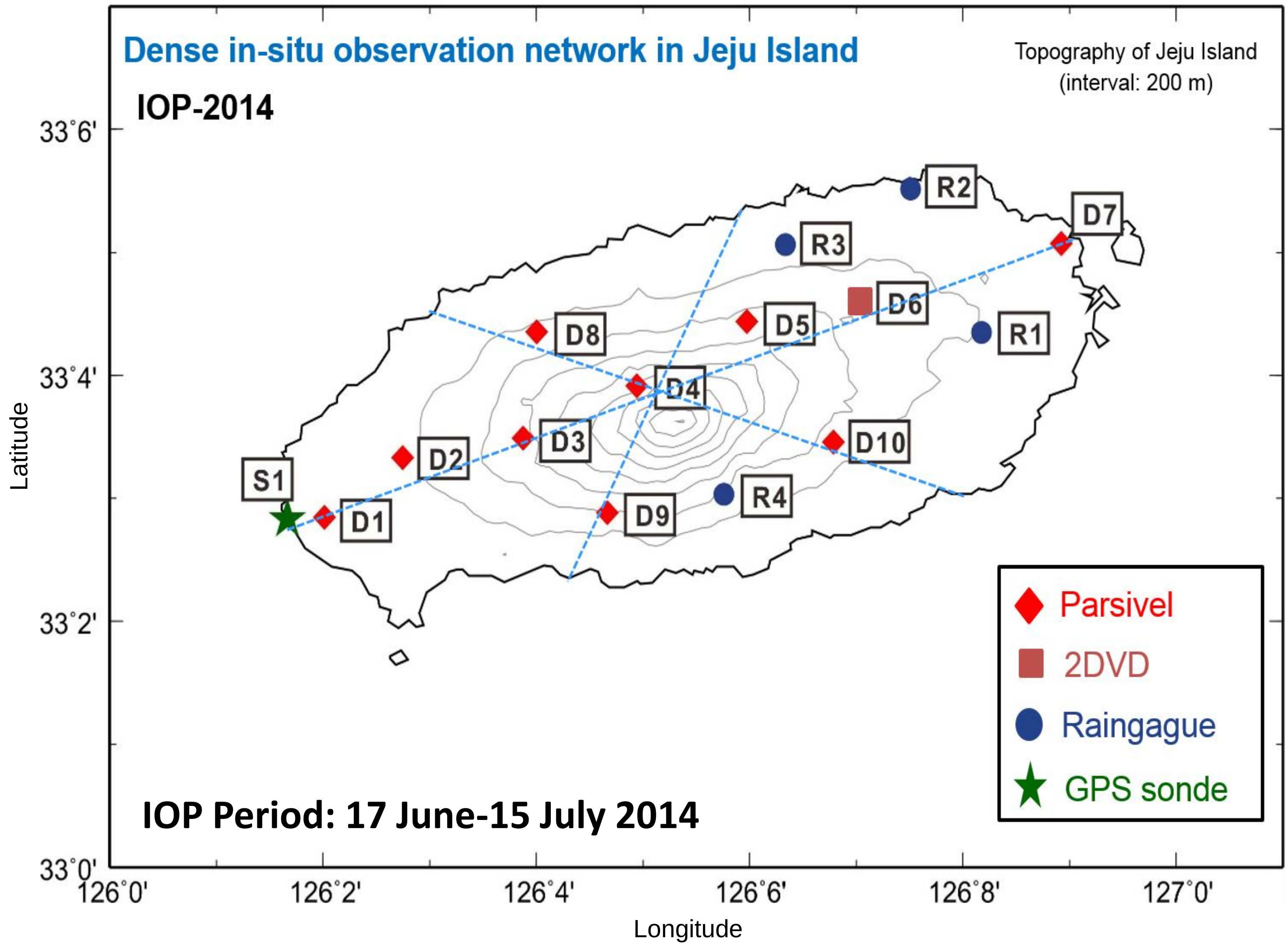

Observation instruments


2DVD - 1


Parsivel - 9

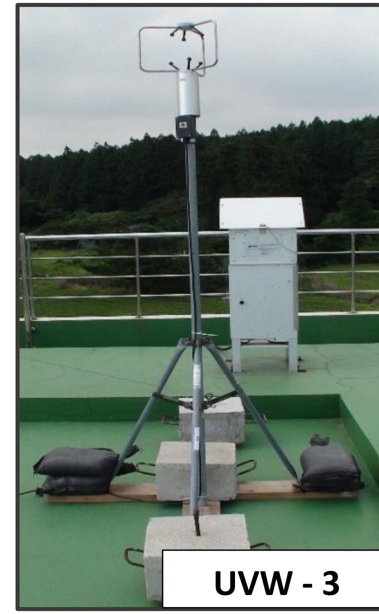
UVW - 3


Rain gauge - 14

LPC - 1


Sonde - 1


AWS - 1

Typhoon Neoguri, 2014

Synoptic Environment

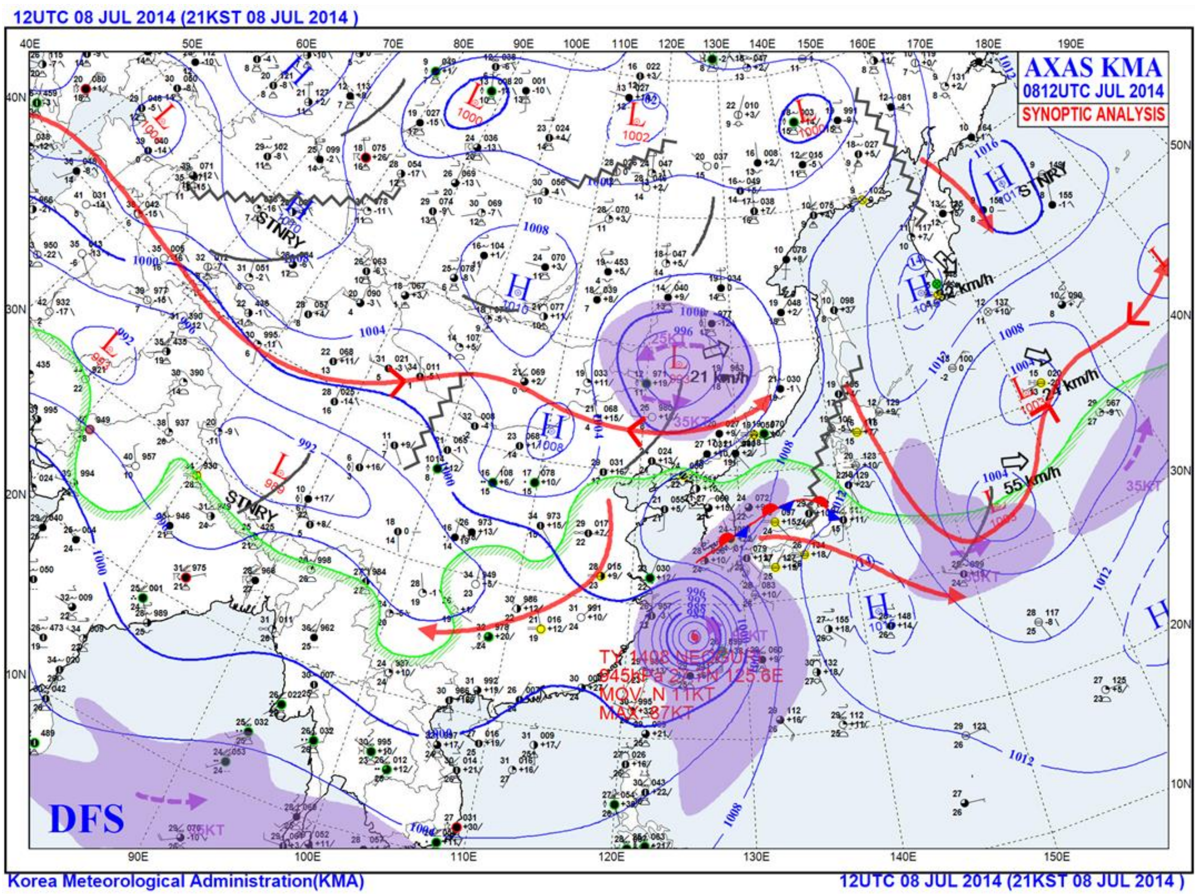

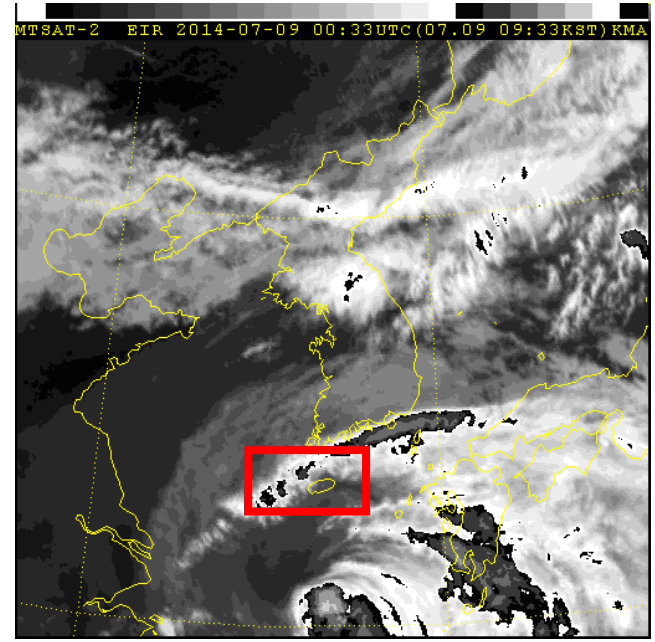

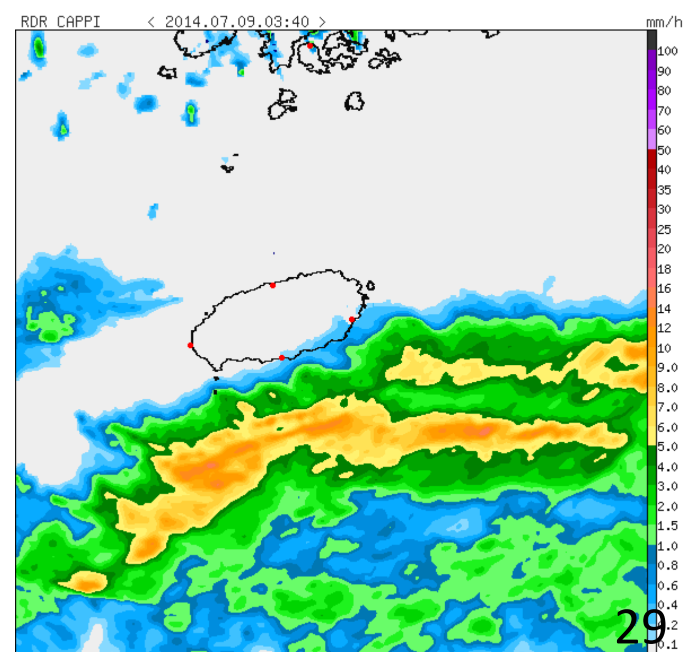

Typhoon Neoguri, 2014

Typhoon Neoguri

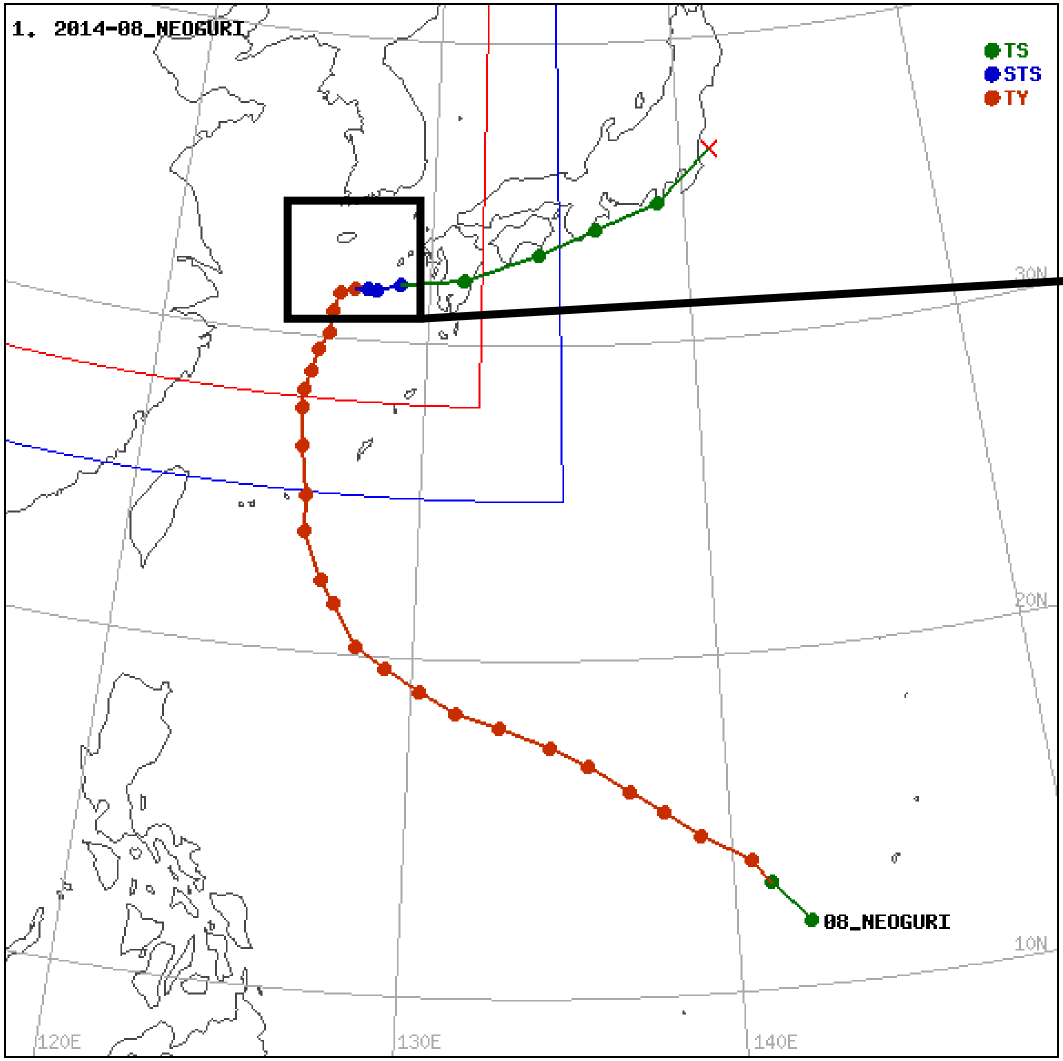

- Formed: 2 July 2014
- Dissipated: 13 July 2014

Parameter	201407090600
Eye of typhoon(Lat.)	31.5
Eye of typhoon(Lon.)	126.6
Propagation	NNE
Moving speed (km/h)	23
Center pressure (hPa)	965.0
Max. wind speed (m/s)	38.0
Intensity	TY
Radius (km)	360.0

Typhoon Neoguri, 2014

Radar analysis

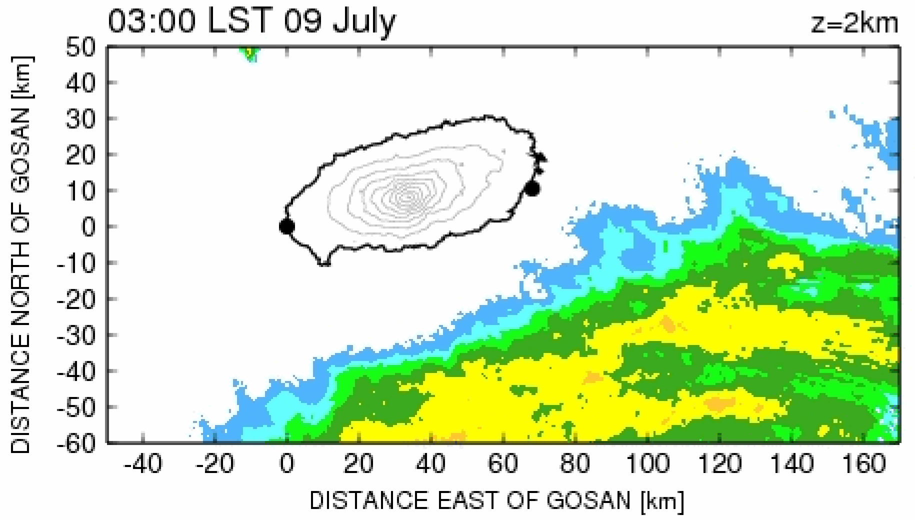

- Reflectivity distribution at 2 km ASL from 0300 to 0710 LST on 09 July 2014

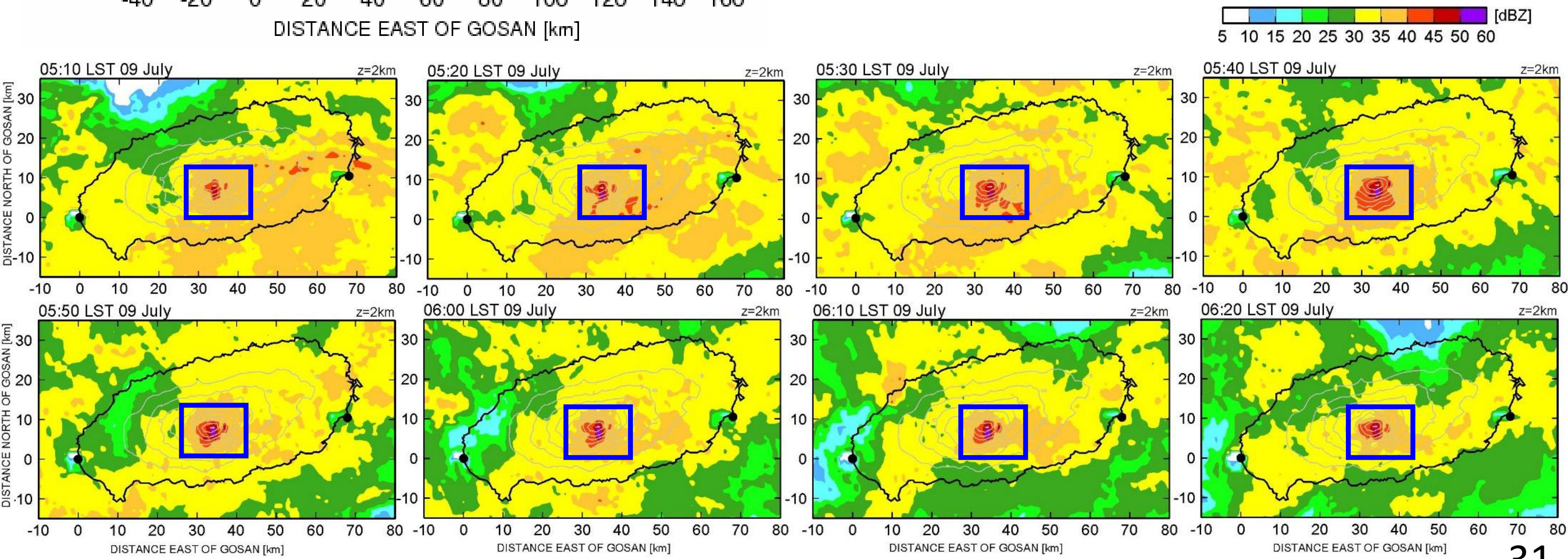

Typhoon Neoguri, 2014

Upper air Sounding

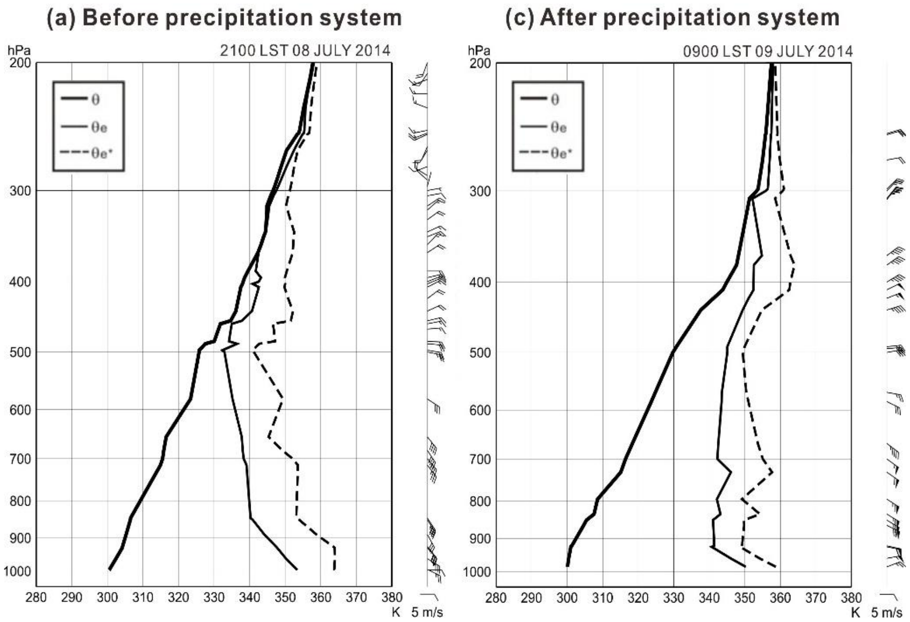

Parameter	20140708 2100 LST	20140709 0900 LST
LCL (hPa)	931	914.5
LFC (hPa)	829.2	840.9
CAPE (J/kg)	430.3	0.9
CIN (J/kg)	-68.2	-1.1
PW (mm)	58.8068	51.9516

Typhoon Neoguri, 2014

Total Vertical Wind Shear
; Strength of temperature gradient

$$\left|\frac{dV}{dz}\right| \equiv \sqrt{\left(\frac{du}{dz}\right) + \left(\frac{dv}{dz}\right)}$$

Directional Vertical Wind Shear
; Warm (or Cold) advection

$$\frac{dD}{dz} \equiv -\left(\overline{u}\frac{dv}{dz} - \overline{v}\frac{du}{dz}\right)$$

(Neiman, 2003)

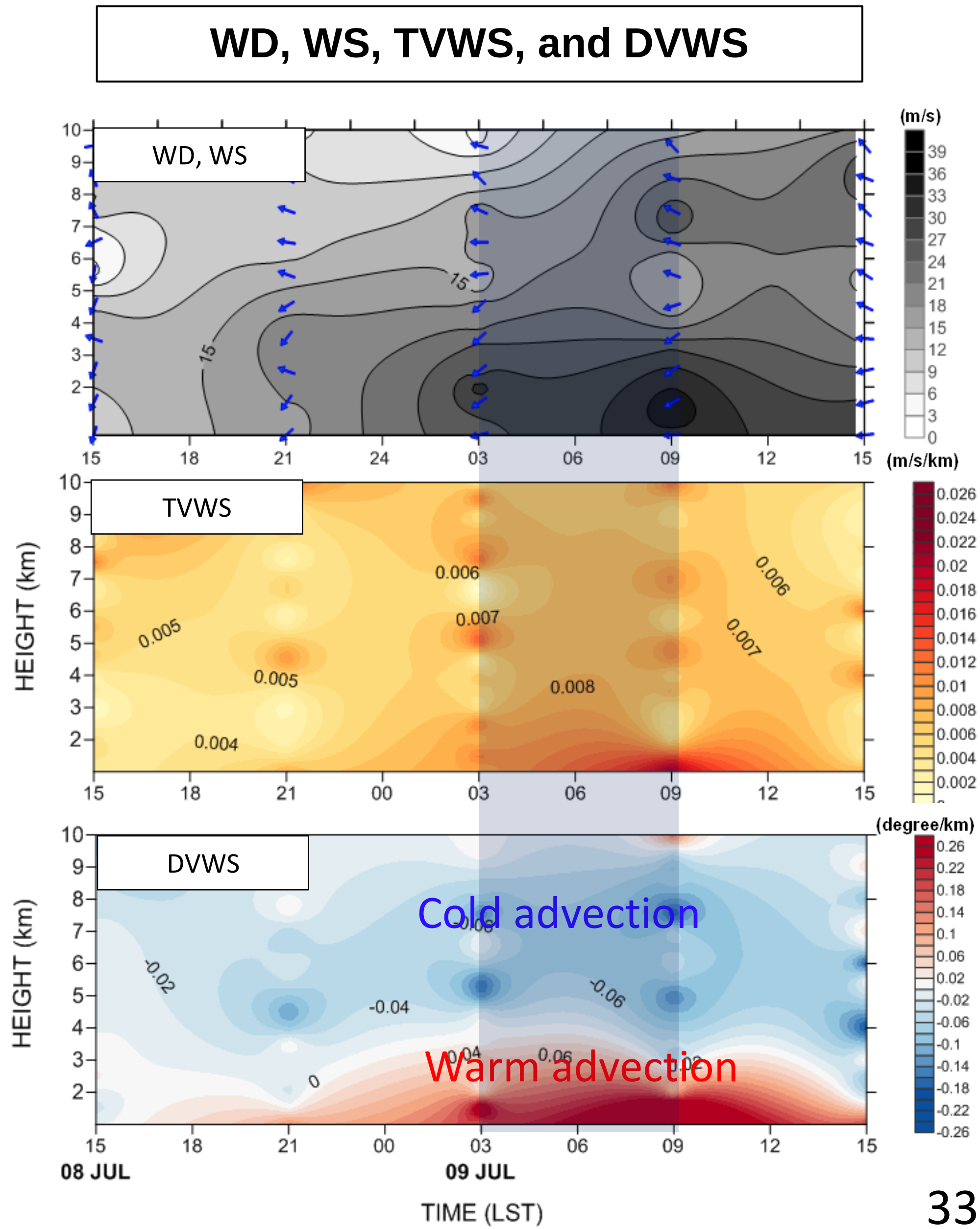

Typhoon Neoguri, 2014

Time series of sounding

Launching interval 6 hour

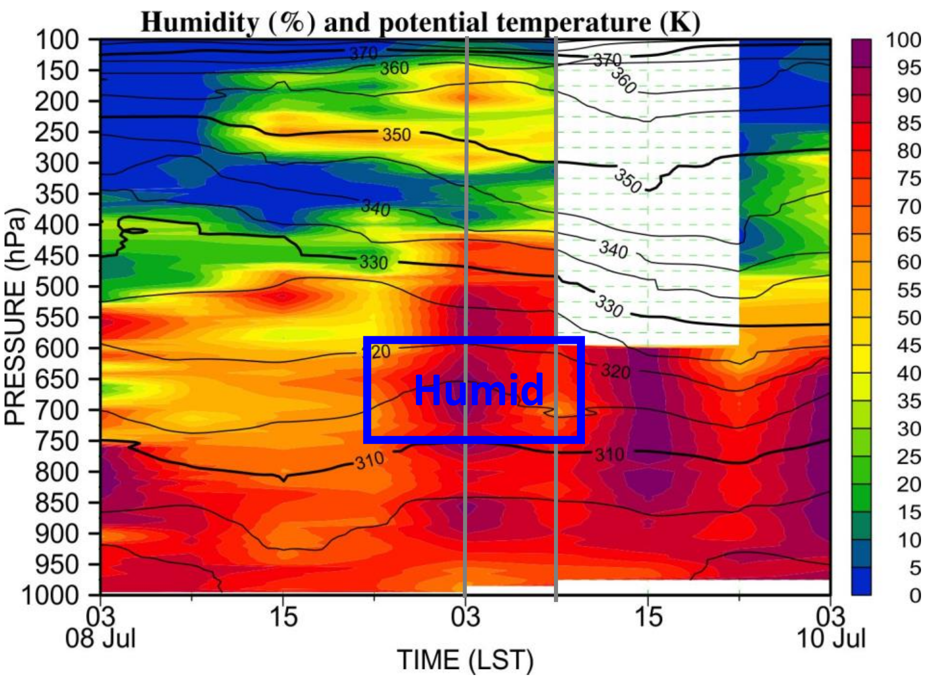

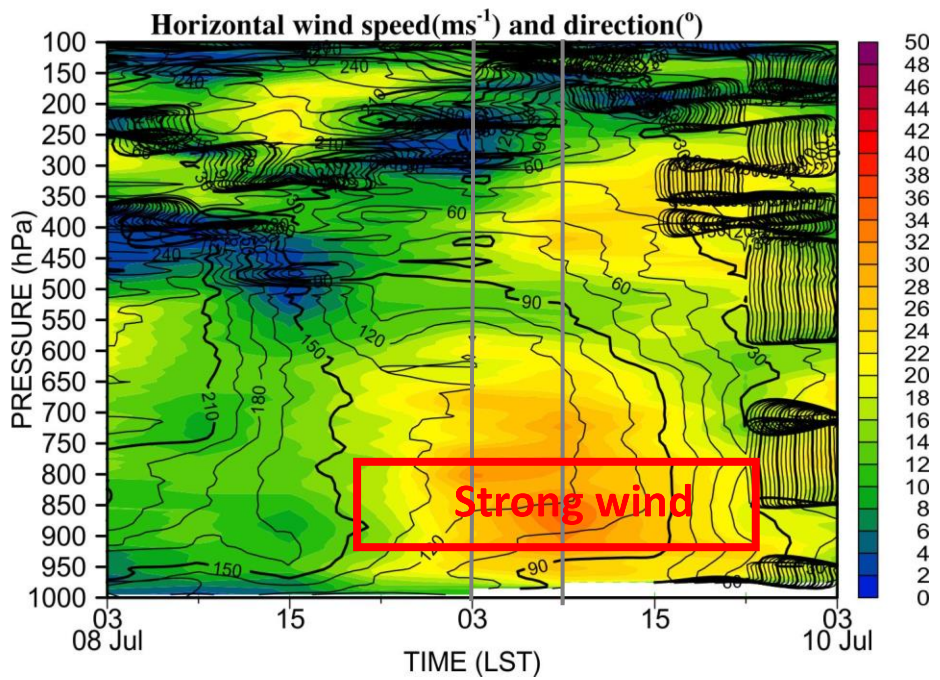

- Humid air condition (0300 LST, 1500 LST 09 Jul).
- Strong wind is represented at 950 hPa – 800 hPa (0900 LST 09 Jul).

Typhoon Neoguri, 2014

Retrieved horizontal wind (u-v) and reflectivity

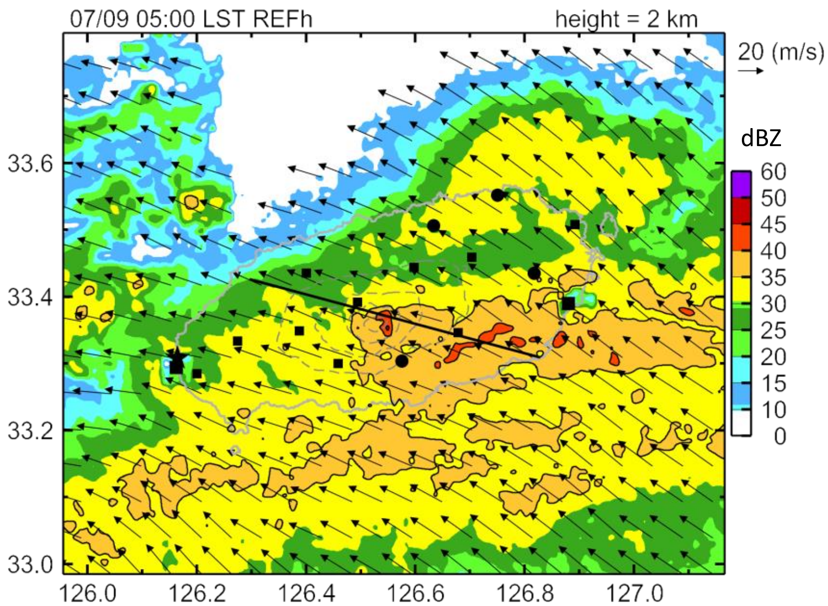

Convergence and reflectivity (35dbz↑) *(Liou et al., 2012)*

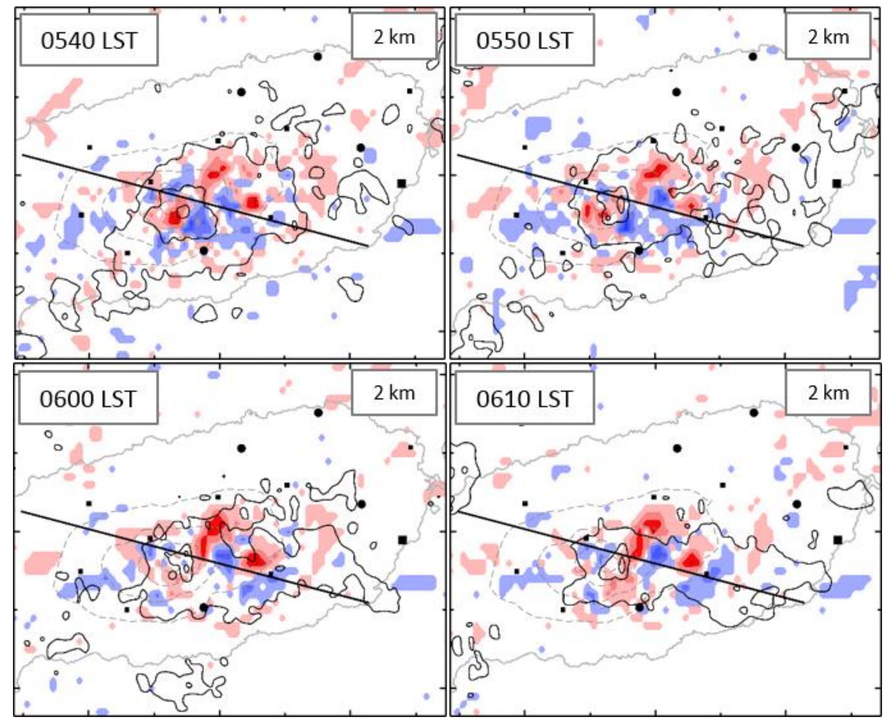

Convergence and reflectivity (cross section)

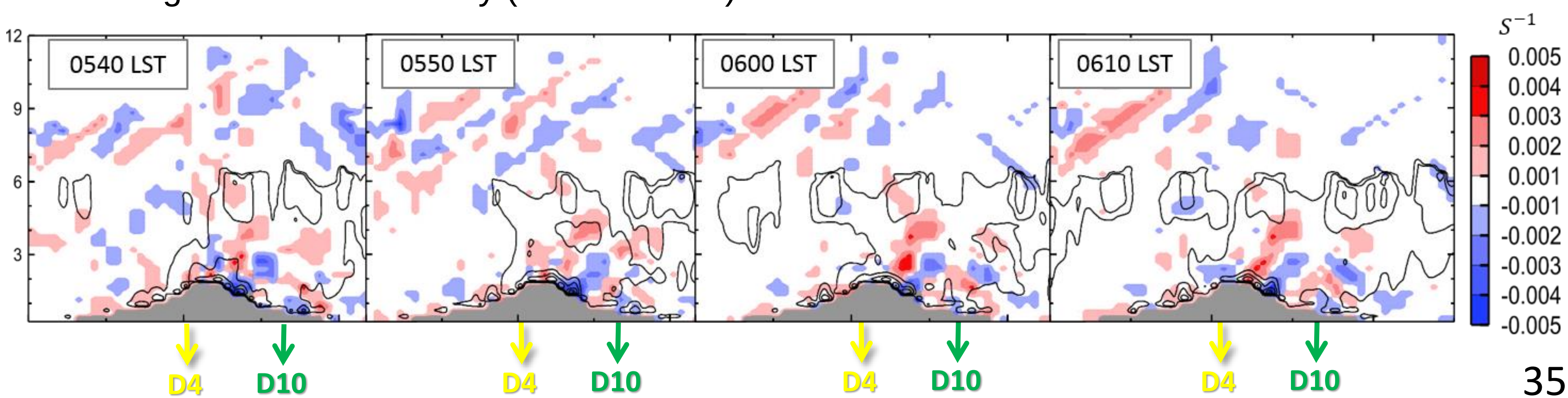

Typhoon Neoguri, 2014

Retrieved horizontal wind (u-v) and reflectivity

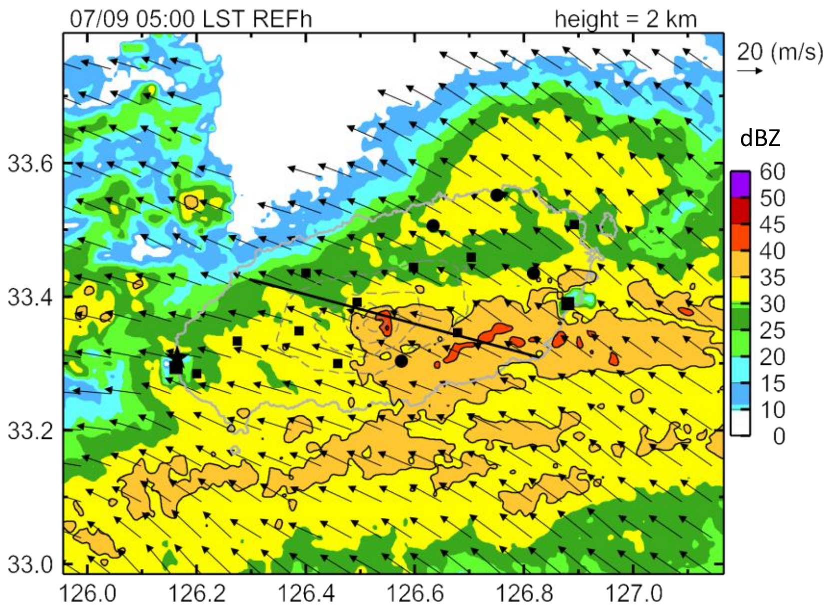

W and reflectivity (35dbz↑)

(Liou et al., 2012)

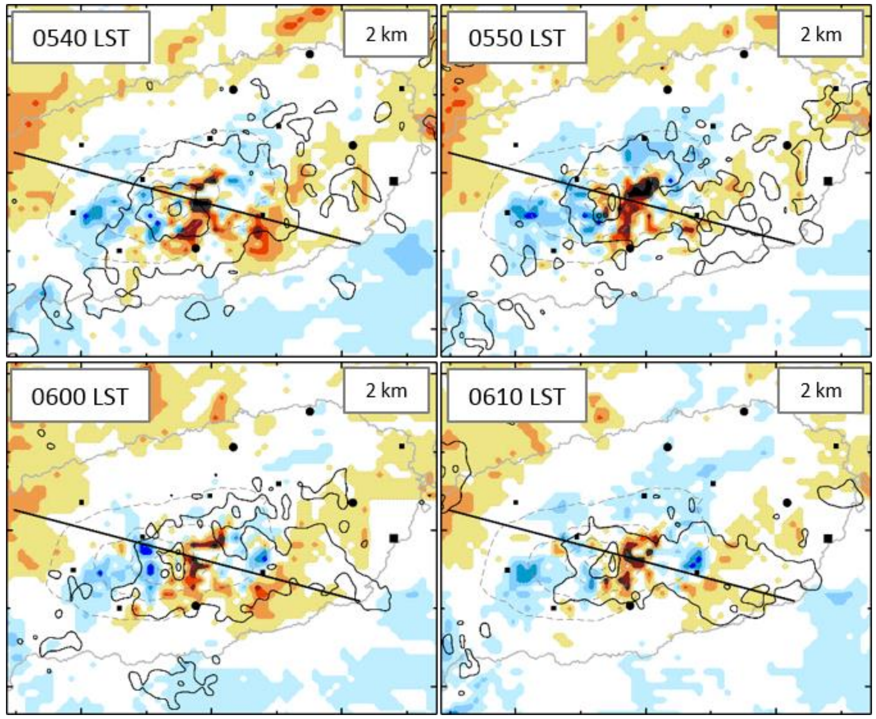

W and reflectivity (cross section)

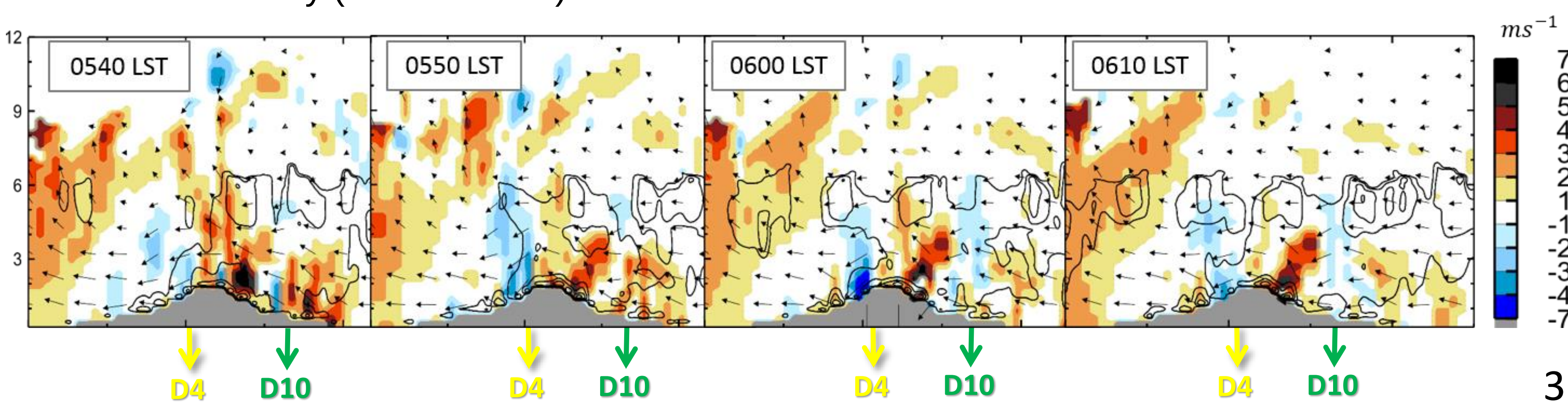

Typhoon Neoguri, 2014

Surface weather condition_disdrometer

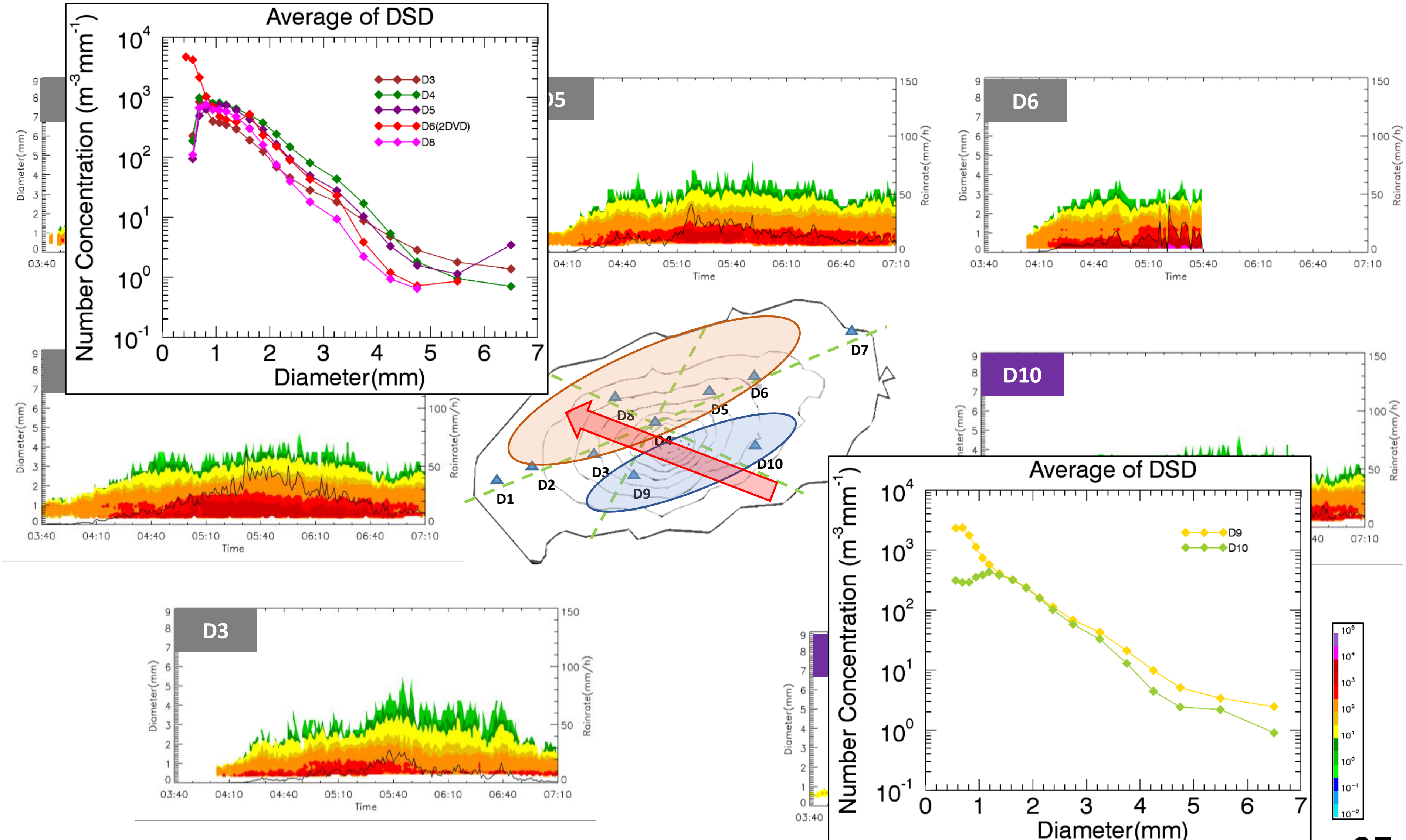

Typhoon Neoguri, 2014

Parsivel analysis

Analysis of DSD parameter and contribution r

Parameter	Equation
Liquid water content	$w = 10^{-9}\rho_w \frac{\pi}{6}\sum N(D)D^3dD$ $\rho_w = 10^6\ {}^{g}/_{m^3}$ for rain
Intercept parameter	$N_0 = \frac{\Lambda^{(\mu+4)}m_3}{\Gamma(\mu+4)}$

Parameter	Equation
Median Volume Diameter	$\int_0^{D_0} D^3N(D)dD = \frac{1}{2}\int_0^{D_{max}} D^3N(D)dD$
Rain Rate	$R = \int_0^{D_{max}} v(D)D^3N(D)dD$

Parameter	Equation
Shape	$\mu = \frac{(8-11m)-(m^2+8m)^{1/2}}{2(m-1)}$
Slope	$\Lambda = \frac{m_3}{m_4}(\mu+4)$

(Kozu, and Nakamura, 1991; Chu et al., 2008; Yuter et et al, 2006)

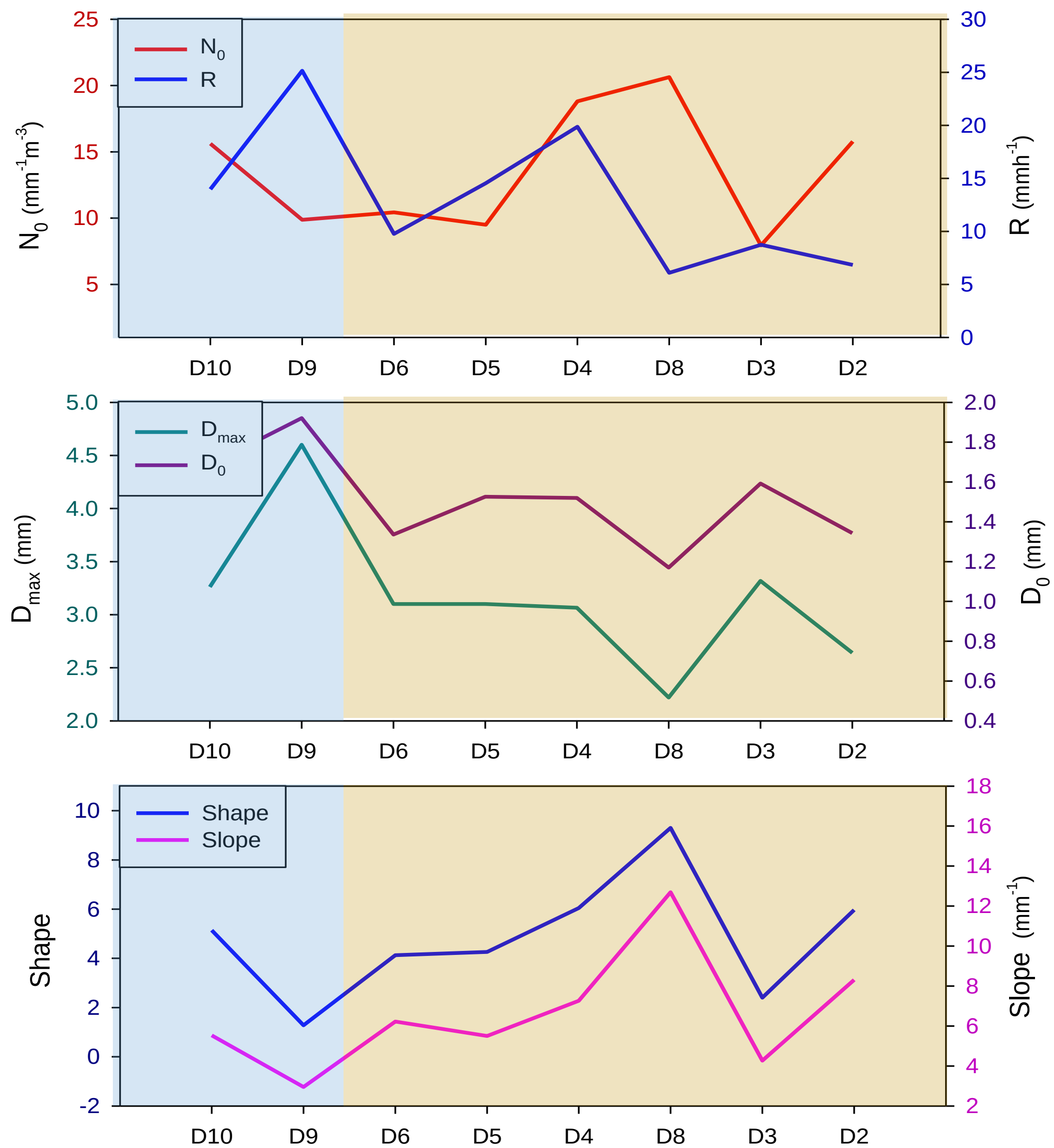

Typhoon Neoguri, 2014

Parameters	Front side	Lee side (Except for D2, D7, D8)
Atmospheric Condition		
$W(ms^{-1})$	0.897	0.280
R(mmh^{-1})	19.554	13.225
DSD Parameters		
$Log(N_0)(mm^{-1-\mu}m^{-3})$	4.483	5.263
$D_0(mm)$	1.804	1.518
$D_{max}(mm)$	3.931	3.156
μ	3.212	4.309
$\Lambda(mm^{-1})$	4.244	.5.818

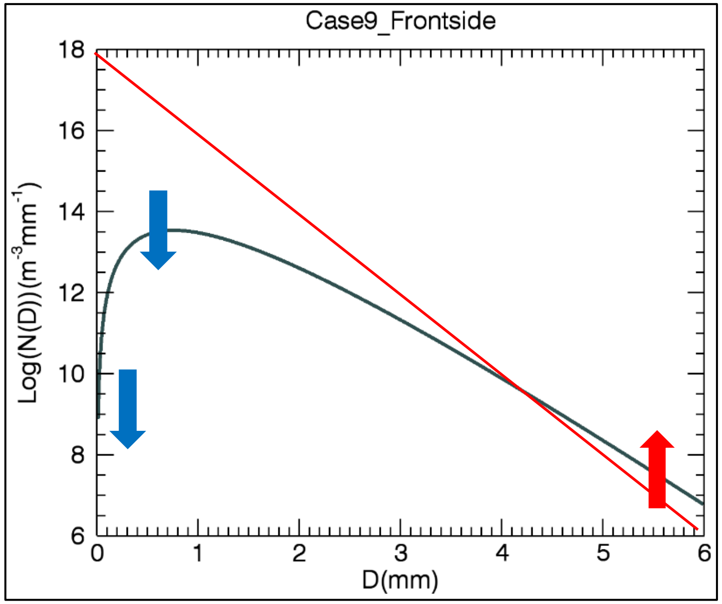

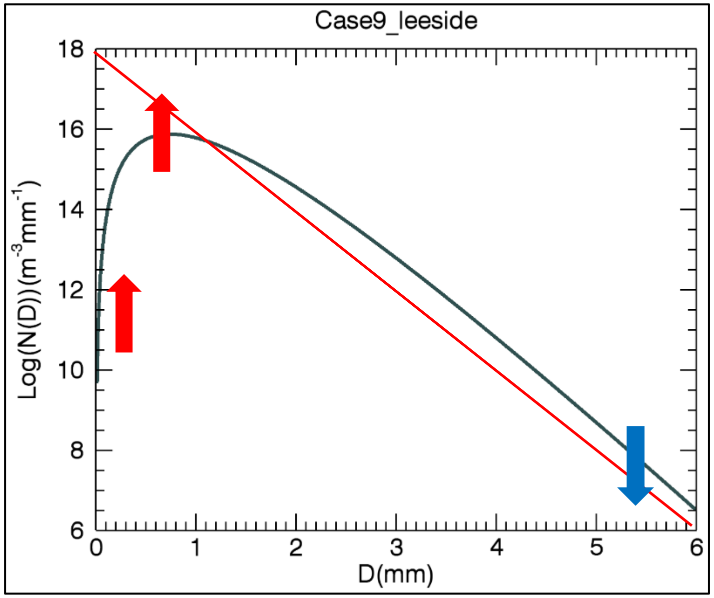

Typhoon Neoguri, 2014

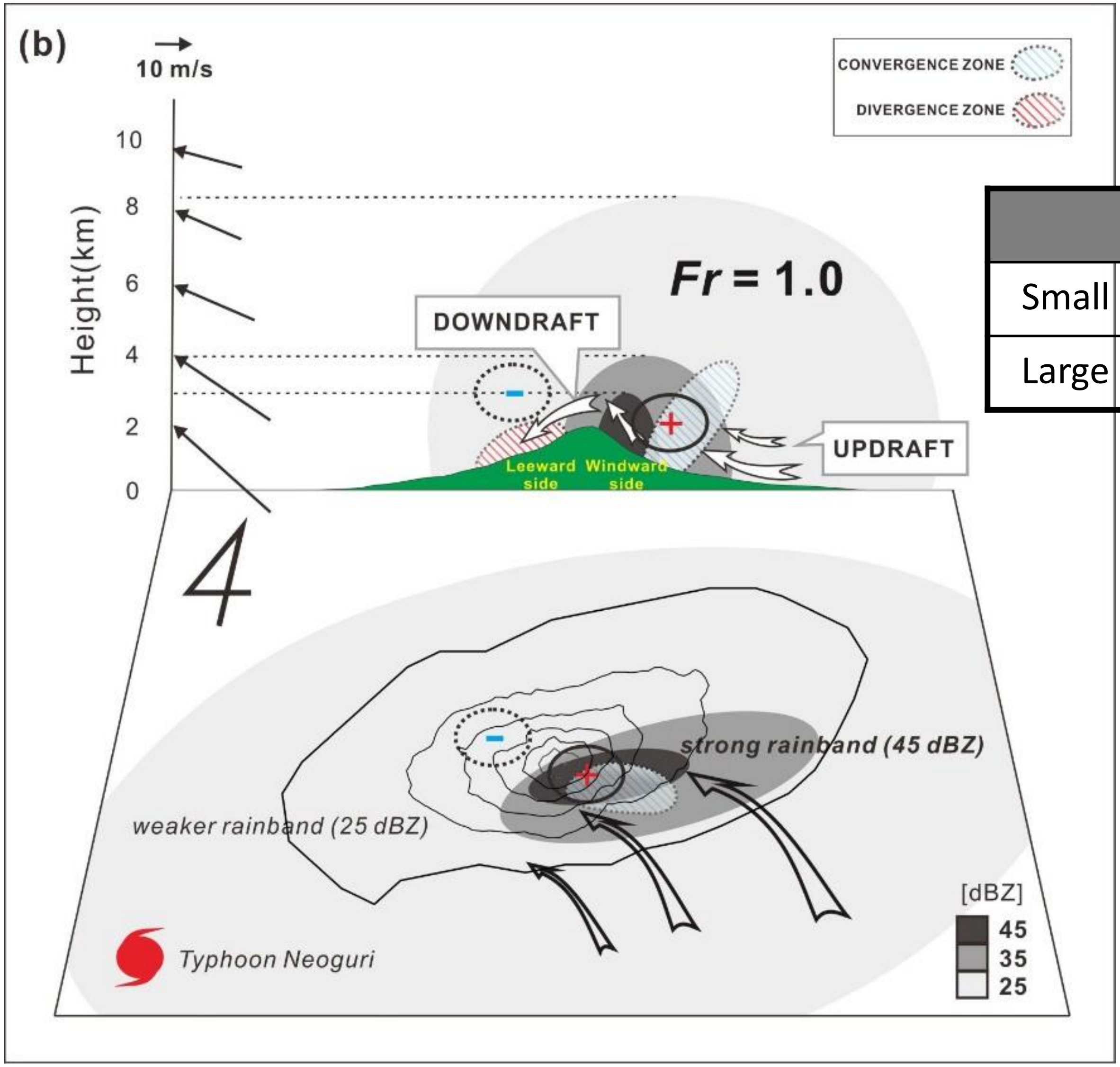

	Windward side	Lee side
Small Drop	↓	↑
Large Drop	↑	↓

2. TY observation in Boseong Bolaven(2012)

Ground-based multi-meteorological observation instruments

1. Jindo(JNI), Gosan(GSN), Sungsan(SSP) S-band Doppler radar

- 240 km range volume scan observation
- **Variables:** Radar reflectivity (Z_H) and radial velocity (V_R)
- Resolution : 10 min, Bin : 250m, Ray : 1°

2. Wind profiler (1290-MHz), Boseong

- UHF Vertical orientation Doppler radar
- **Variables:** 3D wind components, SNR, Doppler vertical velocity, Spectral width
- Resolution : 1-10 min / 100m

3. Parsivel disdrometer (Ver. 1), Boseong

- Optical disdrometer
- **Variable:** Number concentration (N(D)) and terminal velocity (V_T)
- Resolution : 1 min / 54 cm^2

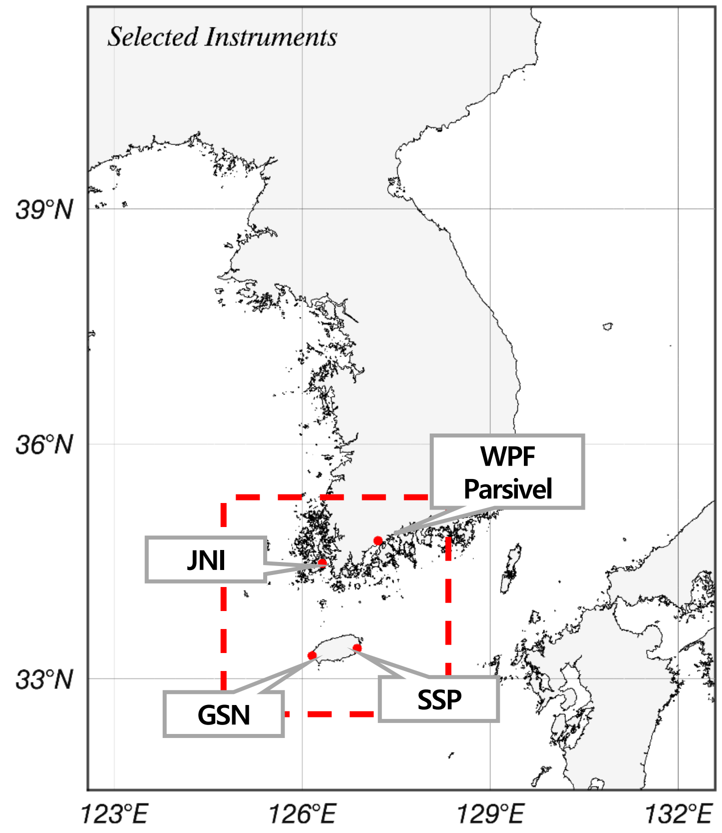

Radar 3km CAPPI Image

Bolaven (2012)

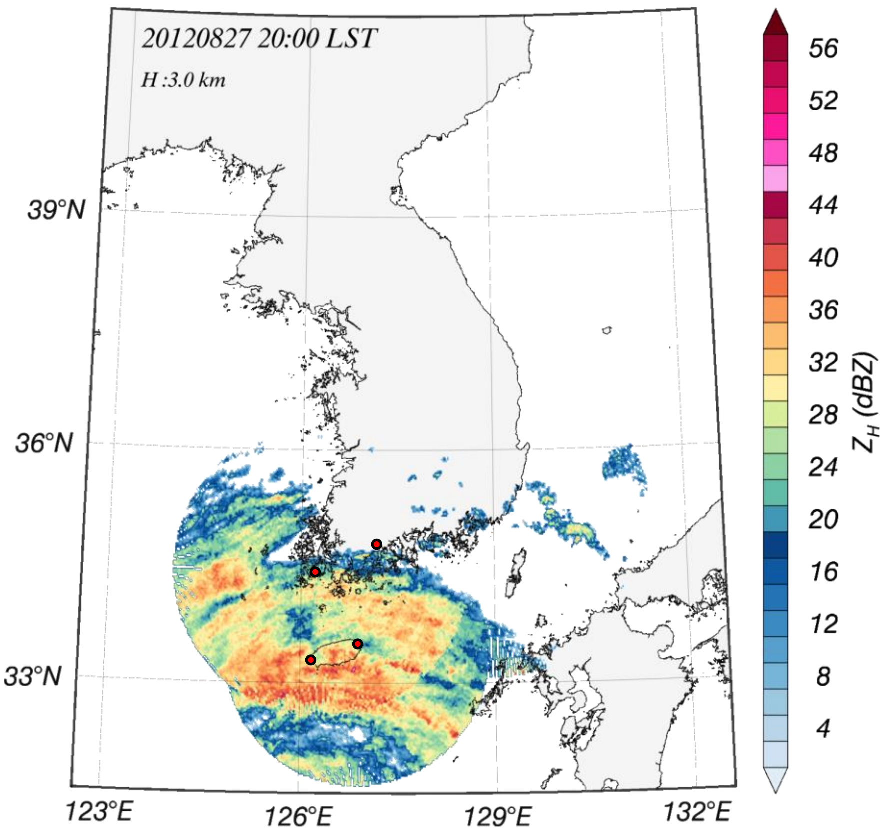

Nakri (2014)

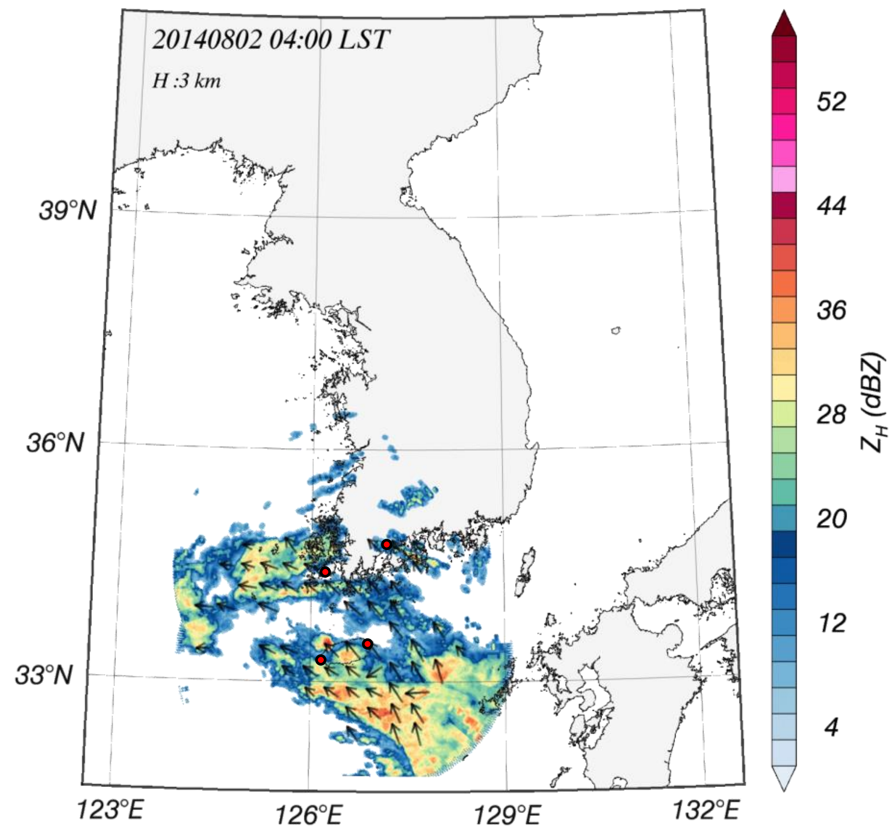

3.1. Rainfall type classifications - WPF

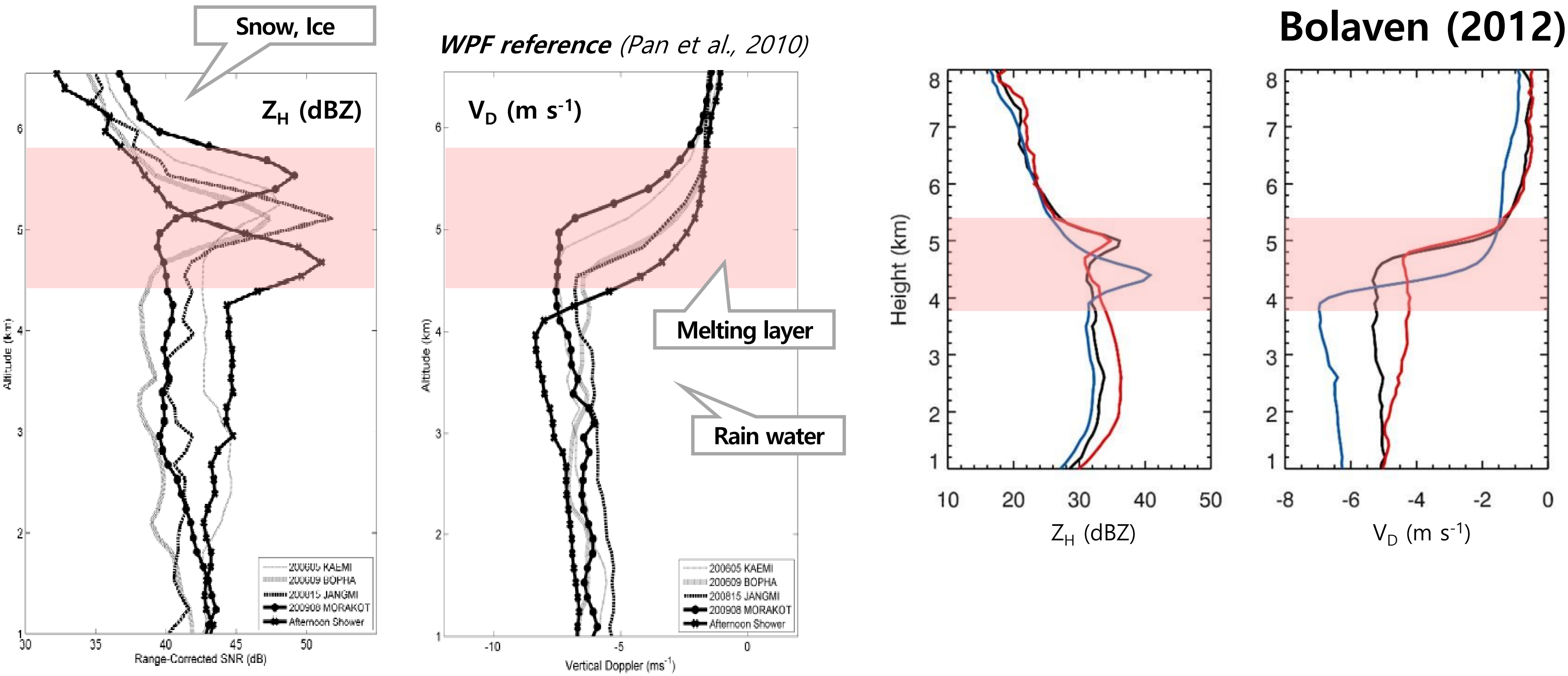

A phenomenon in which Z_H is increased sharply at the melting layer altitude
due to the difference in dielectric constant between ice (~0.197) and liquid water (~0.93).

Vertical Doppler velocity (V_D) is increased sharply around the melting layer altitude
due to the increase of the particle terminal velocity caused by the phase change.

1). Rainfall type classifications – Radar CFAD

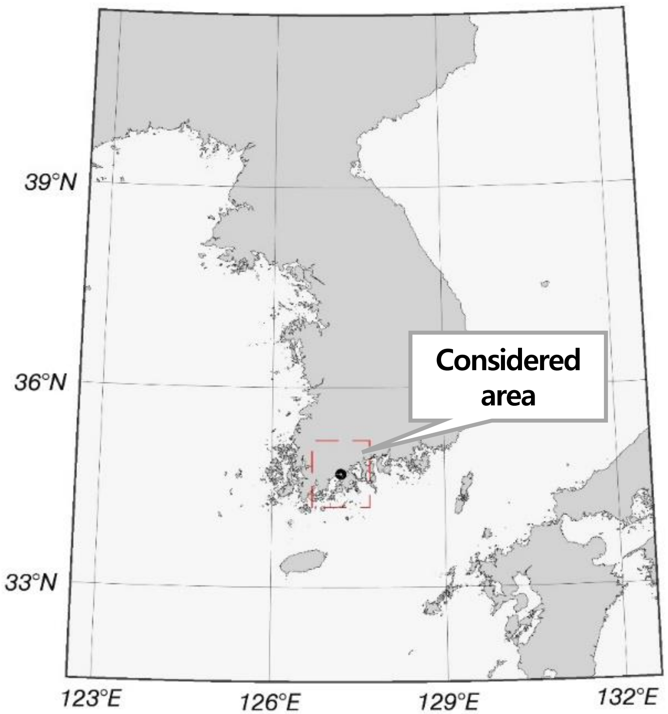

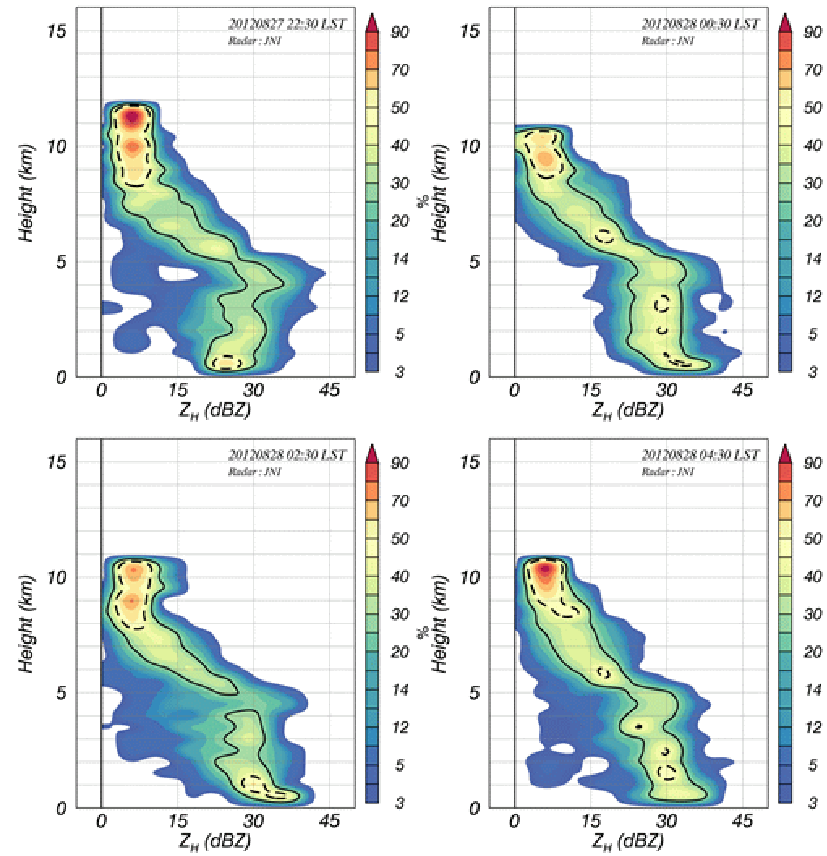

CFAD(Contoured Frequency Altitude Diagram) method was applied

The observation point as the center with the range of **±0.5°N, ±0.5°E** to consider the scale of rain band of Typhoon (~100 km).

2). Rainfall type classifications – Radar CFAD

Bolaven (2012)

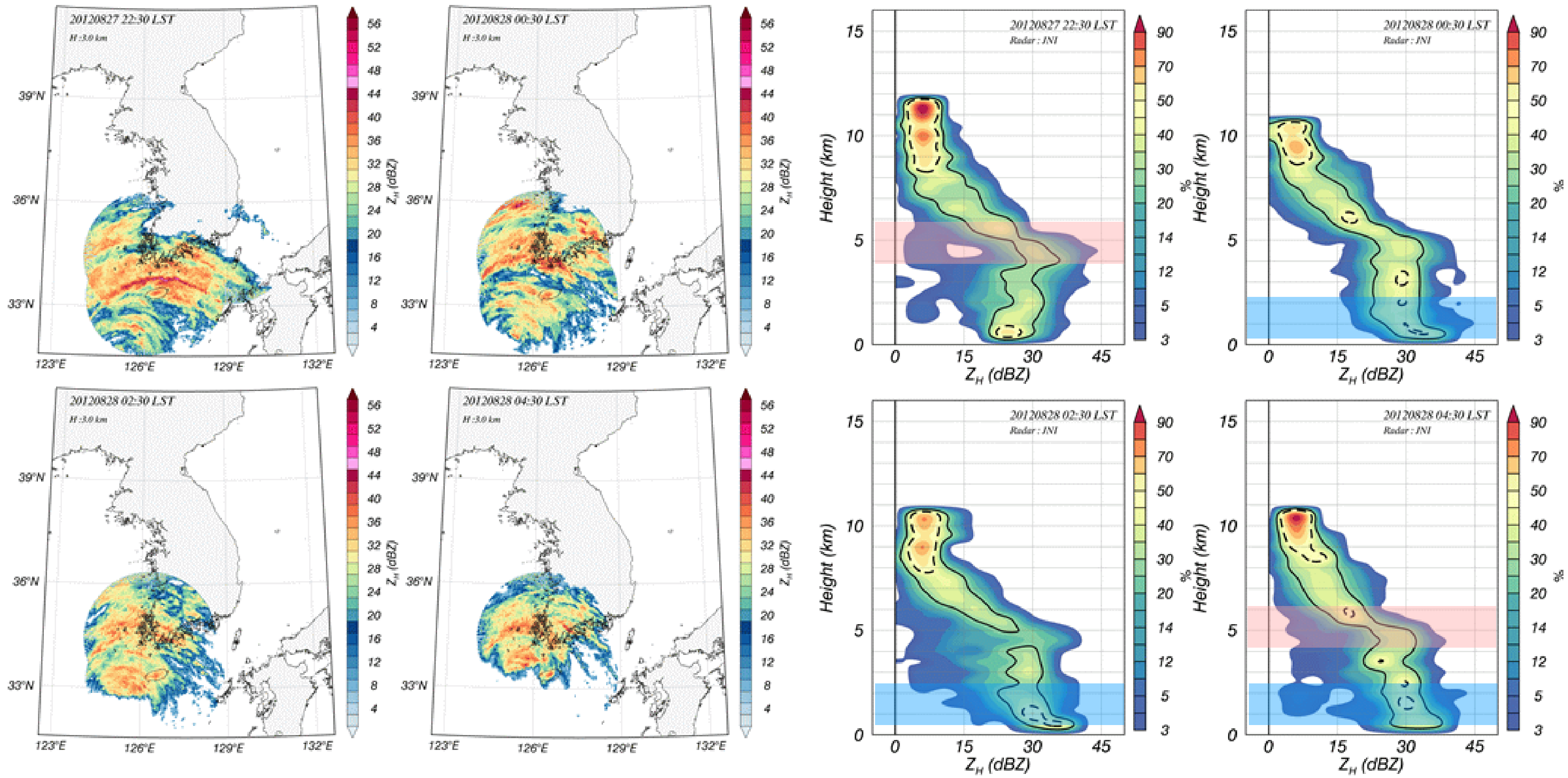

3). Precipitation Band Structure Analysis

Typhoon Bolaven Case – Analysis of radar reflectivity characteristics according to ground landing in typhoon precipitation band

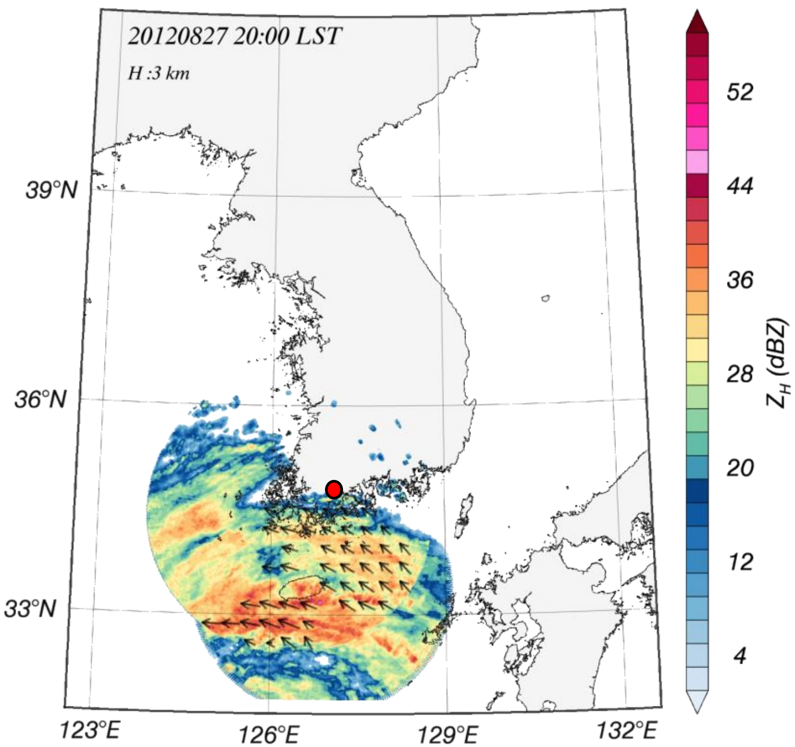

Radar CAPPI and dual wind field distribution at 3 km altitude

Time-Height analysis :

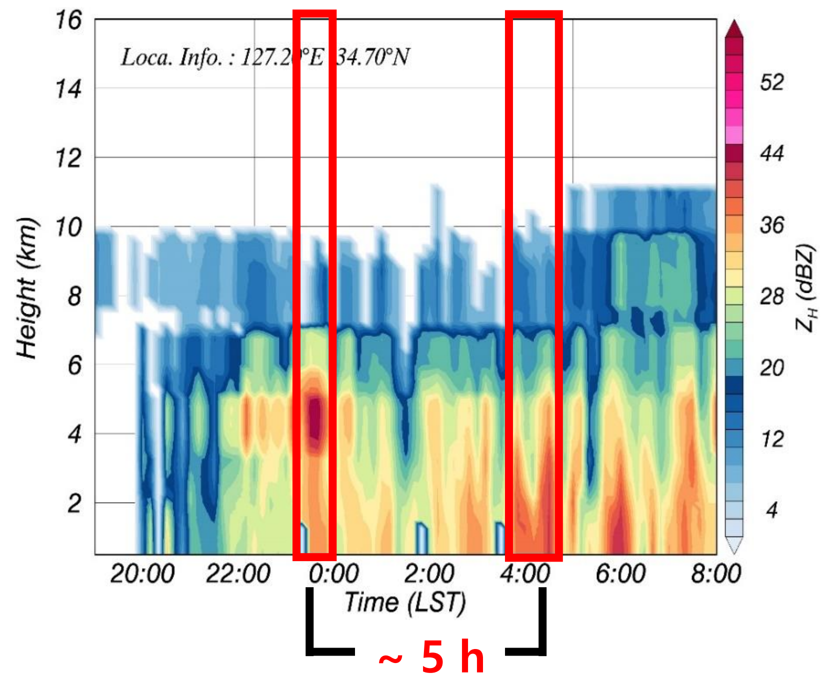

Time series of vertical radar reflectivity distribution for analysis time

4). Time-Height analysis

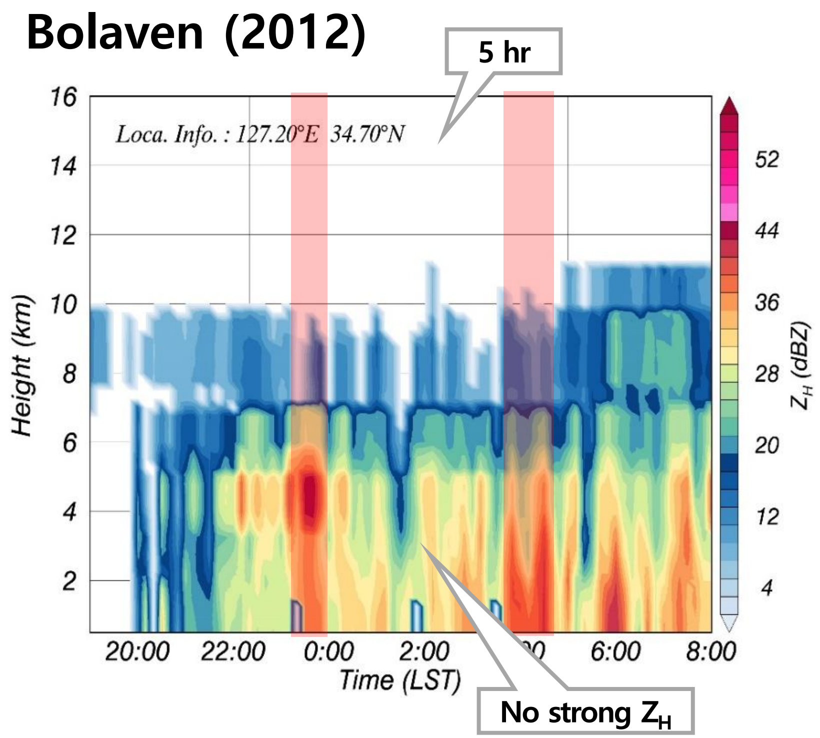

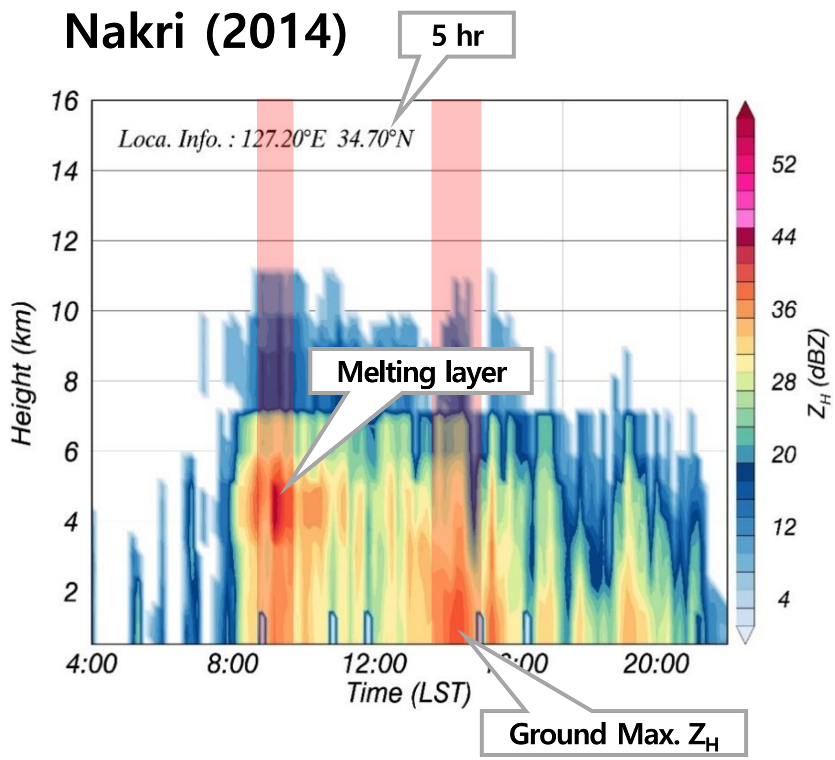

It could be confirmed from the two cases that the maximum rainfall intensity was observed after 5 hours from the observation time when the melting layer was detected regardless of the strength of the moving speed of Typhoon.

5). Procedure for Structure Analysis of TY Bolaven (Precipitation) using Radar and Wind Profiler

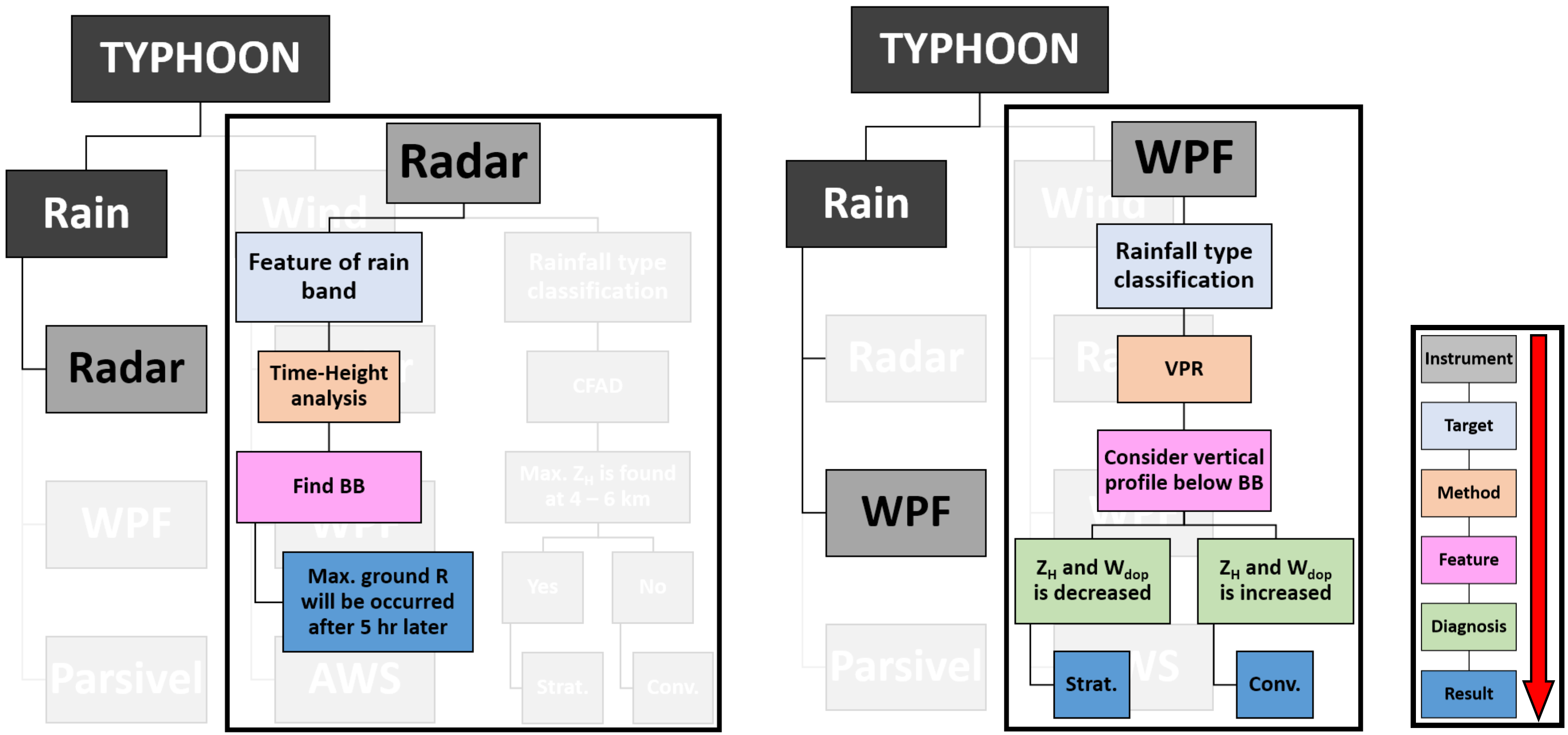

1). Microphysics of Typhoon rainband

DSD Model and basic parameters

Normalized gamma DSD :

(Testud et al., 2001)

Mass-weighted volume median diameter :

$$D_m = \frac{\int_0^{D_{max}} D^3 N(D) dD}{\int_0^{D_{max}} D^4 N(D) dD}$$

Normalized intercept parameter :

$$N_w = \frac{4^4}{\pi \rho_w}\left(\frac{W}{D_m^4}\right)$$

Gamma DSD :

(Ulbrich et al., 1989)

M246 triple moments :

$$\eta = \frac{M_4^2}{M_2 M_6}$$

Shape parameter :

$$\mu = \frac{(7-11\eta)-(\eta^2+14\eta+1)^{0.5}}{2(\eta-1)}$$

Slope parameter :

$$\Lambda = \left[\frac{M_2}{M_4}(\mu+3)(\mu+4)\right]^{0.5}$$

Basic parameters :

Terminal velocity for raindrop :

(Atlas et al., 1979)

$$v(D) = 9.65 - 10.3\exp(-0.6D)$$

Rainfall rate :

$$R = \frac{3.6}{10^3}\frac{\pi}{6}\int_0^{D_{max}} v(D) D^3 N(D) dD$$

Liquid water contents :

$$LWC = \frac{\pi}{6}\rho_w \int_0^{D_{max}} D^3 N(D) dD$$

2). Microphysics of Typhoon Rainband – DSD Variable Characteristics 1

Bolaven (2012)

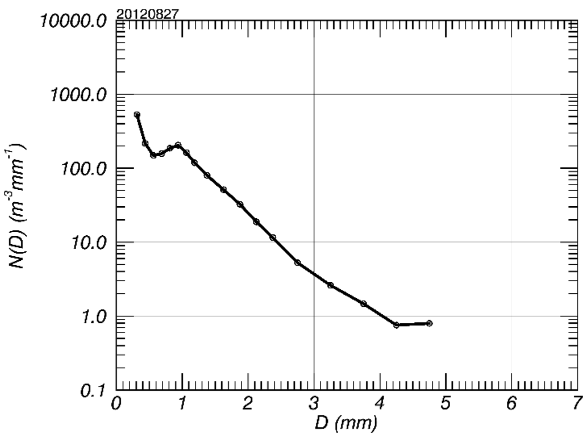

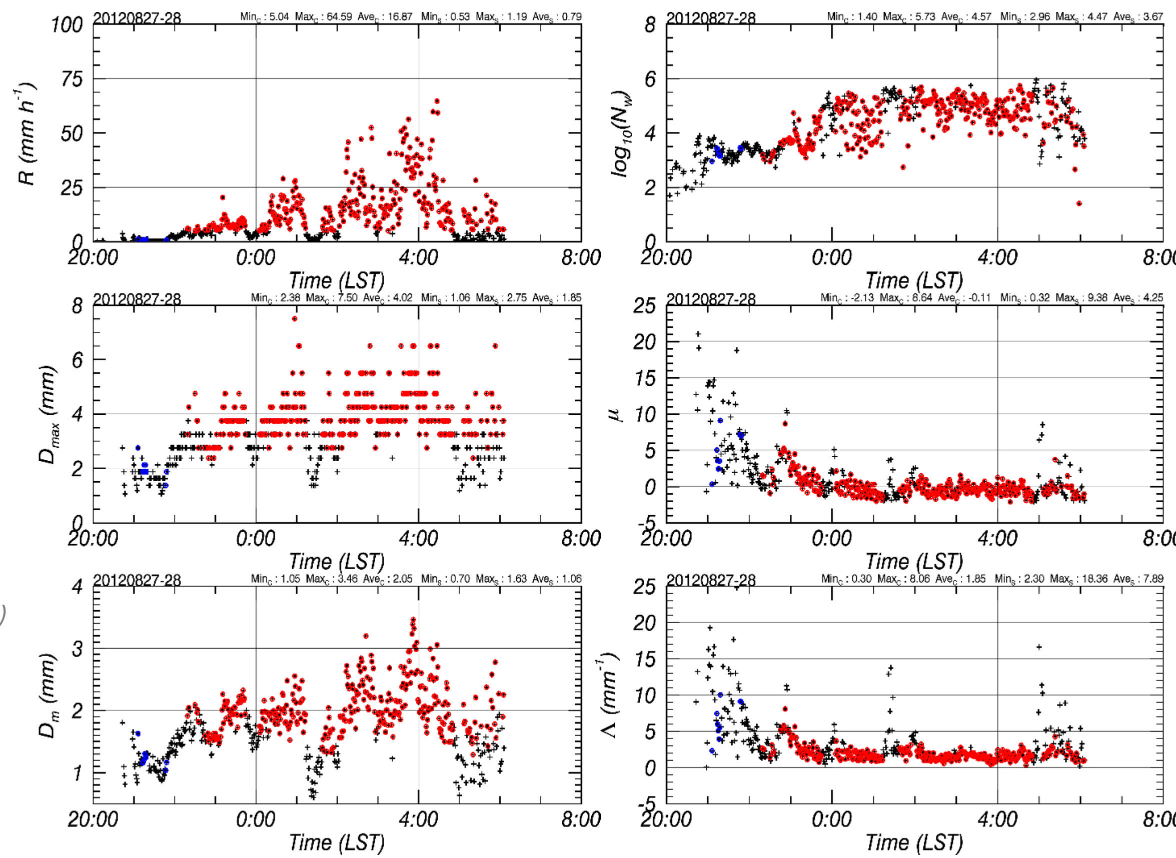

Rainfall type classification

(Bringi et al., 2003a)

Stratiform :

$R > 0.1\ mm\ h^{-1}$ and $\sigma_R < 1.5$

Convective :

$R > 5\ mm\ h^{-1}$ and $\sigma_R > 1.5$

3). Microphysics of Typhoon Rainband – DSD Variable Characteristics 2

Bolaven (2012)

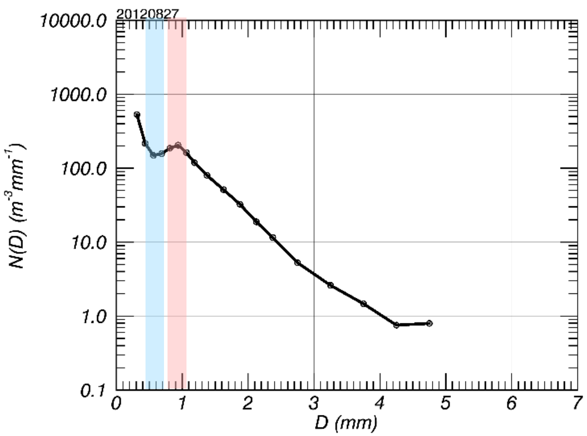

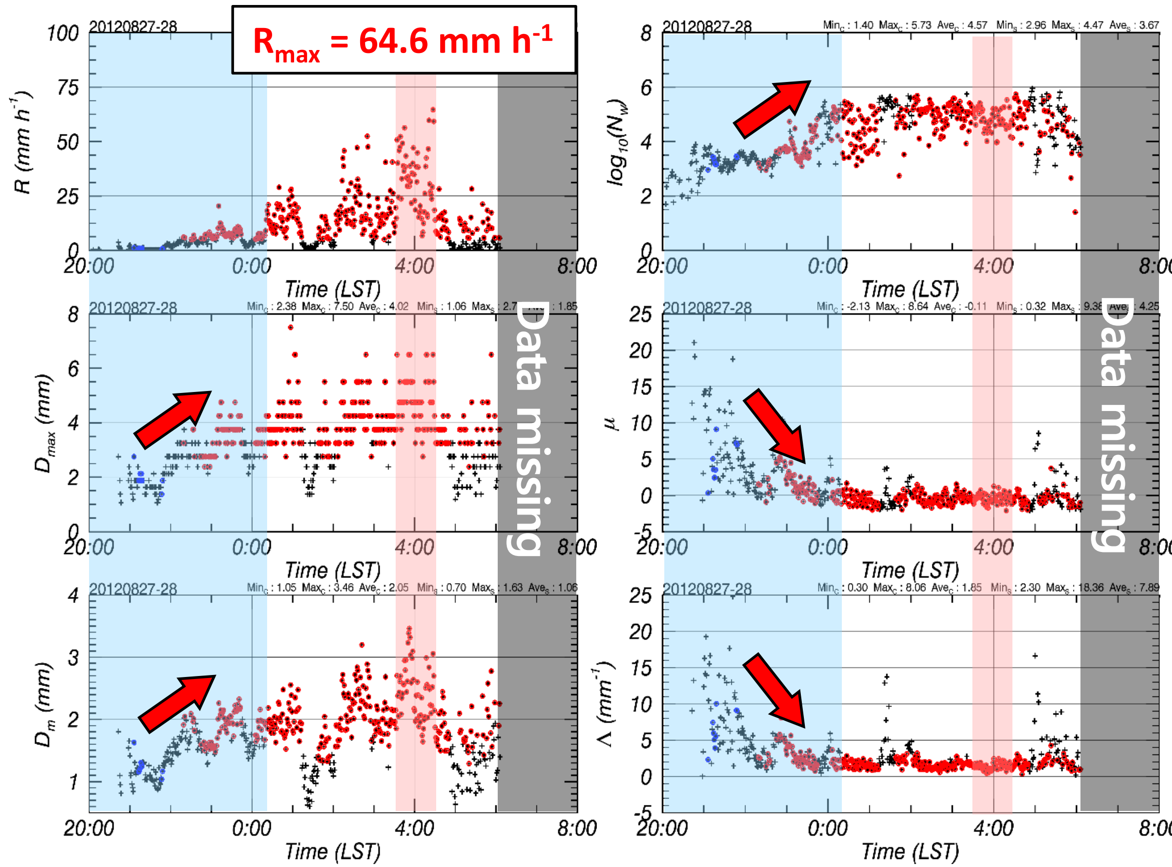

DSD	Approach	Landing	Decaying
D_m	Increased	Max	
N_w	Increased	Steady	?
μ	Decreased	Steady	
Λ	Decreased	Steady	

4). Procedure for Microphysics Analysis of TY Bolaven (Precipitation) using Parsivel Disdrometer

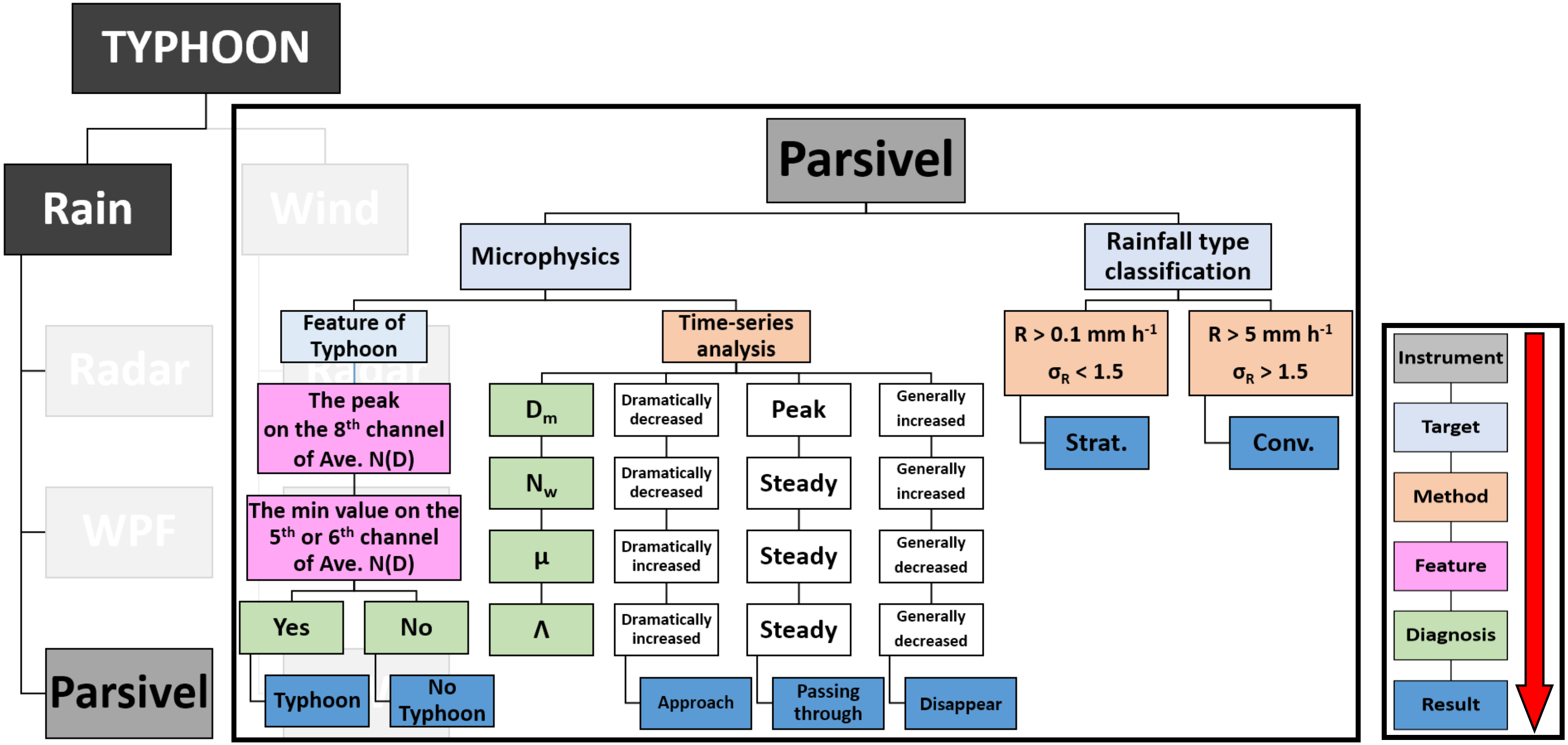

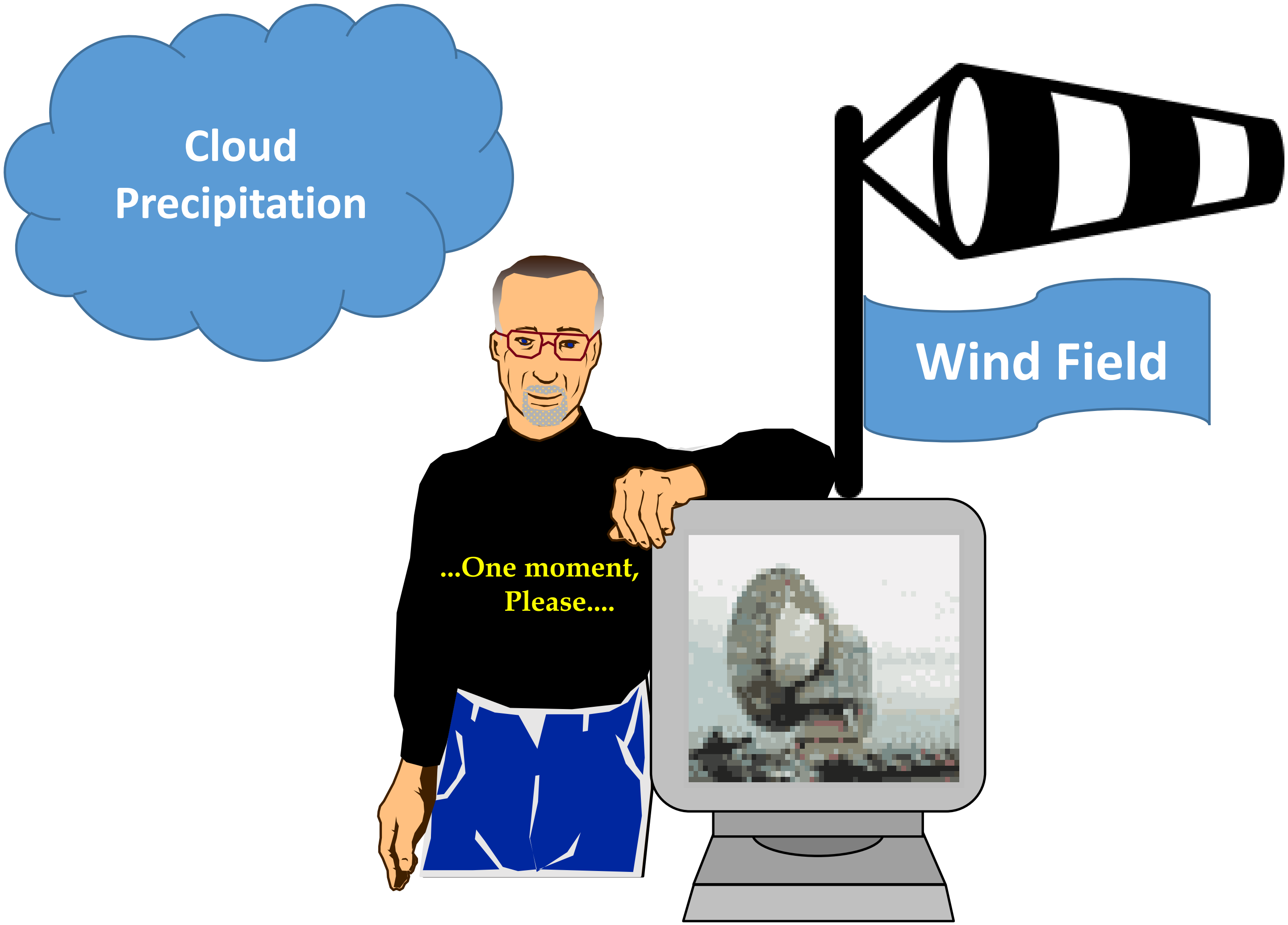
Cloud
Precipitation
Wind Field
...One moment,
Please....

3. Wind field analysis by Radar and Wind profiler

1). Dual Radar Wind Field Analysis Using Variational Method – TY Bolaven

A method for implementation a 3D wind field using radar data

Adopt the wind field value when the cost function (J) is the minimum value

$$J = J_O + J_B + J_D + J_S$$

$$J_O = \frac{1}{2}\sum_m \lambda_m (c \cdot Vr_m - u\cos A - v\cos B - (w + w_t)\cos C)^2$$

$$J_B = \frac{1}{2}\left[\sum_{ijk}\lambda_{ub}(u-u_b)^2 + \sum_{ijk}\lambda_{vb}(v-v_b)^2 + \sum_{ijk}\lambda_{wb}(w-w_b)^2\right]$$

$$J_D = \frac{1}{2}\sum_{i,j,k}\lambda_D D^2$$

$$J_S = \frac{1}{2}\left[\sum_{ijk}\lambda_{us}(\nabla^2 u)^2 + \sum_{ijk}\lambda_{vs}(\nabla^2 v)^2 + \sum_{ijk}\lambda_{ws}(\nabla^2 w)^2\right]$$

$$D = \frac{\partial \bar{\rho} u}{\partial x} + \frac{\partial \bar{\rho} v}{\partial y} + \frac{\partial \bar{\rho} w}{\partial z}$$

J_0 : analyzed ($V_r^{m,n}$) and observed($V_{rob}^{m,n}$) radial velocity
m : the number of radar
n : the number of observation

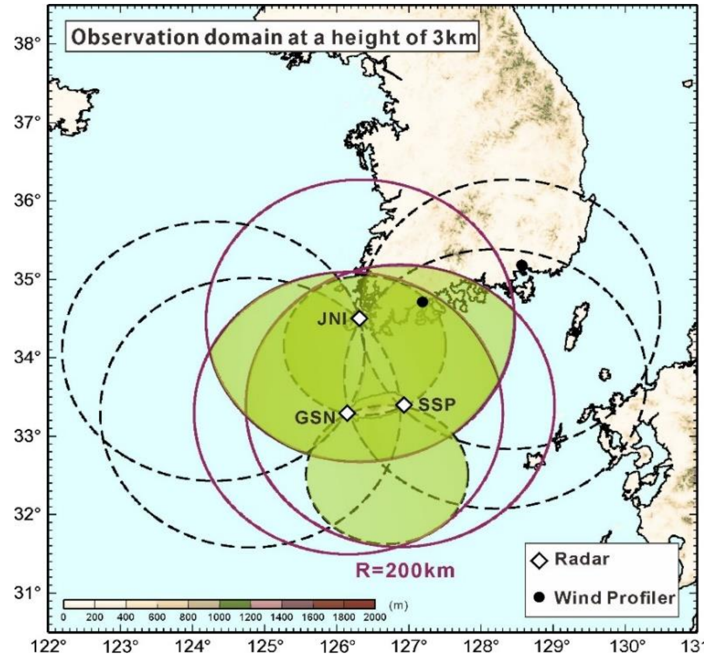

Fig. Wind field expression area by variational method using 3 weather radars at 3 km height

3. Wind field analysis by Radar and Wind profiler

1). Dual Radar Wind Field Analysis Using Variational Method – TY Bolaven

1. Wind field by weather radar

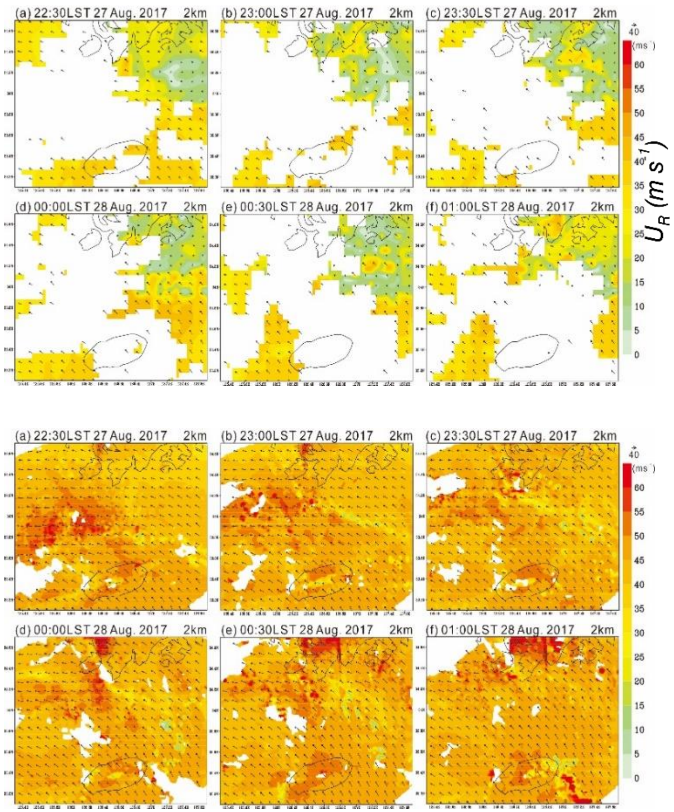

Dual wind field by operating weather radar (up) ,
Variational method dual wind field (down)

2. Wind profiler in Boseong Standard Observatory

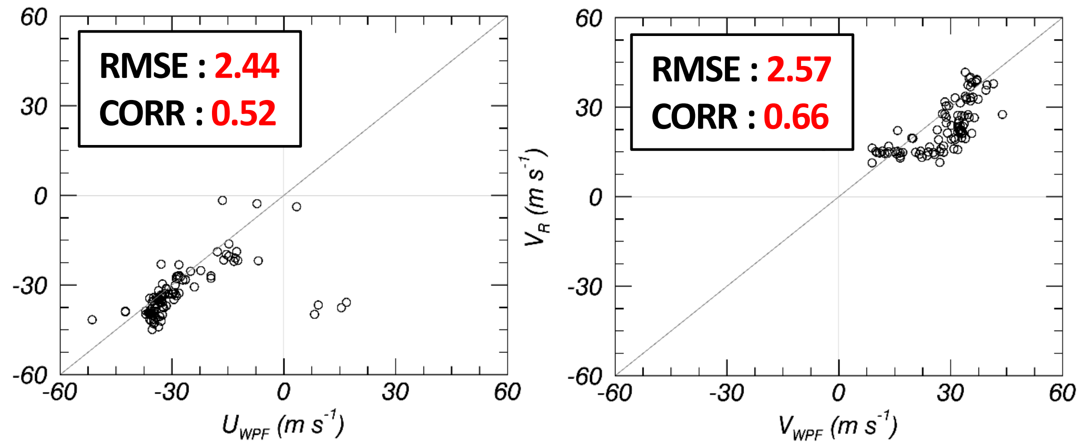

Fig. Comparison of the horizontal wind component of the variational dual wind field and the wind profiler of the Boseong Standard Observatory

- The wind field of the operating radar has an insufficient display area and a very small value compared to the wind component (45 - 50 m s-1) presented in the MSM reanalysis data.

- Most of the results of the variational method dual wind field were calculated within the expression area, and a horizontal wind component similar to the reanalysis data was presented.

- In comparison with Wind Profiler, it shows a relatively high correlation.

3. Wind field analysis by Radar and Wind profiler

2). Algorithm of the wind field retrieval

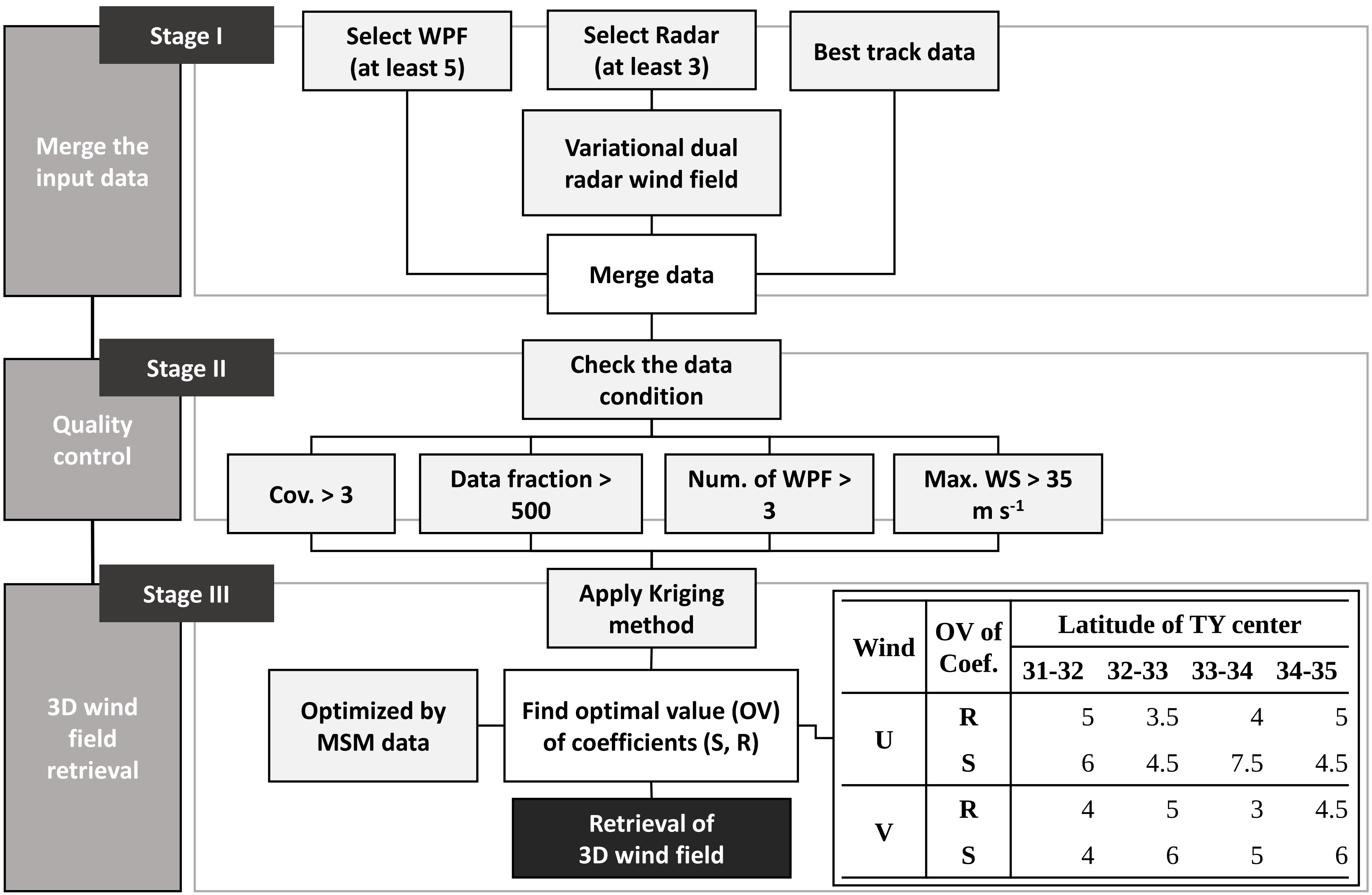

Wind	OV of Coef.	Latitude of TY center			
		31-32	32-33	33-34	34-35
U	R	5	3.5	4	5
	S	6	4.5	7.5	4.5
V	R	4	5	3	4.5
	S	4	6	5	6

3. Wind field analysis by Radar and Wind profiler

3). TY Bolaven Case Analysis – Surface wind calculation using the variational method for radar dual wind field

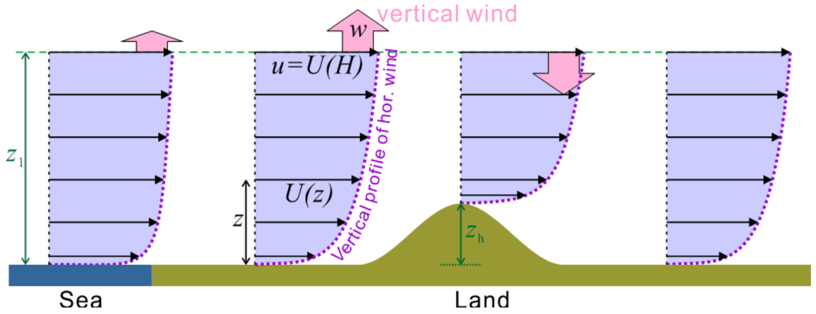

Fig. Conceptual diagram of surface wind estimation algorithm assuming a logarithmic profile of wind speed

(Maesaka et al., 2007)

Wind speed at the specific height z :

$$U(z) = \frac{u^*}{\kappa} log \frac{z - z_h}{z_0} \qquad V(z) = \frac{v^*}{\kappa} log \frac{z - z_h}{z_0}$$

z_h : terrain height, κ: von Karman constant
z_0 :roughness depth on the ground

Friction velocity :

$$u^* = \kappa u \left(\log \frac{z - z_h}{z_0} \right)^{-1} \qquad v^* = \kappa u \left(\log \frac{z - z_h}{z_0} \right)^{-1}$$

Advantages :

- **Complement dual wind field from 10 m to 1 km**
- **It could detect ground gust wind without AWS**
- **Supplement of the resolution of AWS field**
- **It could calculate the ground wind on the ocean**

Vertical profile of horizontal wind speed :

$$U(z) = u \left(\log \frac{z_1 - z_h}{z_0} \right)^{-1} \log \frac{z - z_h}{z_0}$$

$$V(z) = v \left(\log \frac{z_1 - z_h}{z_0} \right)^{-1} \log \frac{z - z_h}{z_0}$$

4. Wind field analysis by Radar, Wind profiler and AWS

1). TY Bolaven Case Analysis – Typhoon structure analysis procedure– Wind Part

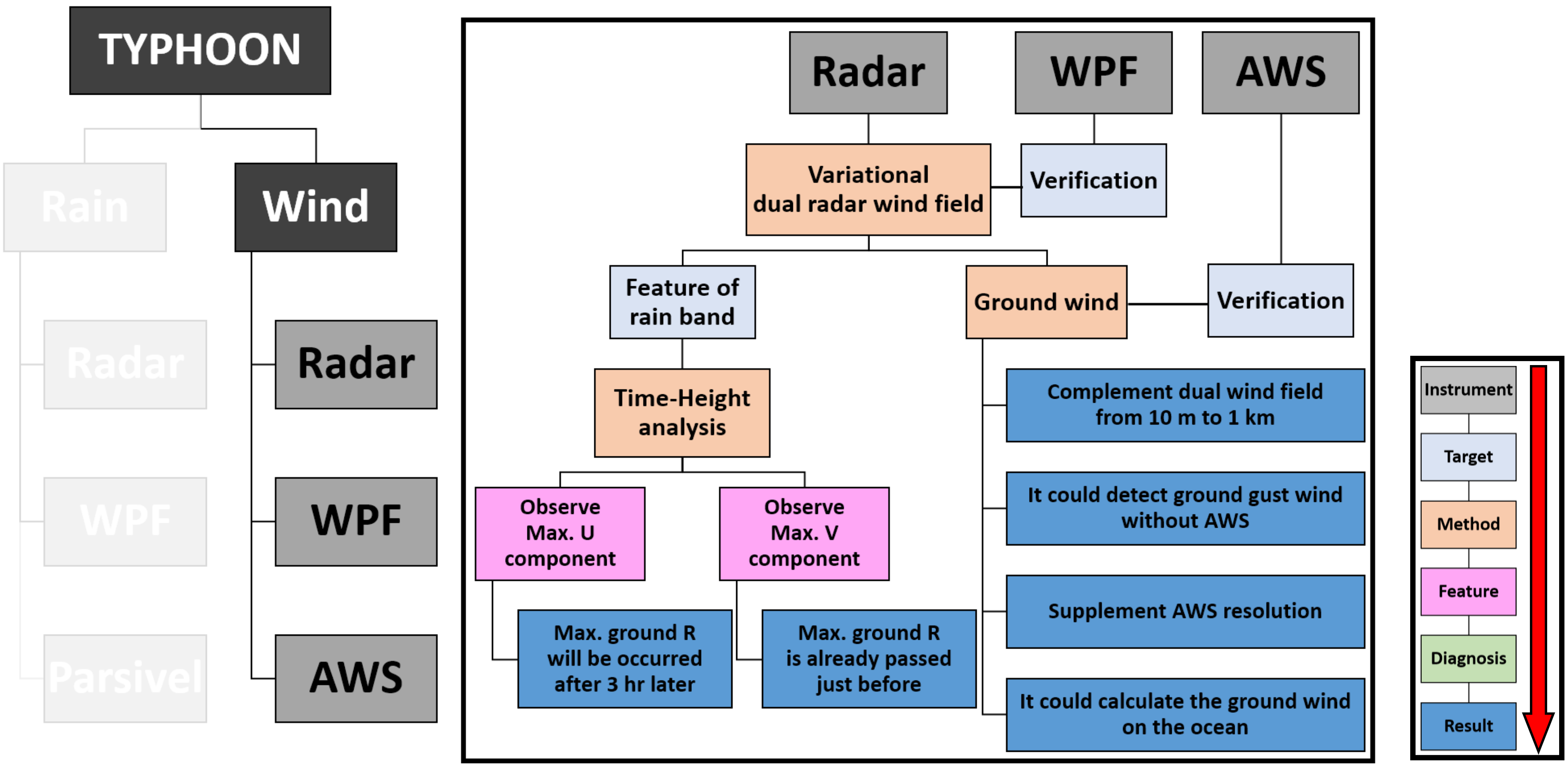

5. Analysis of wind field characteristics according to landfall of typhoon (Bolaven) precipitation band

1). Distribution of East-West Wind Component (U) of Typhoon Bolaven for Key Times

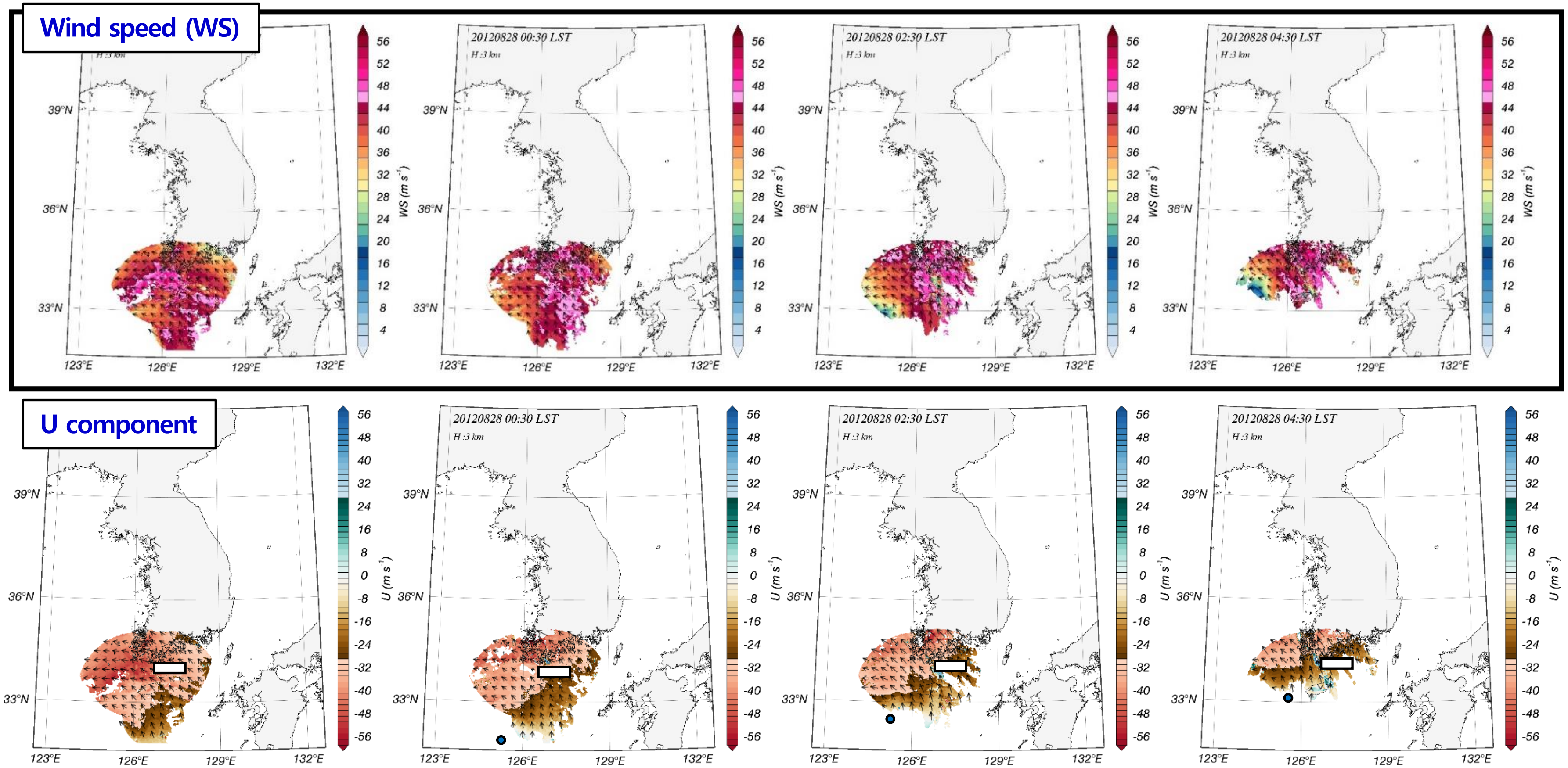

5. Analysis of wind field characteristics according to landfall of typhoon (Bolaven) precipitation band

2). Distribution of South-North Wind Component (V) of Typhoon Bolaven for Key Times

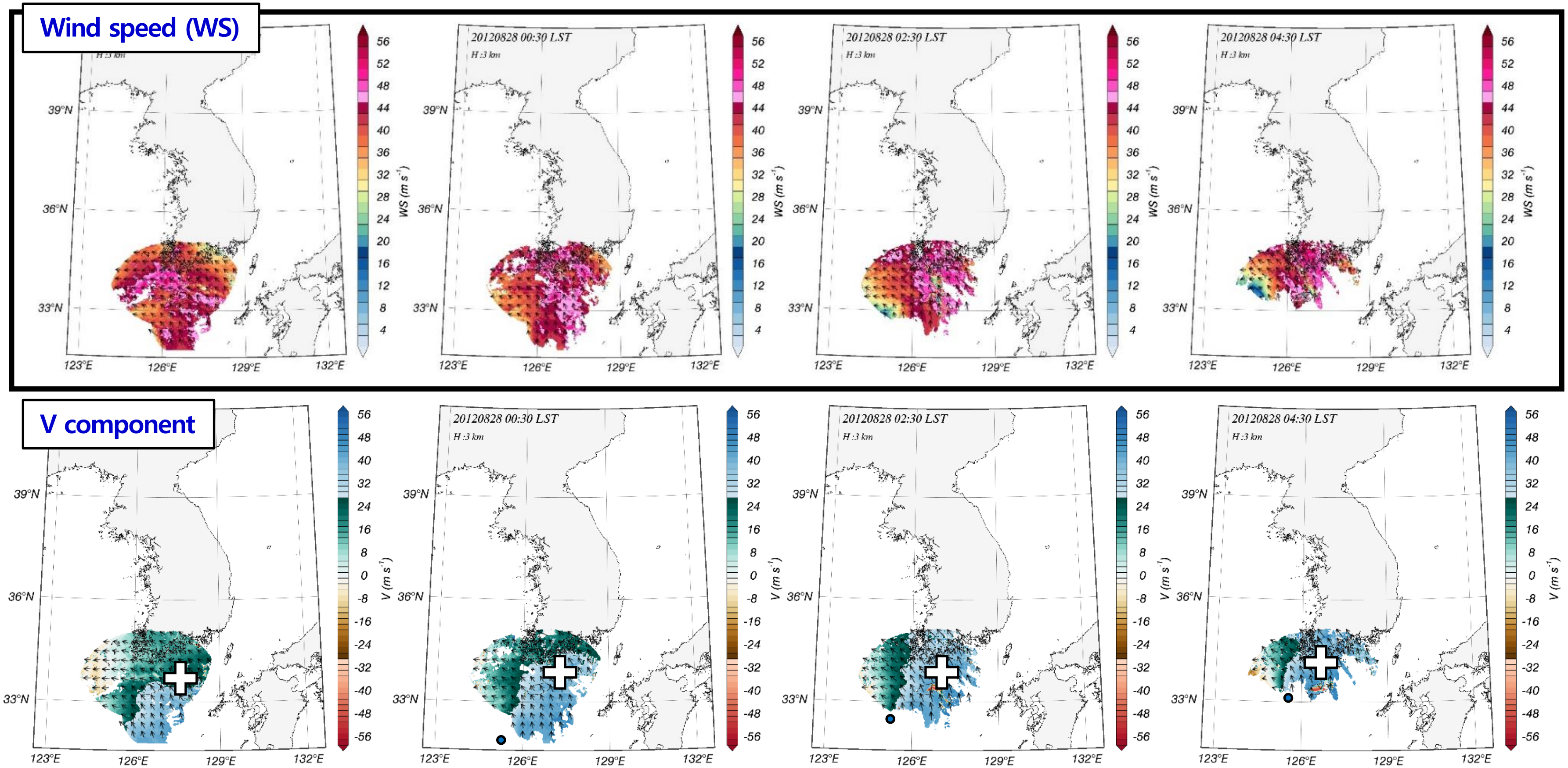

5. Analysis of wind field characteristics according to landfall of typhoon (Bolaven) precipitation band

3). Altitude-time distribution of the wind field of Typhoon Bolaven for analysis time

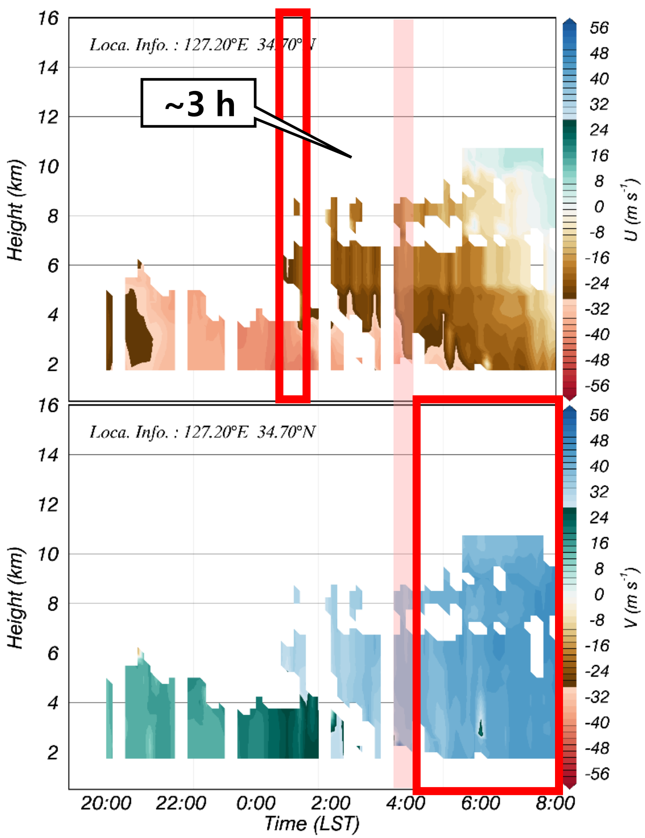

*** From U,V data***

- The maximum east-west (U) wind component was observed and the maximum rainfall intensity on the ground was observed after about 3 hours.
- Observation of the maximum north-south (V) wind component after observation of the maximum rainfall intensity on the ground
- Strong vertical wind component (V) was observed when maximum rainfall intensity occurs.

Radar reflectivity and wind component characteristics according to the inflow of typhoon precipitation band

Variable	Characteristic
Z_H	The reflectivity center gradually descends
U	The maximum U occurs approximately 3 hours before the maximum ground rainfall intensity value appears.
V	Immediately after the maximum rainfall intensity value on the ground appears, the maximum north-south wind on the ground occurs.
W	Presence of strong downdrafts

3. Comparative verification of **typhoon structure analysis guide** with other Typhoon(Nakri) case

3. Application of Typhoon Internal Structure Analysis Guide

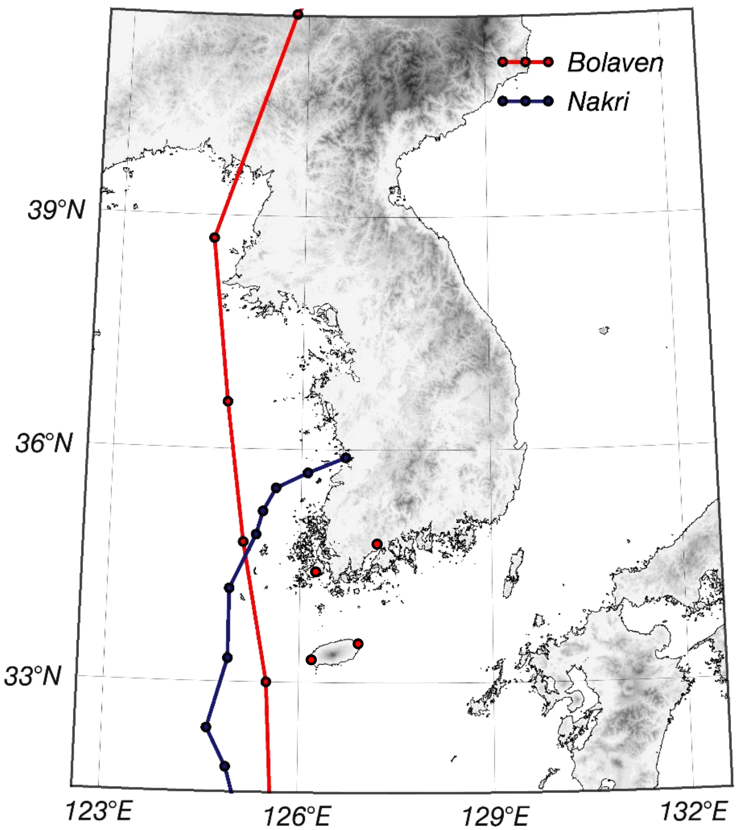

Verification of Typhoon Nakri case

Best track of the 6-hour interval between typhoons Bolaven (2012) and Nakri (2014) (provided by JMA)

3. Application of Typhoon Internal Structure Analysis Guide

Verification of Typhoon Nakri case

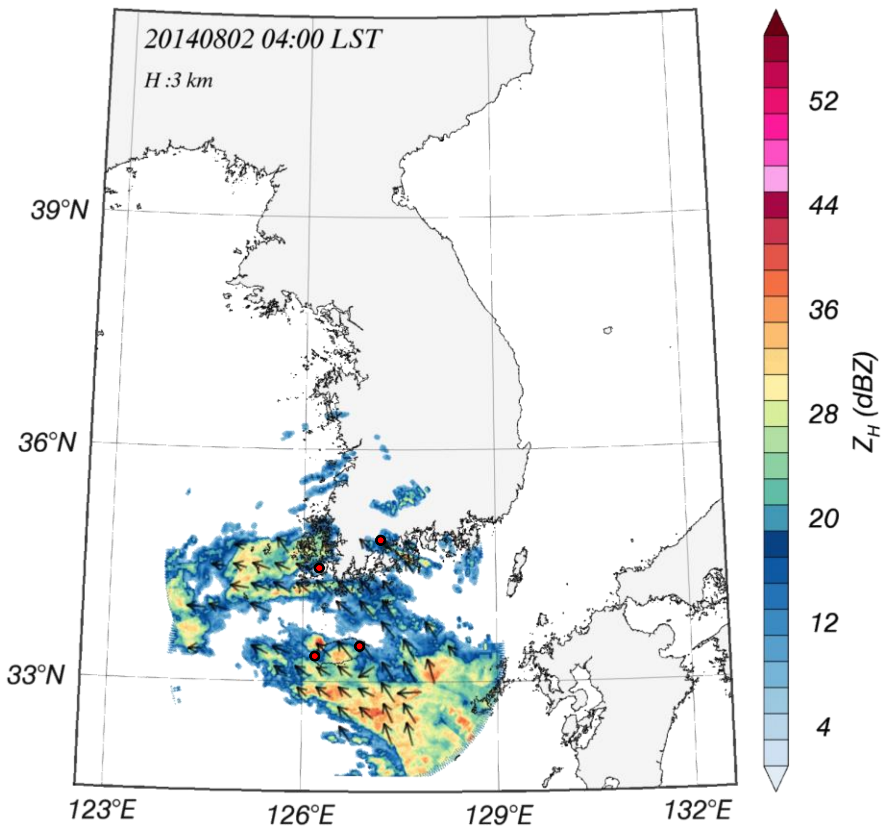

Fig. Synthetic Radar CAPPI (3km) and dual Wind Field Distribution by variation method of Typhoon Nakri

The 12th Typhoon Nakri in 2014...

- Although it is an impact typhoon that passed through the Korean Peninsula, it had relatively weak intensity and the overall wind speed is weaker than that of existing typhoons.

- Precipitation is concentrated in the southern coastal area

- The precipitation band of Typhoon Nakri passes through the southern coast → Daily cumulative precipitation of more than 300 mm was recorded at the Boseong Standard Observatory.

- The precipitation band passing through the southern coast of the Korean Peninsula at the same time was observed from JNI, GSN, SSP S-band weather radar, Parsivel disdrometer and rain gauge (Boseong Standard Observatory).

3. Application of Typhoon Internal Structure Analysis Guide

Typhoon Nakri case – Verification of precipitation type classification using CFAD

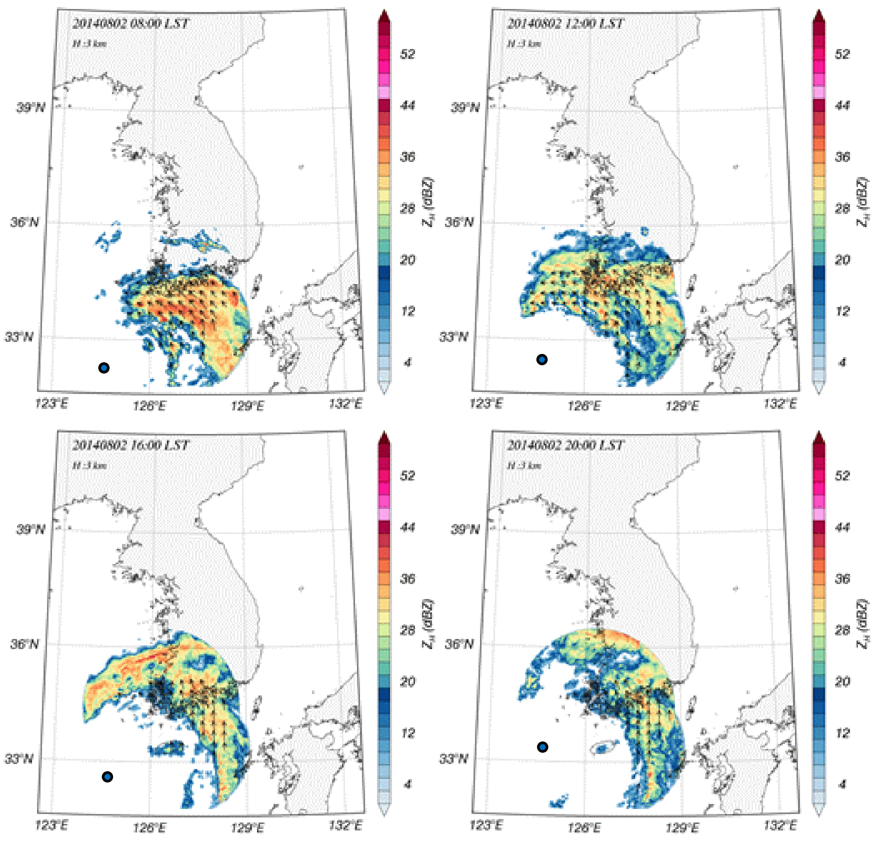

Fig. Synthetic CAPPI (3km) for Typhoon Bolaven precipitation bands at key times

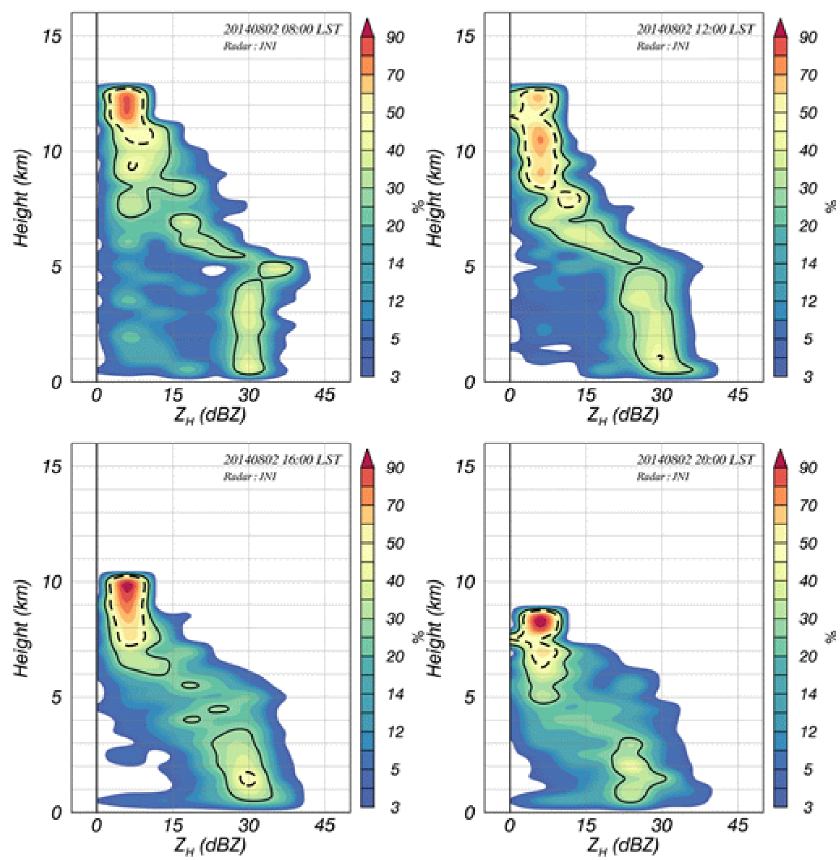

Fig. CFAD observed by JNI for Typhoon Bolaven precipitation band at key times

3. Application of Typhoon Internal Structure Analysis Guide

Typhoon Nakri case – Verification of precipitation type classification using CFAD

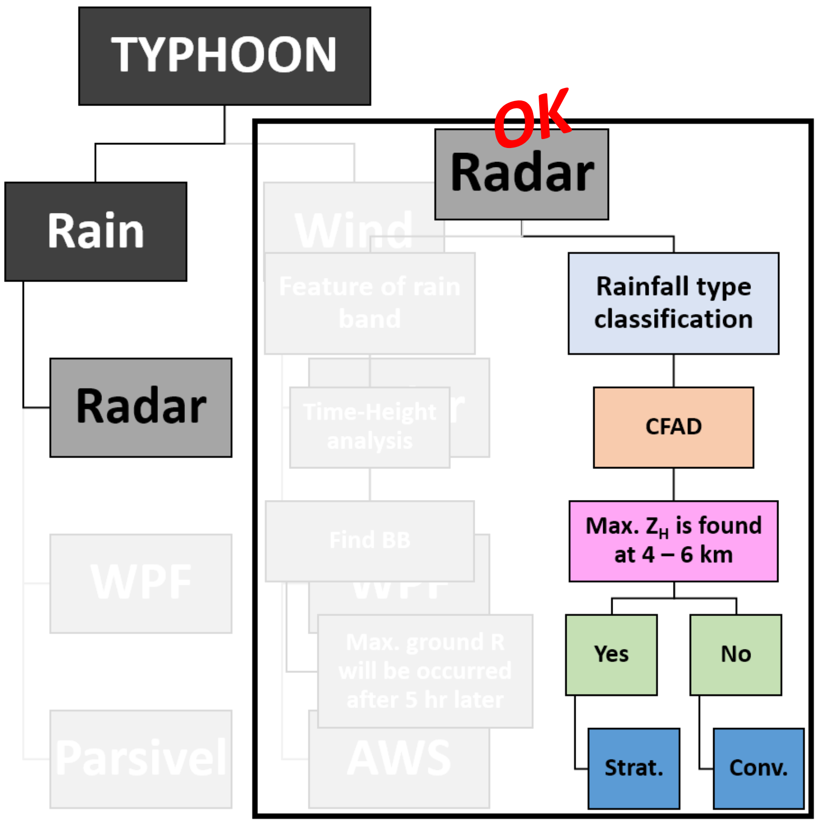

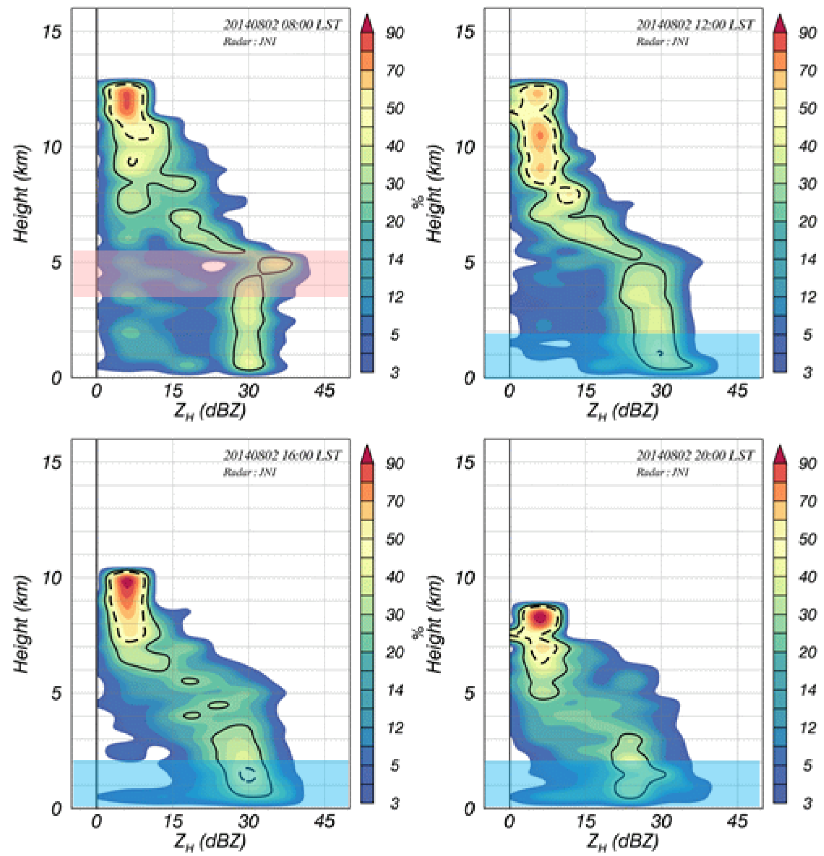

Fig. CFAD observed by JNI for Typhoon Bolaven precipitation band at key times

3. Application of Typhoon Internal Structure Analysis Guide

Typhoon Nakri case – Analysis and verification of radar reflectivity characteristics according to landfall of typhoon precipitation band

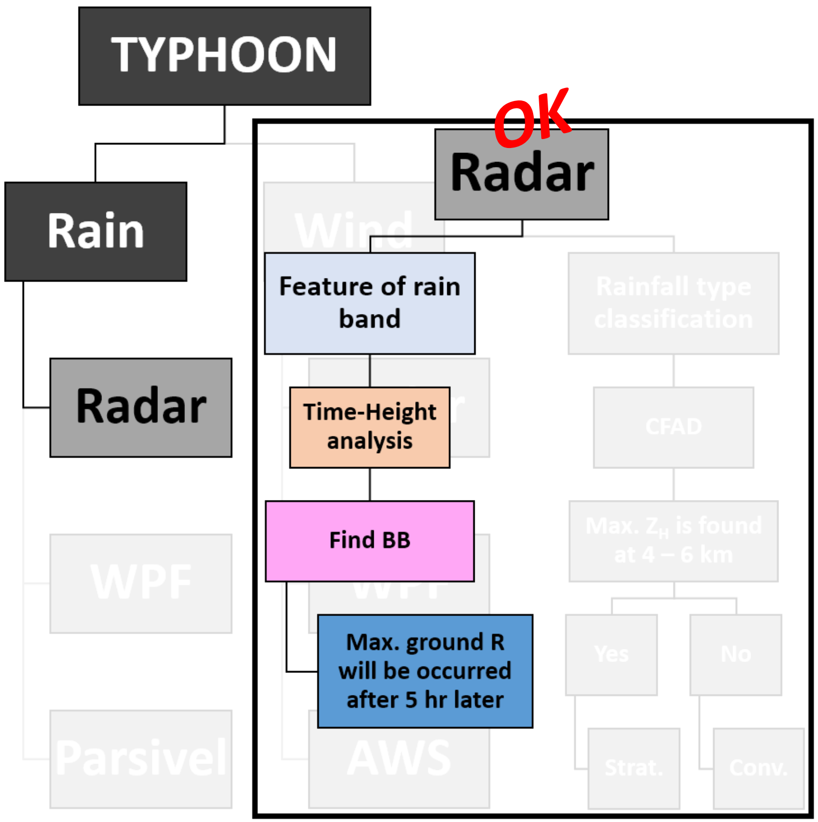

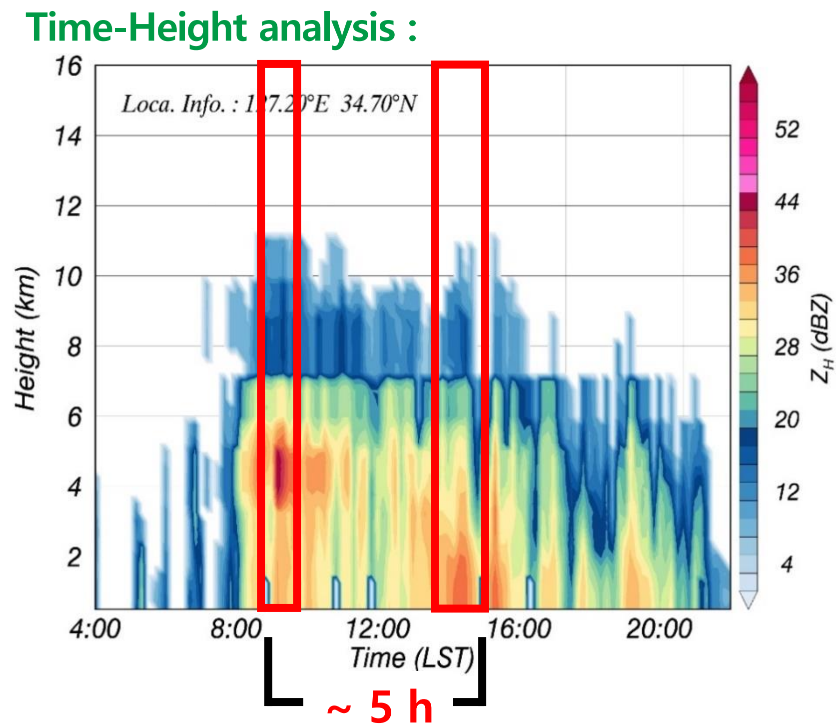

Fig. Vertical radar reflectivity time series distribution

3. Application of Typhoon Internal Structure Analysis Guide

Typhoon Nakri case – Verification of Typhoon characteristics and precipitation type classification using Parsivel disdrometer

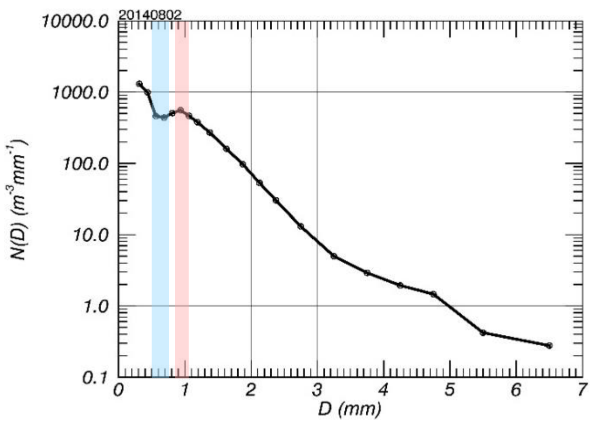

Fig. Distribution of average number concentrations of Typhoon Nakri

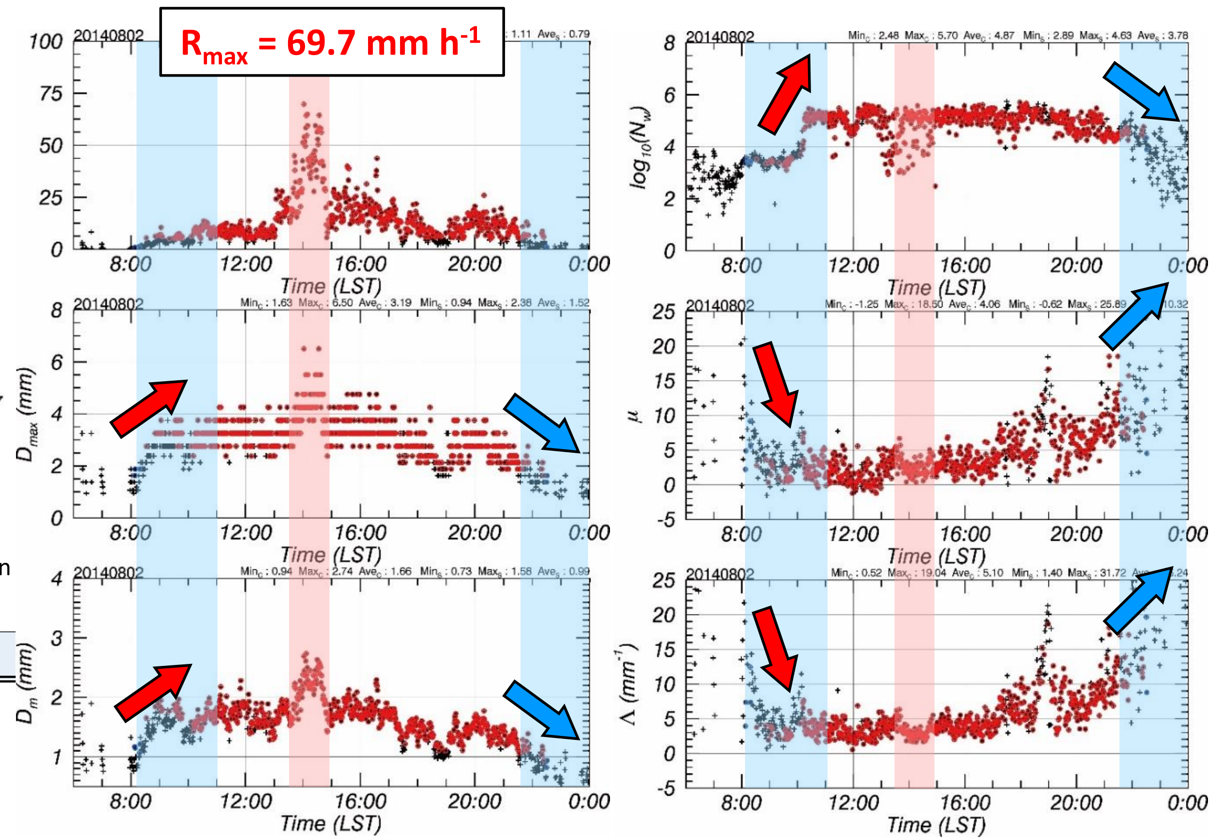

Fig. Time series distribution of DSD variables for Typhoon Nakri observed by Parsivel disdrometer

Characteristics of DSD Variables in the Inflow of Typhoon Nakri Precipitation Band

Variable	Inflow	Landing(Max)	Extinction
D_m	Sharp increase	Max	Gradually decrease
N_w	//	Maintain	//
μ	Sharp decrease	//	Gradually increase
Λ	//	//	//

3. Application of Typhoon Internal Structure Analysis Guide

Typhoon Nakri case – Verification of Typhoon characteristics and precipitation type classification using Parsivel disdrometer

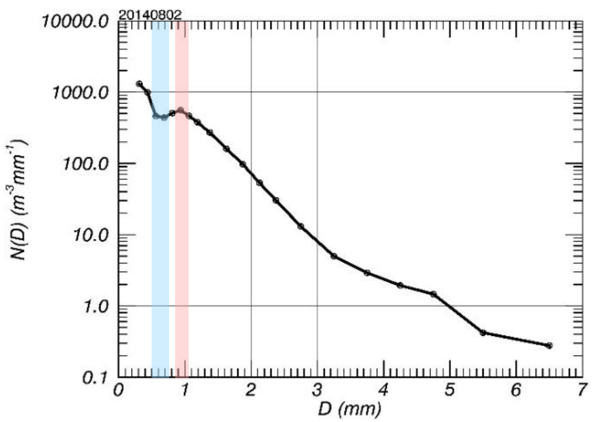

Fig. Distribution of average number concentrations of Typhoon Nakri

Characteristics of DSD Variables in the Inflow of Typhoon Nakri Precipitation Band

Variable	Inflow	Landing(Max)	Extinction
D_m	Sharp increase	Max	Gradually decrease
N_w	//	Maintain	//
μ	Sharp decrease	//	Gradually increase
Λ	//	//	//

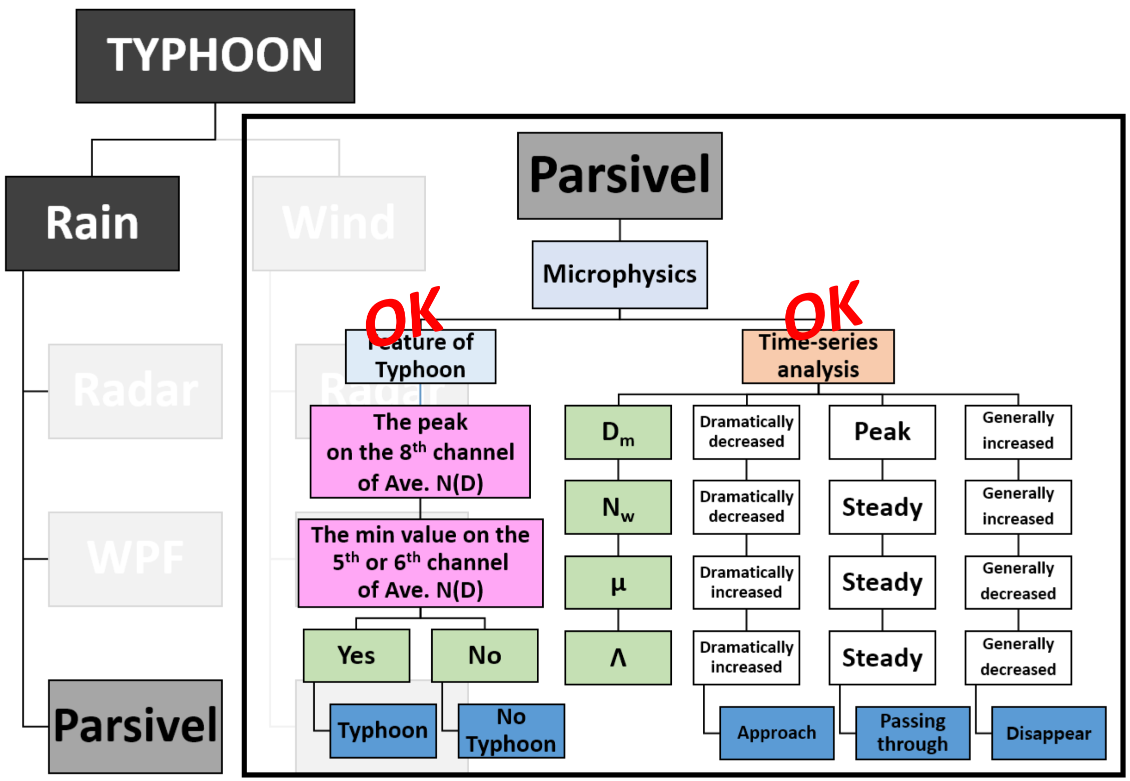

3. Application of Typhoon Internal Structure Analysis Guide

Typhoon Nakri case – Analysis of wind field characteristics according to landfall of typhoon precipitation band

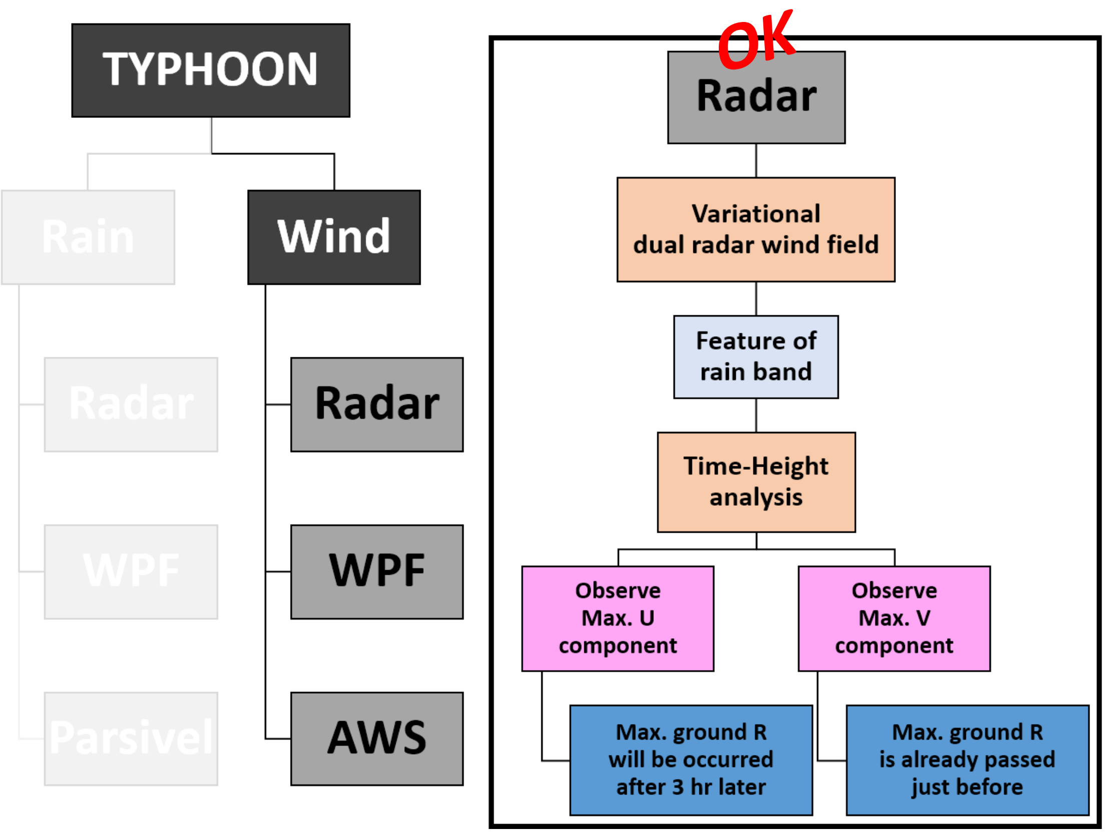

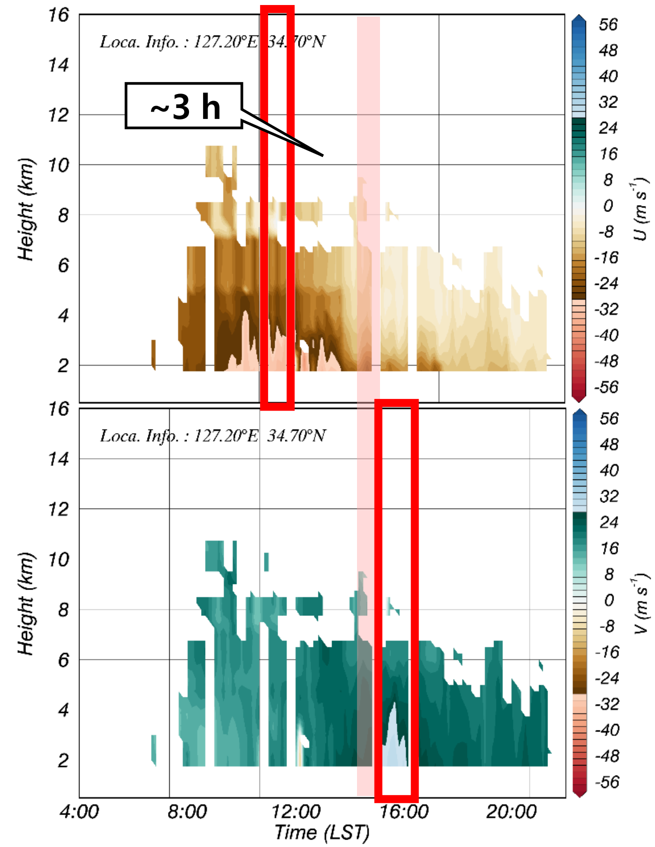

Fig. Altitude-time distribution of the dual wind field of Typhoon Nakri

Summary (Ch.2 & 3)

Development of Typhoon Structure Analysis Technology Using Real-time Observation Data

Internal structure analysis of typhoon precipitation band using multiple ground-based meteorological instruments located on the southern coast of the Korean Peninsula.

1. JNI, GSN, SSP S-band Doppler radars:
   (precipitation type classification, variational dual wind field, typhoon precipitation band inflow characteristics).

2. Installed at the Boseong Standard Observatory, Wind profiler:
   (precipitation type, dual wind field verification)

3. Parsivel disdrometer:
   (precipitation micro-physics, typhoon precipitation band inflow characteristics)

Using analysis of internal structural characteristics of typhoon Bolaven precipitation band
→ Development of typhoon internal structure analysis technology based on these results
→ It was verified with the case of Typhoon Nakri.

The results are very similar to the internal structural characteristics of the typhoon precipitation band confirmed in Bolaven.

Typhoon analysis guidance according to the phenomena

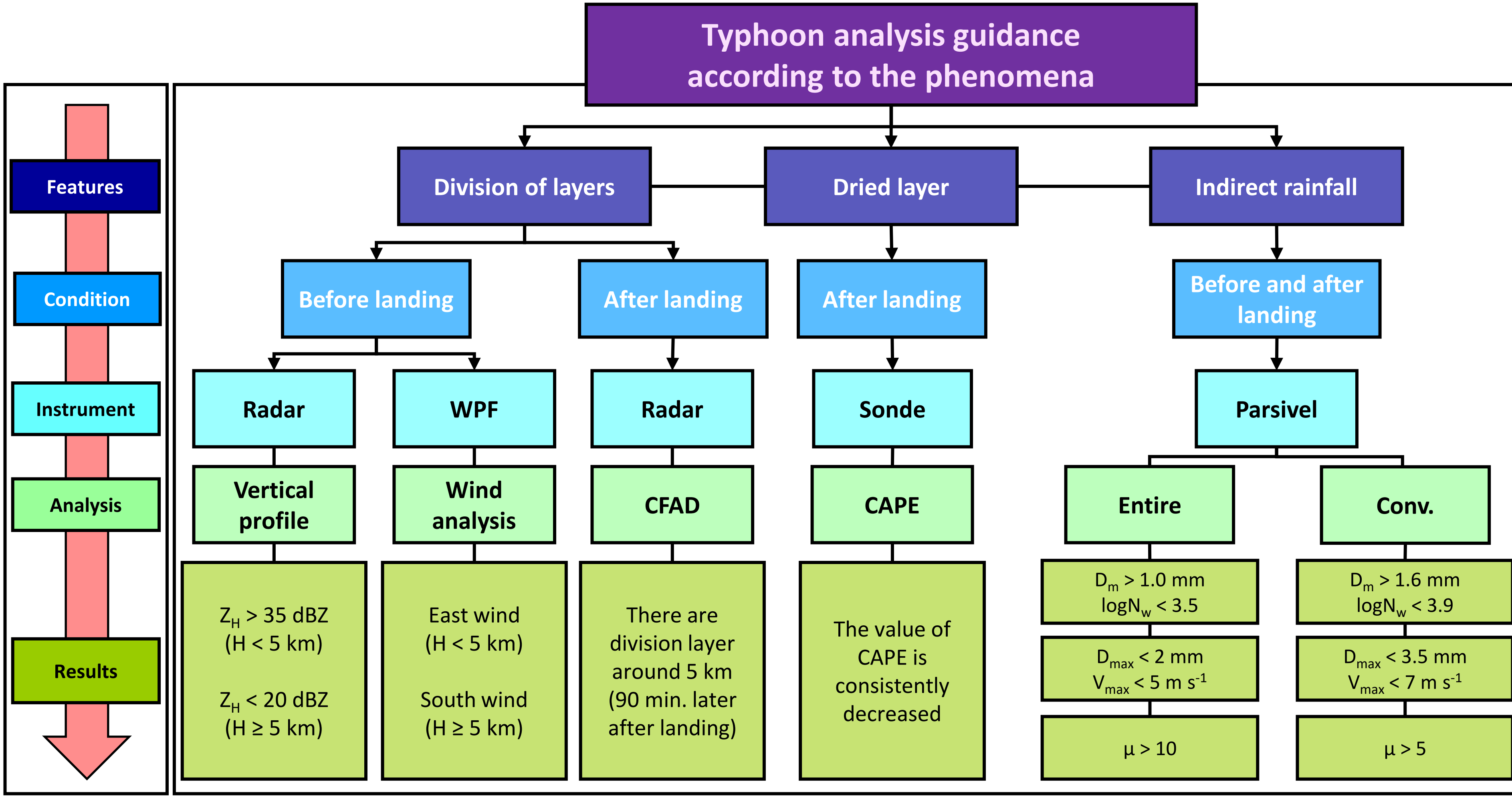

Development of Typhoon Structure Analysis Technology Using Real-time Observation Data

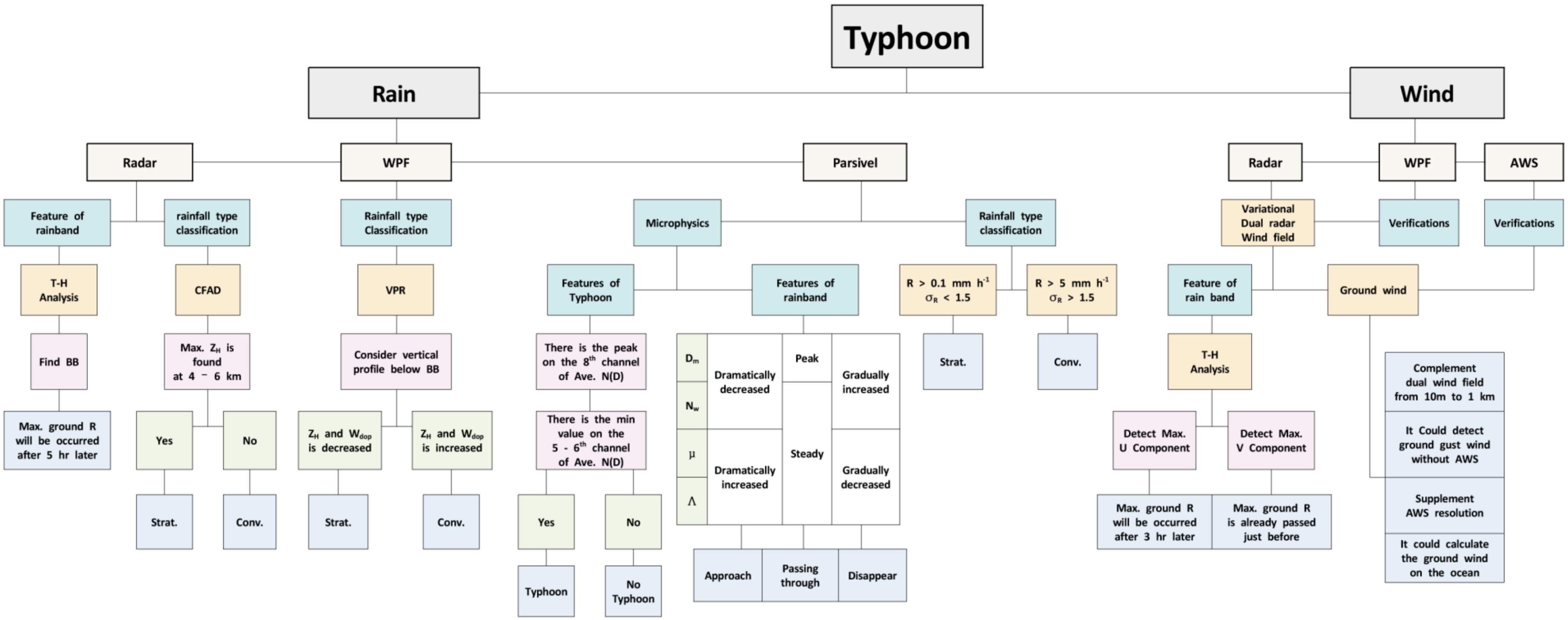

Can the typhoon internal structure analysis technology and guidance developed in this study be used in Vietnam or Asia?

Answer : I believe it's possible.

Thank you, any questions?

e). Wind profiler

1). UV wind distribution and data filter (Circle type)

Circle-shaped distributions

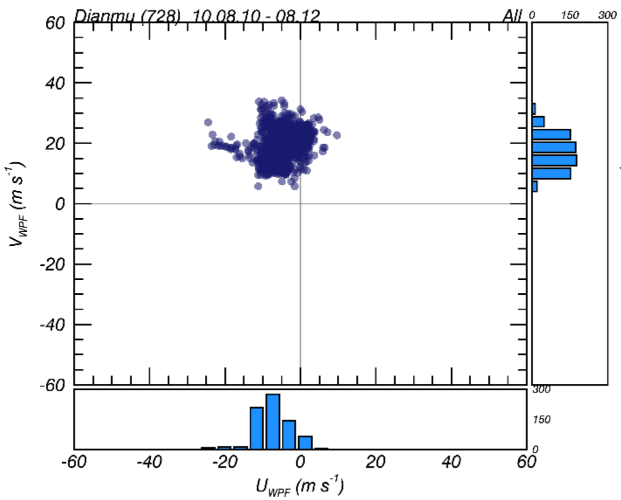

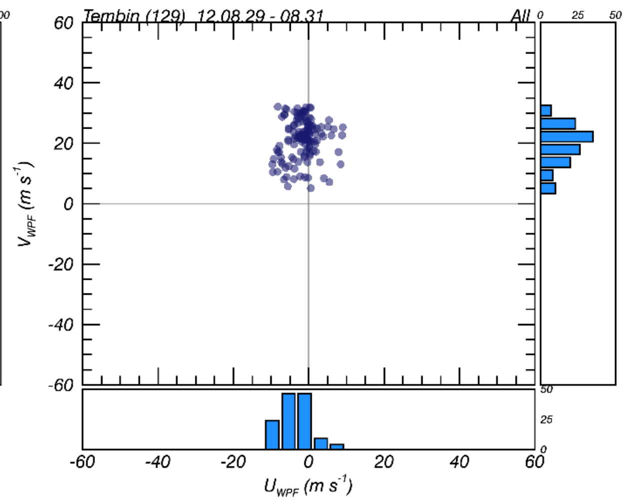

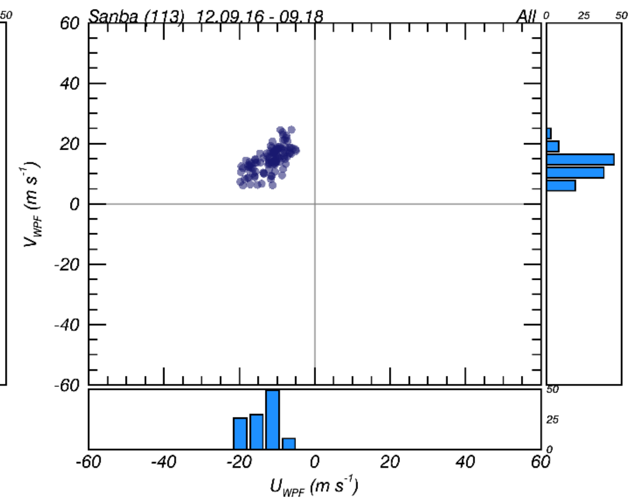

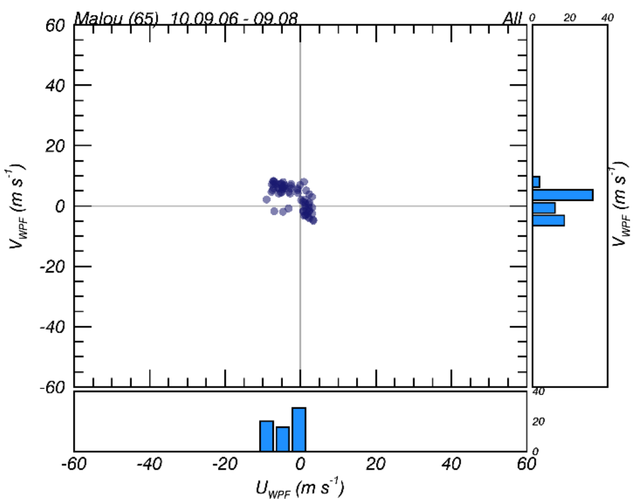

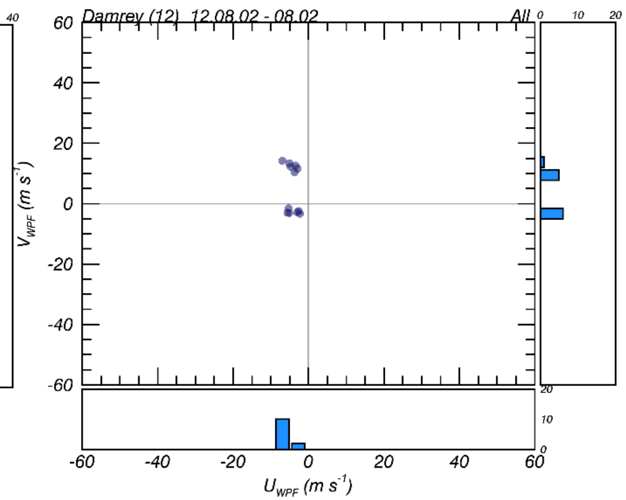

Circle-shaped cases
(Dianmu, Malou, Tembin)

Typhoons were passed through **the southern sea.**

e). Wind profiler

2). UV wind distribution and data filter (Arch, Line type)

Arch-shaped distributions

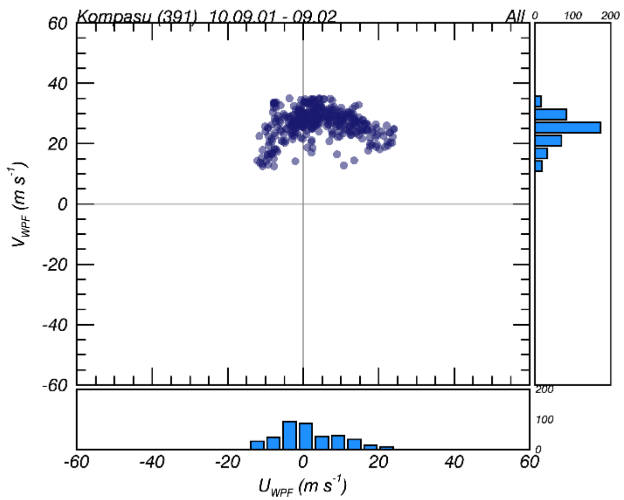

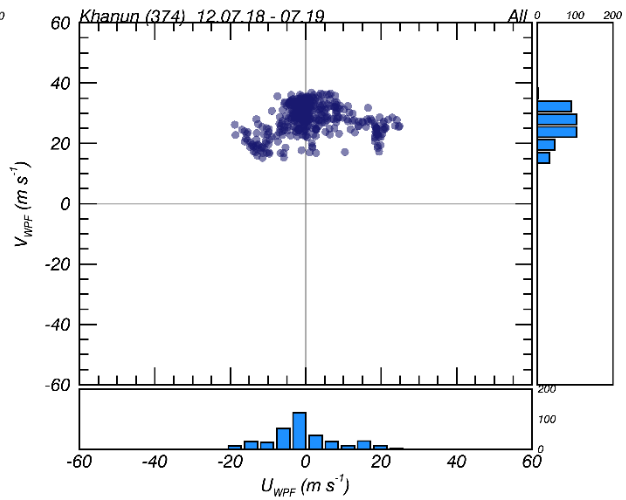

Line-shaped distributions

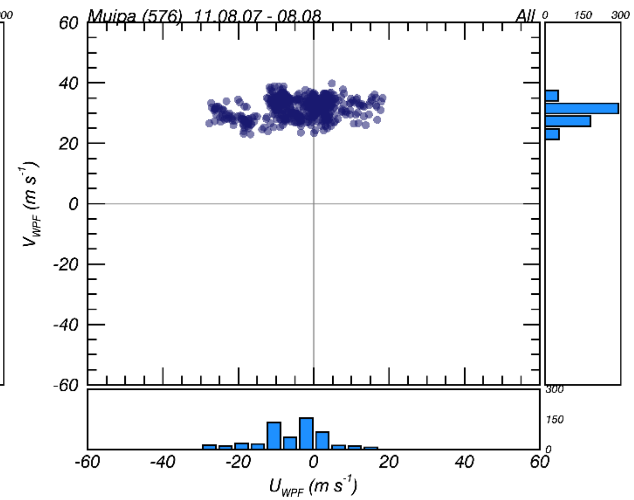

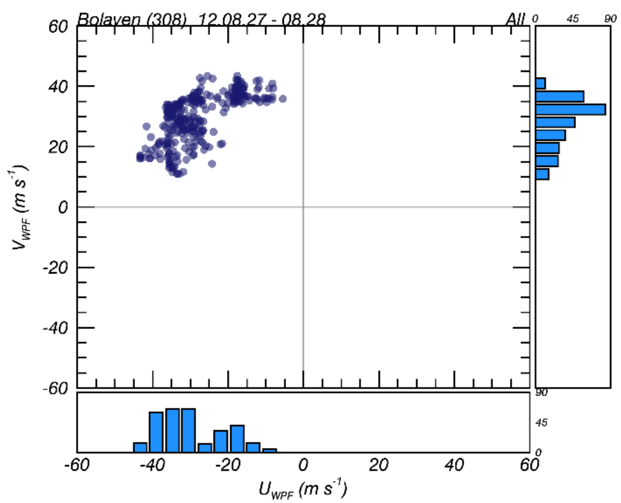

Arch-shaped Case
(Khanun, Kompasu)

Typhoons were passed through **the center of Korean peninsula.**

Line-shaped Case
(Muipa, Meari)
Typhoons were passed over **the Yellow sea.**

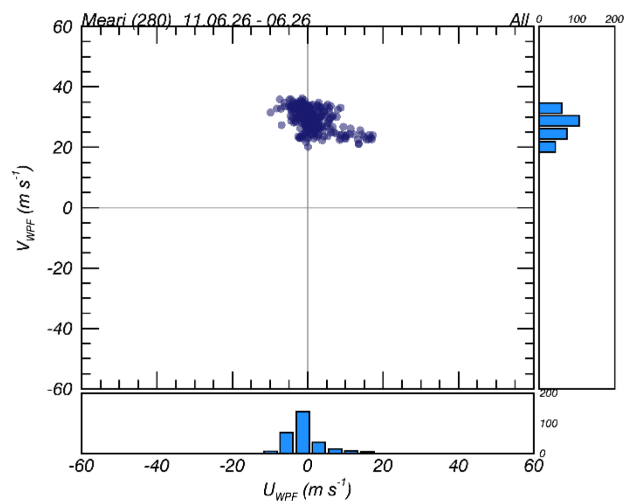

e). Wind profiler

3). UV wind distribution (Circle, Arch, Line type)

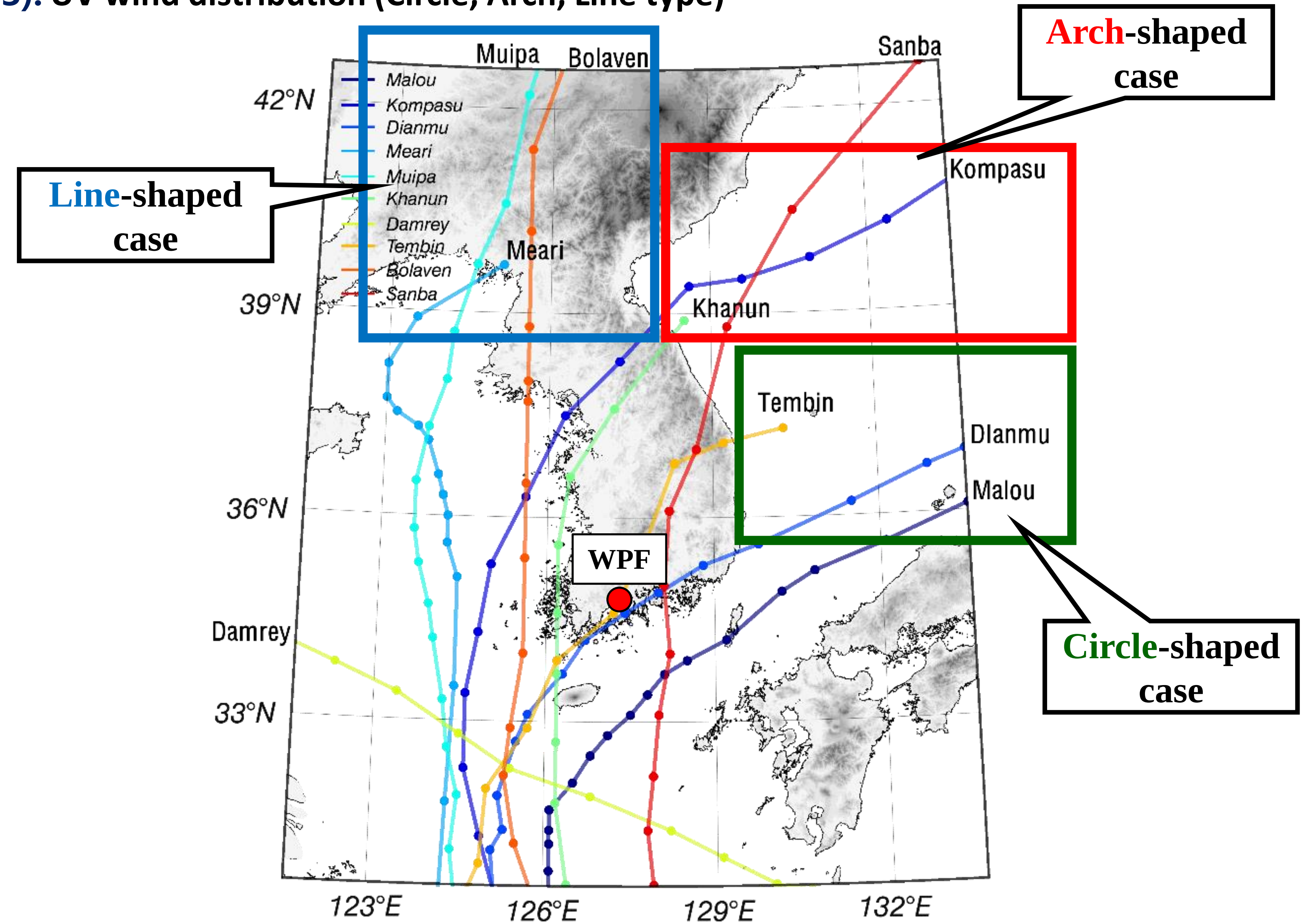

4. Summary

Stage	Radar	Parsivel					AWS	Sonde
Before								CAPE ↓ CIN ↑
Beginning	C_{max} ↑ H_C ↑ H_{Max} ↑	N(D <1 mm) ↓ N(D >3 mm) ↑	Higher V(D) for the same D	D_m ↓ Higher D_m for same R	N_w ↓	Lower μ for the same R	T ↓(~4ºC) RH ↑(70→90%)	CAPE ↓ CIN ↓
Middle	C_{max} ─ H_C ↓ H_{Max} ↓	N(D <1 mm) ↑ N(D >3 mm) ↓	Max V(D)	D_m ↑	N_w ─	Min μ (→0)	P ↓ (Depends on the central P)	CIN ↓
After	C_{max} ↓ H_C ─ H_{Max} ↓	N(D <1 mm) ↓ N(D >3 mm) ↓	Lower V(D) for the same D	D_m ↓ Lower D_m for same R	N_w ↑	Higher μ for the same R		

UV wind observed by WPF

Circle-shaped cases
(Dianmu, Malou, Tembin)

Typhoons were passed through **the southern sea**

Arch-shaped Case
(Khanun, Kompasu)

Typhoons were passed through **the center of the Korean peninsula**

Line-shaped Case
(Muipa, Meari)

Typhoons were passed over **the Yellow sea**